Centre for Minerals Research
Department of Chemical Engineering
University of Cape Town

Investigating the Potential of using Hydrocyclone-Fine Screen Hybrid Systems to improve the Performance of Classification Circuits

A dissertation presented for the degree of Master of Science in Chemical Engineering

Prepared by: Saliya L. Muketekelwa
Supervised by: Prof. Aubrey Mainza & Dr. Paul Bepswa

May, 2017

PLAGIARISM DECLARATION

I hereby declare that all the work presented in this dissertation is the result of my own research, except as cited in the reference. This dissertation has not been accepted for any degree or is being submitted in the candidature of any other degree.

Signed by candidate

signature removed

Signature:

Date: 25th May, 2017

ABSTRACT

Classification is an integral part of comminution operations that controls the performance of the circuit. Hydrocyclones are normally used to perform the classification function. They offer numerous advantages that include, the ability to handle high throughputs, low floor space occupation and relatively low capital and running costs. Despite these advantages, hydrocyclones are inherently inefficient classifiers as they are predominantly dependent on hydrodynamics to effect separation. This effect is more prominent in operations handling complex ores such as a dual-density ore, where the heavy fine particles are misplaced to the underflow and the lighter middling particles report to the overflow. Several attempts have been made to improve the separation efficiency of cyclones either by modification of the cyclone or use of multi-stage cycloning. Most of the results obtained from experimental and simulation studies have shown considerable improvements. Even though some have not yet found wide application in the minerals industry due to practical limitations related to control and unstable operations.

More recently, fine screening has gained recognition in the classification role. This development has allowed the use of fine screens in closed-circuit grinding operations resulting in significant metallurgical and economic benefits. Screens provide a sharper cut at the desired size and reduce the fraction of fines bypassing classification compared to hydrocyclones but have capacity limitations at smaller apertures. In an effort to mitigate the classification challenges of both the hydrocyclone and fine screen, this study investigated the potential of combining the high throughput performance of the hydrocyclone operation and the high precision classification characteristics of fine screening to result in a hybrid classification circuit

Plant scale tests were conducted using five different classification circuit configurations at an operational Base Metal Concentrator treating a polymetallic ore. The classification circuit configurations considered included (i) a two-stage hydrocyclone with primary underflow reclassification (ii) an inclined hydrocyclone, (iii) a fine screen and (iv) selected permutations of hybrid circuit designs that included a hydrocyclone-fine screen (2 stage) and two hydrocyclones-fine screen (3 stage) variants of the hybridised configurations.

The efficiency curves and their respective key performance indicators were used to assess the performance of the circuit configurations tested. The results showed that classification circuits that included fine screens exhibited higher sharpness of separation compared to circuit configurations comprised of hydrocyclones. The fine screen configuration showed the sharpest separation while the hydrocyclone-fine screen hybrid configurations gave relatively higher separation efficiencies than the configurations with hydrocyclones only. The overall sharpness of separation values obtained for the two stage and three-stage hybrid circuits were 3.0 and 2.4, respectively. The two-stage hydrocyclone and inclined hydrocyclone circuits had sharpness of separation values of 1.7 and 0.5, respectively. The inclined hydrocyclone circuit configuration performed the poorest. Furthermore, the two-stage hybrid circuit showed a higher degree of separation compared to the three-stage hybrid configuration. However, it was observed that a finer corrected cut size was realised for the three-stage hybrid circuit design. The fishhook effect was seen at particle sizes less than 38μm for the configurations incorporating a fine screen and an inclined hydrocyclone. Notably, the effect appeared to be more pronounced in configurations involving a fine screen stage.

The results have shown that application of hybrid classification configurations can improve the performance of classification circuits. In addition, reclassification of hydrocyclone underflow on fine screens will results in a sharper classification while reclassifying the overflow stream on fine screens will provide a clean circuit final product. An evaluation of the capital and operating costs associated with fine screens should be done to determine the economic feasibility of incorporating the units in conventional milling circuits.

DEDICATION

I am forever indebted to mom and dad for their inspiration, love, support and prayers. I can never ask for better parents than them. I dedicate this milestone to them.

ACKNOWLEDGEMENTS

I am deeply grateful to my supervisors, Prof. Aubrey Mainza and Dr. Paul Bepswa for the insightful comments, suggestions, immense knowledge and continuous support during my MSc. Study.

Besides my supervisors, I would like to thank Mr. Mussa Lisso for the support rendered during the period of the surveys at Black Mountain Mine (BMM) and the valuable contributions to this thesis. I could not imagine conducting the surveys alone.

My sincere thanks go to Mr. Adolph Mwale for the insightful suggestions and comments, also to the Centre for Minerals Research (CMR) group for their support.

My appreciation also go the metallurgy crew at Black Mountain Mine for the support rendered during the period of survey campaigns.

It is a pleasure to thank my friends Prisca Chikuta and Joseph Banda for their continuous support, prayers and encouragements, especially during the sleepless nights.

Special thanks to my family: mom and dad, my brothers and sisters for always being there for me, providing unfailing support and encouragement throughout my years of study.

Lastly, but most important I want to thank my Heavenly Father for giving me the strength, courage, wisdom and knowledge to complete this thesis. *"I can do everything through **Christ** who gives me strength"*

TABLE OF CONTENTS

LIST OF FIGURES

LIST OF TABLES

NOMENCLATURE

F	Mass solid flowrate in feed stream	t/h
U	Mass solid flowrate in coarse stream	t/h
O	Mass solid flowrate in fine stream	t/h
f_i	weight fraction of size i in feed stream	
u_i	weight fraction of size i in coarse stream	
o_i	weight fraction of size i in fine stream	
E_i	Actual efficiency to the coarse product	
C_i	Corrected efficiency to the coarse product	
P_i	Actual efficiency to the fine product	
α	Sharpness of separation	
R_f	Water recovery to the coarse product	
$d50_c$	Corrected cut size	µm
β	Beta	
D_c	Cyclone diameter	m
D_u	Apex diameter	m
D_o	Vortex finder diameter	m
Q_f	Feed flowrate	m^3/hr.
u	Fluid viscosity	Pa.s
C_w	Solid concentration by weight	%
C_v	Solid concentration by volume	%
P	Pressure drop	Pa
ρ_l	Liquid density	Kg/m^3
ρ_s	Solids density	Kg/m^3
ρ_p	Pulp density	Kg/m^3
A	Screen aperture	µm
f_o	Screen open area	m^2
BMM	Black Mountain Mines	

1 CHAPTER ONE: INTRODUCTION

1.1 Background

The purpose of this thesis is to investigate the potential of applying hybrid hydrocyclone-fine screen circuit configurations in closed-circuit grinding by comparing their separation efficiencies with different conventional circuit configurations tested in this study. Classification plays an important role in the comminution circuits as mill capacity and the quality of the final product for the next processing step solely depends on its effectiveness. The misplacement of liberated fine particles to the coarse stream results to high circulating loads leading to loss in mill capacity while misplacement of coarse particles in the fine product stream coarsens the final product. Therefore, overlooking the process of classification can have detrimental effects on the overall plant performance. Napier-Munn et al. (2005) noted that an efficient classification process will results into 5-10% better performance while poor classification leads to 5-10% below average performance.

There are different types of classifiers used to close grinding circuits in mineral processing plants and these include hydrocyclones also referred to as cyclones, high frequency screens, spiral classifiers, rake classifiers, and air classifiers. In most concentrators, either cyclones or high frequency screens are employed to perform the task of classification. For many years, cyclones have been extensively utilised because of their simplicity in unit design, ability to handle high throughputs on a relatively small footprint, and relatively low capital and maintenance costs. However, cyclones are inherently poor classifying devices because of hydrodynamic effects. These units suffer from the deviation from ideal classification, described by the sharpness of separation indicator and assumed bypass which occurs when some fraction of the fine particles bypasses the classification forces and report to the underflow stream (Kelsall, 1953). The hydrodynamic effect is more pronounced in operations treating complex ores such as dual-density ores, where high density mineral particles accelerate faster than the low density mineral particles at equal size (Heiskanen, 1993). Many attempts have been made to improve the separation efficiency of cyclones either by modification of the cyclone or use of multi-stage cycloning. Most of the results obtained from experimental and simulations studies have shown considerable improvements (Kelsall & Holmes, 1960; Hukki & Heiskanen, 1981; Dahlstrom &

Kam, 1988) including some tested on full plant-scale (Heiskanen, Vesanto & Eronen, 1987; Mainza, Powell & Knopjes, 2004a). But, some cyclone modifications and multi-stage cycloning operations have proven unproductive or with little improvements in full plant-scale for various reasons (Hukki, 1975; Chu & Luo, 1994). Due to the inefficient performance of the conventional cyclones, recent advances in classification technology has allowed an increase in the application of high frequency screens in closed grinding circuits. Where modern high frequency screens have been implemented successfully, metallurgical benefits have been reported. Due to the encouraging reports, several plants around the world are considering replacing cyclones with high frequency screens.

High frequency screens were considered inapplicable in closing grinding circuits in the past due to their inability to effectively handle high throughputs in relation to the unit size, high wear rate of the screening media and the tendency of aperture blinding. Even with the afore-mentioned limitations, several studies performed many years ago demonstrated that a sharper separation could be achieved by closing grinding circuits with high frequency screens compared to other units such as spiral, rake and cyclone classifiers (Davies, 1925; Albert, 1945; Hukki, 1975). Nonetheless, recent innovations have led to improvements in the design and material of construction for the screening media. The modern high frequency screens have a 'unique' stack design where individual screen decks are stacked above the other and operate in parallel. This novelty allows for a relatively high throughput on a small foot print. Valine et al. (2009) argue that a stack sizer comprising of five individual decks is capable of handling throughputs as high as 350t/h of dry ore. Furthermore, polyurethane material is now used for the construction of the screening media which is specially designed to reduce aperture blinding and high wear rate (Albuquerque et al., 2008). Despite the numerous improvements made to the modern high frequency screen, the efficiency decreases rapidly with aperture size due to challenges of handling high throughputs. Application of high frequency screens only in large tonnage operations will increase the magnitude of screening units required to efficiently process the material, which will result into high capital and running costs.

Combining cyclones and high frequency screens to form a hybrid classification system is one of the methods considered to improve the performance of classification in this study. The main

purpose of the hybrid combination is to minimise the predominant challenges of cyclone circuit and screen circuit operations by taking advantage of the high throughput performance of the cyclones in the primary stage and the high precision classification characteristics of fine screening in the subsequent stage of classification. The concept of implementing a hybrid classification system acknowledges the shortfalls of the cyclone in the initial stage in terms of the inherent bypass fraction and corrects that by using high frequency screens. This also addresses the challenges of throughput limitations for screens operated with sub 500µm apertures (Mainza, 2016). Different types of classification hybrid system configurations can be implemented and the choice depends on the process requirement. For example, reclassification of cyclone overflow stream on a high frequency screen could provide the best quality product leaving the grinding circuit. Mainza et al. (2004a) made design modifications to the three-product cyclone developed at Julius Kruttschnitt Mineral Research Centre (JKMRC) (Obeng & Morrell, 2003) in an effort to mitigate the particle density effect commonly encountered in conventional cyclones. The authors postulated that the second overflow stream in which the fine dense liberated and middling particles report could be reclassified on a separate screening unit, thus producing the desired results. Whereas, cyclone underflow reclassification on fine screens could be best suited for minimal fines bypass and improvements in circuit capacity (Brodzik, 2009; Jankovic & Valery, 2013). Also, about 40 years ago Hukki (1975) postulated that a sharper separation could be realised by using a hybrid classification system in closed-grinding circuits.

1.2 Research objectives

The objectives of this study are as follows:

- Conduct plant surveys to collect data from different classification configurations comprising hydrocyclone(s) and fine wet screening technologies.
- Assess the performance of different classifiers and classification configurations which include: a two-stage hydrocyclone, an inclined hydrocyclone, a fine screen, a hybrid hydrocyclone-fine screen (2 stage) and a hybrid two hydrocyclones-fine screen (3 stage).
- Quantify the performance of different classification configurations using the efficiency curve properties by fitting the Whiten model.

1.3 Hypotheses

Hypothesis One

The application of hybrid classification configurations containing hydrocyclone(s) and fine screens will give improved classification performance than multi-stage hydrocyclone circuits because the classifier in the primary stage addresses the throughput requirements and the secondary stage rectifies the inherent imperfections of the prior stage as particle separation is not dependent on hydrodynamic principles which involves particle density to effect separation.

Hypothesis Two

Reclassification of the primary hydrocyclone underflow in a separate classifying stage will improve the classification performance of the overall circuit because the fines bypass to the recycle stream is minimised, thus providing a sharper classification. While reclassification of the hydrocyclone overflow will increase the fines bypass for the overall circuit as the fine material will have more chances of short-circuiting to the coarse streams. However, a better-quality product can be achieved as coarse particles short-circuiting to the final product are minimised.

1.4 Key questions

1. Do hybrid classification configurations containing hydrocyclone(s) and fine screens give improved classification performance, assessed by sharpness of separation, water split to coarse product and corrected cut size compared to the configurations with hydrocyclones only?
2. What is the effect of reclassifying the primary hydrocyclone underflow stream in separate classifier units on the sharpness of separation?
3. What is the effect of reclassifying the primary hydrocyclone overflow stream in separate classifier units on the quality of the final product and sharpness of separation?
4. How does the type of hybrid classification configuration influence the overall sharpness of separation, apparent bypass and size of separation?
5. What is the order of efficiency of the different classification configurations tested assessed using reduced efficiency curves?

1.5 Thesis layout

The introduction of this study has been done in the above section, discussing the background of the research, main objectives, hypotheses and key questions. Chapter two covers the literature review relevant to the subject of the study. This will be followed by chapter three, where the experimental apparatus is presented and classification circuit flowsheets considered are given indicating the sampling points. Chapter four discusses the experimental methodology followed during the survey campaigns as well as the experimental conditions and sample processing procedures. The results and discussions are presented in chapter five. Chapter six discusses the conclusions and recommendations drawn from the study.

2 CHAPTER TWO: LITERATURE REVIEW

2.1 Introduction

This chapter discusses the literature relevant to classification systems used in the mining industry. The general definition of classification processes in grinding circuits and a description of various wet classifier units used in processing plants are given. Studies focusing on the two commonly utilised wet classifiers namely, hydrocyclones and high frequency screens are reviewed. Characterisation of classification efficiency and the key properties associated with the important performance indicators are presented. The common mathematical models used to simulate performance of the hydrocyclones and high frequency screens are given focusing on how these can be used to identify key design and operating variables to consider in studies involving classification. Finally, the different circuit configurations adopted in the classification step of mineral processing plants are described.

2.2 Classification process in comminution circuits

Classification in mineral processing, as defined by Drzymala (2007), is a process of separating mixtures of mineral grains into two or more products under the ordering and disordering fields and splitting forces of a particular classifier (Figure 2-1). This process can either be done dry or wet depending on the nature of application. Dry classification usually utilises air as a carrying medium whereas water is used in wet classification. In most grinding circuits, wet classification process is applied. According to Wills and Napier-munn (2006), wet classification is applied to particles that are considered too fine (sub 200μm). As such, since this study focuses on fine slurry classification, the review of literature will focus on wet classification.

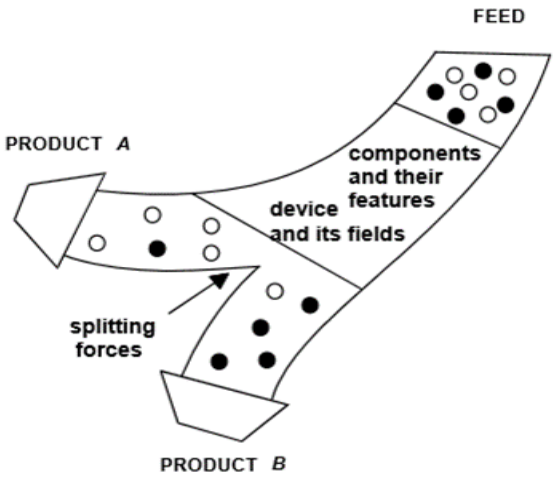

Figure 2-1: Rule of classification based on size and/or density (Drzymala, 2007)

The process of classification is essential in closing grinding circuits as it regulates the degree of grind of the ore particles to produce a product that meets the desired size for the subsequent downstream processes such as flotation and leaching (Napier-Munn et al. 2005). There are different types of wet classifiers used to carry out the function of classification. These classifiers can be categorized into three groups namely: centrifugal classifiers which uses centrifugal force to effect separation and covers a typical size range of about 10μm -100μm (Metso, 2015); physical classifiers which uses a geometrical pattern to effect separation and can separate particles from 300mm down to roughly 40μm (Wills & Napier-Munn, 2006) and gravitational classifiers which utilises the force of gravity to effect separation and covers a particle size range of about 100μm - 1000μm (Metso, 2015).

Gravitational classifiers, such as rake and spiral classifiers are mostly used for coarser wet classification. These units are simple to operate and require low energy input, but the capital cost is relatively high (Heiskanen, 1993; Wills & Napier-Munn, 2006). They also work on the same principle of separation, both taking advantage of the natural settling characteristics of the ore but differ in their application. Presently, they have limited use as classifiers and are only found in older concentrators or in some special cases (Wills & Napier-Munn, 2006). A more detailed guide to the principles of classification and images of the rake and spiral classifiers can be found in (Kelly & Spottiswood, 1982; Heiskanen, 1993; Wills & Napier-Munn, 2006).

Centrifugal classifiers and physical classifiers have gained widespread use in grinding circuits for many different types of ores. A typical example of a centrifugal classifier is the hydrocyclone

and the physical classifier is the high frequency screen (Heiskanen, 1993; Metso, 2015). The hydrocyclone and high frequency screen were used in this study and hence the review of literature is focused on these two units. The subsequent sections of this chapter mainly discuss the classification process and unit description of the hydrocyclone and high frequency screen; the classification efficiency indicators; common mathematical models, highlighting key design and operating variables that influence classification efficiency. Various circuit configurations where these classifiers are used in the grinding ore minerals are reviewed.

2.2.1 Hydrocyclone - unit and process description

Hydrocyclone, commonly referred to as cyclone, is a continuously operating classifying unit that uses centrifugal force to accelerate the settling rate of particles (Bradley, 1965). Cyclones are widely applied in closed-circuit grinding operations as classifiers for the removal of fine particles from the systems (Tarr Jr., 1985; Olson & Turner, 2002; Napier-Munn et al., 2005). Other than being used as classifiers, cyclones are also used as de-sliming, de-gritting, scalping, grading and de-watering units (Wills & Napier-Munn, 2006). Their application offers several advantages such as, ability to handle high capacity relative to unit size, low capital and operating costs compared to other classifiers on the market such as high frequency screens (Dündar et al., 2014; Mainza, 2016). However, precise particle classification is a prominent drawback encountered in convectional cyclones due to hydraulic entrainment (Mainza, 2006; Honaker et al., 2001; Mainza, 2016). The short-circuiting of fine material is more prominent in operations where the difference in specific gravity between the valuable mineral and gangue mineral is large (Gaudin, 1937; Obeng & Morrell, 2003; Mainza, Powell & Knopjes, 2004a). In such instances, the fine liberated heavier minerals tend to report to the underflow stream and the lighter middling minerals are misplaced to the overflow stream. Barrios (2006) and Barkhuysen (2009) reported that cyclones typically operate with separation efficiencies in the range of 45% to 65% and in closed-circuit grinding, the efficiency rarely surpasses 60%.

A conventional cyclone consists of a cylindrical upper section, conical lower body with a cone angle varying from 5 to 40°, a feed inlet, a spigot opening located at the apex of the conical section and a vortex finder opening at the top of the cylindrical part (Heiskanen, 1993). Figure 2-2 presents the systematic view of a conventional cyclone and the flow principal of the slurry inside the unit.

a. Conventional cyclone components

b. Flow principle of slurry inside the cyclone

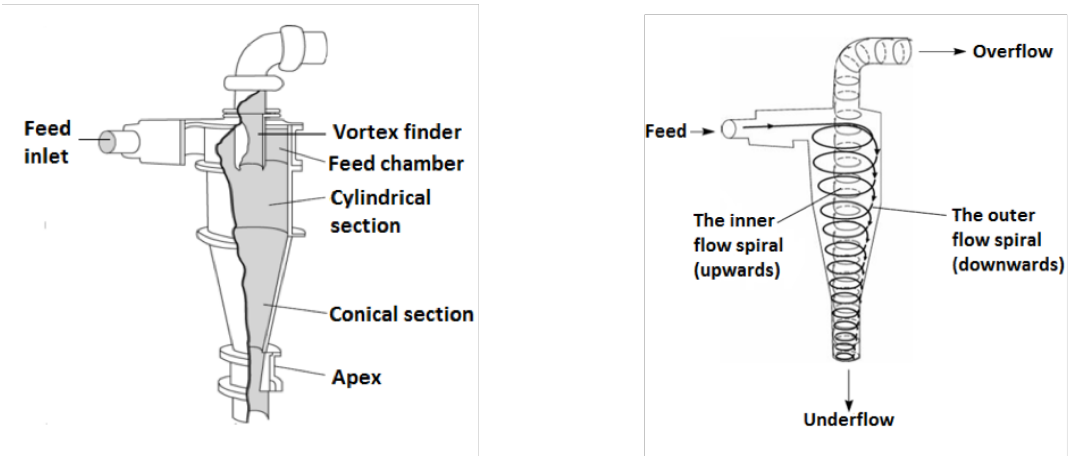

Figure 2-2: Systematic view of a conventional hydrocyclone and flow principle of slurry inside the unit (Napier-Munn et al. 2005)

During operation, the feed slurry is introduced into the cylindrical body tangentially or as an involute under pressure through the feed inlet. As the feed enters, a rotation of the slurry inside of the cyclone begins (Figure 2-2b), causing centrifugal forces to accelerate the movement of the particles towards the outer wall. The lighter particles move toward the center and spiral upward exiting through the vortex finder opening whereas the heavier particles remain in a downward spiral along the walls of the conical section and exit through the apex opening (Bradley, 1965; Arterburn, 1976; Heiskanen, 1993). The product exiting through the vortex finder is called the fines or overflow while underflow or coarse product is the term used for material exiting through the spigot opening (Mainza, Powell & Knopjes, 2004a).

The simple understanding of separation of particles inside the cyclone flow pattern is that particles are subjected to two opposing forces namely: the outward acting centrifugal force and an inward drag force (Wills & Napier-Munn, 2006). The centrifugal force developed accelerates the settling rate of the particles, thereby separating particles based on size and specific gravity (Bradley, 1965). The faster settling particles move to the walls of the cyclone, where the velocity is lowest and migrate down to the apex opening. Due to the action of the drag force, the slower-settling particles move toward the zone of low pressure along the axis and are carried upward

through the vortex finder to the overflow stream (Bradley, 1965; Svarovsky, 1984). A detailed description of the flow patterns inside the cyclone are presented in (Kelly & Spottiswood, 1982; Svarovsky, 1984; Heiskanen, 1993).

In an attempt to rectify the deficiency of conventional cyclones in closed-grinding operations, a number of component modifications to the conventional cyclones have been reported in literature (Kelsall & Holmes, 1960; Heiskanen, Vesanto & Eronen, 1987; Chu & Luo, 1994; Obeng & Morrell, 2003; Rong & Napier-Munn, 2003; Mainza, Powell & Knopjes, 2004b; Mainza, 2006; Farghaly et al., 2010). Most of the modified cyclones developed have demonstrated reduced fines bypass and improved the separation efficiency. But, some of these units have not yet found wide application in the mineral processing industry due to practical limitations related to control and unstable operations. Some of the modified cyclone designs commonly reported in literature are water injected cyclone, twin vortex cyclone, flat bottom cyclone and three-product cyclone.

The water injected cyclone is like the conventional cyclone, the only difference is that the lower part of the cyclone cone consists of nozzles through which water is injected as shown in Figure 2-3. This cyclone is designed to improve the flow dynamics of the slurry inside the cyclone by disrupting the boundary layer to minimise the misplacement of fine particles in the underflow stream (Kelsall & Holmes, 1960; Honaker et al., 2001; Bhaskar et al., 2004; Farghaly et al., 2010). However, Honaker et al., (2001) suggest that the size of benefit in fines bypass reduction is subject to the geometrical parameters of the conventional cyclone. Furthermore, Heiskanen et al. (1987) and Farghaly et al. (2010) noticed that water-injected cyclones are limited to coarser size separations; sensitive to variations in feed conditions; and the addition of water at the apex disrupts the cyclone flow, thus can easily deteriorate separation.

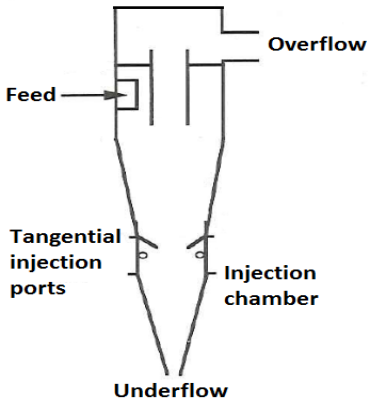

Figure 2-3: Schematic showing a water injected cyclone and the key components, adapted from (Kelsall & Holmes 1960)

The Twin Vortex cyclone is a combination cyclone with two separate stages. The primary part operates as a conventional cyclone but the conical section is replaced with a cylindrical part having a larger diameter then the cyclone main body as shown in Figure 2-4. The cylindrical part has a centrical adjustable cone and tangential water injection ports. The coarse product of the primary cyclone is diluted with additional water and leaves tangentially from the side of the washing section to a conventional secondary cyclone (Heiskanen, 1993). Heiskanen et al. (1987) performed comparison test between the Twin Vortex cyclone and conventional cyclone based on pilot plant using different test materials and industrial scale using apatite-mica slurry. They found that the bypass flow of fines to underflow was reduced, with the coarse product containing less fines than a conventional cyclone. Unlike the water injected cyclone, a finer cut size was also achieved in the Twin Vortex finder.

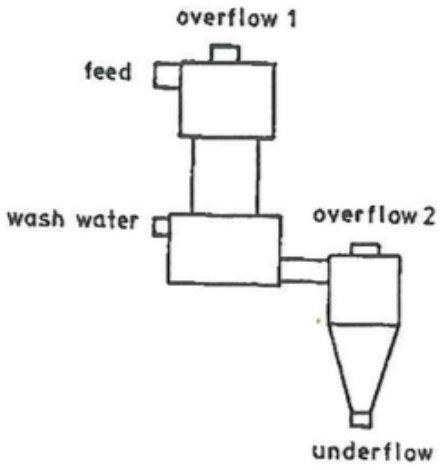

Figure 2-4: Schematic view of the Twin Vortex cyclone (Heiskanen et al. 1987)

The flat bottom cyclone also has similar features as the conventional cyclone, the main differences lies in the length of the cylindrical section and the cone angle (Heiskanen, 1993; Mainza, Powell & Knopjes, 2004b). Normally, the flat bottom cyclone has a longer cylindrical part with wider cone angle ranging from 120° to 180° (Heiskanen, 1993) as shown in Figure 2-5. However, in some flat bottom cyclone designs, the conical part is completely absent (Trawinski, 1980; Gupta & Yan, 2006). Mainza et al. (2004b) performed comparison tests on different cyclone designs and they found that employing a flat bottom cyclone gave a coarser separation than the conventional cyclone.

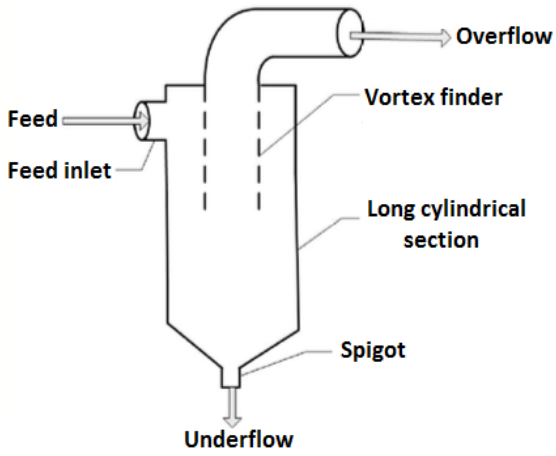

Figure 2-5: Schematic showing a flat bottom cyclone and the key components adapted from (Mainza et al. 2004)

The three-product cyclone has two overflow streams instead of one as is with the conventional cyclone (Obeng & Morrell, 2003; Mainza, Powell & Knopjes, 2004a; Mainza, 2006; Ibrahim & Ahmed, 2007) as shown in Figure 2-6. The conventional vortex finder is the outer vortex finder in the three-product cyclone whereas, the inner vortex finder is the additional vortex finder (Mainza, Powell & Knopjes, 2004a). The three-product cyclone is designed to minimise the dense media effect (Obeng & Morrell, 2003). Mainza (2006) conducted tests using a 600mm diameter three-product cyclone fed with a dual-density ore. The results showed that the fraction of the middling particles misdirected to the final fines product and the fines bypass reduced because they reported to the additional overflow product, which could be screened to recover the fines and returned the middling material to the mill for further size reduction.

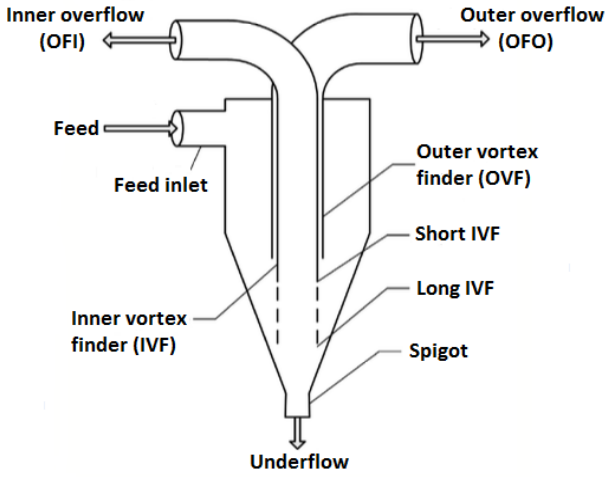

Figure 2-6: Schematics showing a three-product cyclone and the various parts (Mainza et al. 2004)

Hydrocyclones in processing plants can be installed on simple supports either as single units or clusters (Heiskanen, 1993). In closed-circuit grinding operations, small cyclones are preferred as they are said to achieve finer separation (Tarr Jr., 1985; Wills & Napier-Munn, 2006) and to meet the capacity required, the cyclones are connected in parallel to form clusters (Figure 2-7). Whereas, in instances where the efficiency of classification needs to be improved cyclones are connected in series to reclassify the overflow, underflow or both streams (Kelsall, Stewart & Restarick, 1974; Hukki & Heiskanen, 1981; Rogers et al., 1981; Peterson & Herbst, 1984;

Dahlstrom & Kam, 1988; Heiskanen, 1993; Firth & O'Brien, 2003; Napier-Munn et al., 2005; Honaker, Boaten & Luttrell, 2007). Some common circuit configurations comprising of cyclones adopted in most concentrators around the world are presented in section 2.6.

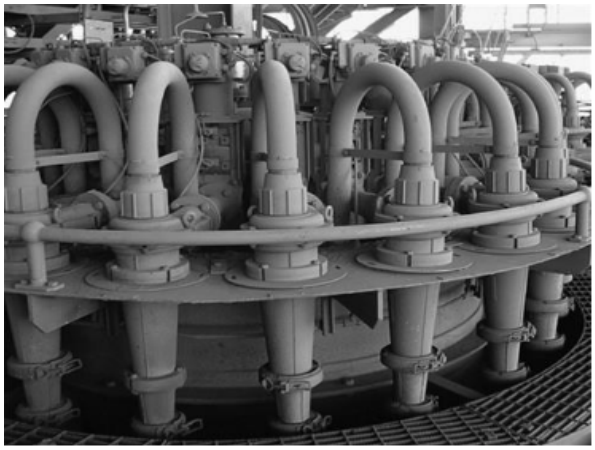

Figure 2-7: A cluster of hydrocyclones (Wills & Napier-Munn 2006)

2.2.2 Fine screen – unit and process description

Industrial screening is defined as a mechanical process which uses a barrier to achieve separation of particles on the basis of size (Matthew, 1985). Particles are presented to the screening surface and are retained if larger than the opening or pass through if smaller. There are different types of screening units in the minerals industry. The choice is dependent on the screening objective such as classifying, scalping, grading, media recovery, de-watering, de-sliming or de-dusting and trash removal (Wills & Napier-Munn, 2006). Screening can be classified into two groups namely; coarse screening, size separation at 4.75mm and above; and fine screening, size separation smaller than 4.75mm and larger than 300µm (Matthew, 1985), though with recent advances in fine screening, separation can be done as low as 40µm (Wills & Napier-Munn, 2006).

Generally, fine screening is accomplished with high frequency, low amplitude vibrating screens using either straight-line or elliptical motion (Pryor, 1965; Wills & Napier-Munn, 2006). This process can be done either dry or wet depending on the ore type, target size to be separated and capacity. Gaudin (1937) and Gupta and Yan (2006) commends that dry screening can be done up to about 75µm while, wet screening up to about 40µm (Wills & Napier-Munn, 2006). High frequency screens sometimes referred to as fine screens are used to perform the function of fine

screening. These units are widely used in closed-circuit grinding operations for size control as classifiers (Matthew, 1985).

In wet screening, particles are fed to the screen as slurry. The particles smaller than the screen aperture size are carried through with the fluid forming the undersize product while, those larger than the screen opening are retained on the screen surface forming the oversize product (Drzymala, 2007) as shown in Figure 2-8. The addition of water plays a significant role in the screening processing. The screen efficiency decrease rapidly once the free water has been removed (Valine, Wheeler & Albuquerque, 2009). Normally, the fine screens are equipped with spray nozzles for re-pulping to achieve maximum removal of fine particles from the oversize material (Brodzik, 2009; Mainza, 2016)

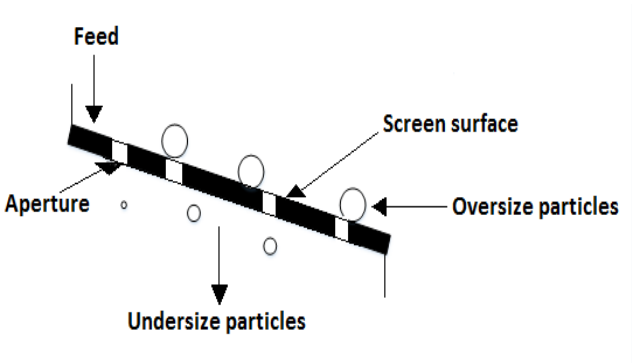

Figure 2-8: Particle size classification on screen classifiers adapted from (Drzymala, 2007)

The process of stratification in wet screening operations is not as important as in dry screening because the process is negated for most parts by wetness and adhesiveness of the material (Matthew, 1985). Nonetheless, in dry screening stratification is a crucial factor that contributes to the effectiveness of classification (Wills & Napier-Munn, 2006). During stratification, material bed is built up on the screen surface and particles stratify with the motion of the screening, reducing the internal friction in the particles. This allows finer particles to pass between coarser particles providing a sharper separation (Napier-Munn et al., 2005). It has been found that stratification tends to increase the rate of particle passage in the middle section of the screen (Soldinger, 1999). Figure 2-9 illustrates the process of stratification on a screen with the middle section presenting a high rate of fine particle passage

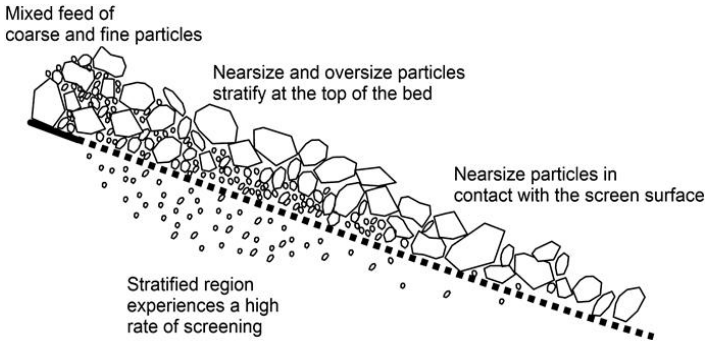

Figure 2-9: Stratification of particles on a screen during dry screening **(Napier-Munn et al., 2005)**

Generally, screens are considered to be 'perfect' classifiers as particle separation is independent of density and based on size only, thus providing a sharper cut at the desired size (Valine & Wennen, 2002; Albuquerque et al., 2008). Normally, a sharper separation is as a result of reduced circulating load, which in turn leads to increased circuit capacity (Mainza, 2016). Several authors have reported case studies demonstrating the benefits of closing grinding circuits with fine screens (Albuquerque et al., 2008; Valine, Wheeler & Albuquerque, 2009; Dündar et al., 2014; Mainza, 2016). In industrial practices, the fine screens are stacked one above the other and operate in parallel in an effort to increase capacity at relatively small footprints (Valine et al. 2009). The screen configuration employed in closed-circuit grinding operations is presented in section 2.6. Even though screens are efficient at size control, they usually suffer from aperture blinding. This problem tends to become more persistent as the aperture size decreases and results in capacity reduction (Dündar et al., 2014; Mainza, 2016).

2.3 Efficiency curves

Tromp (1937) first developed a graphical method of assessing and comparing the performance of a classifier, referred to as tromp curve or efficiency curve or performance curve or partition curve. The efficiency curve relates the weight fraction of each size fraction of the solid in the feed which reports to the coarse or fine product. Either of the two curves can be used, as one curve is the reverse of the other (Napier-Munn et al. 2005). Much of the literature utilises the curve to the coarse product and thus, has been adopted in this work.

According to Gupta and Yan (2006), an efficiency curve can be obtained from performing a mass balance around the classifier in operation by size analysis of the feed, coarse and fine product as shown in Figure 2-10.

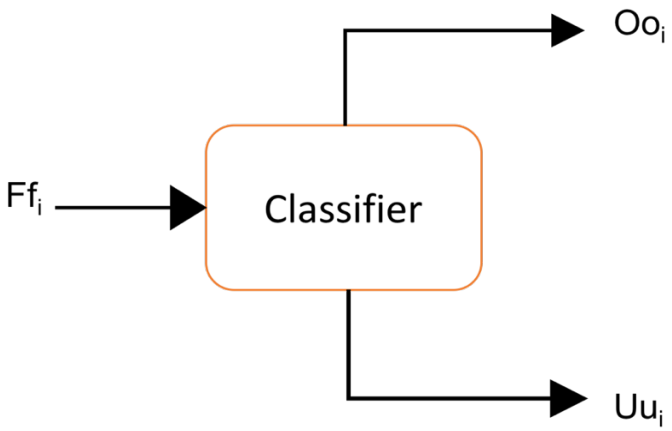

Figure 2-10: Mass balance around a solid-liquid classifier

From the mass balance, Equation 2-1 can be formulated to give the efficiency number of the particle size class i to the coarse product by relating the mass flowrates of coarse and feed fractions.

$$E_{ui} = \frac{Uu_i}{Ff_i}$$

Equation 2-1

Where; F and U are the mass flow rate of solids (t/h), f_i and u_i are the weight fractions of particle size i in the feed and coarse product streams, respectively.

The efficiency number can also be calculated from the particle size data using the two-product formula given in Equation 2-2. Napier-Munn et al., (2005) argues that the two-product formula can be used to estimate the mass split to either products of a classifier. According to Heiskanen (1993) Equation 2-1 and Equation 2-2 very rarely give the same result due to sampling errors.

$$E_{ui} = \frac{u_i(f_i - o_i)}{f_i(u_i - o_i)}$$

Equation 2-2

Where; o_i is the weight fractions of particle size i in the fine product streams.

The efficiency number is plotted against the geometric mean size of the particle size class to produce the uncorrected or actual efficiency curve shown in Figure 2-11. Generally, the actual curve does not pass through the origin but rather approaches some constant value called bypass (Rogers, 1982; Tarr Jr., 1985; Mainza, 2006; Narasimha et al., 2014). Bypass is defined as an assumed value resulting from the misplacement of fine particles that do not respond to classification forces and follow the feed water flow to the coarse product (Kelsall, 1953). Kelsall (1953), suggested that bypass is directly proportional to the amount of water in the feed reporting to the underflow product. Kelsall's general assumption has been questioned by some researchers. Frachon and Cilliers (1999) studied the effect of fish-hook on a 10mm diameter cyclone and observed that the apparent bypass value was notably higher than the fraction of water recovered to the underflow. They commend that in small diameter cyclones, the bypass fraction consists of the misplaced fines recovered in proportion to water and an additional fraction possibly due to boundary layer flows directly to the underflow unlike, in the large cyclones were the effect of the boundary layer could be negligible. Similar observations were reported by Kilavuz and Gülsoy (2011) who studied the effect of cone ratio on the performance of a 25.4mm and 50.8mm diameter cyclone. However, Kelsall's assumption is still widely used as it leads to Equation 2-3 used to describe the corrected and reduced efficiency curve, giving a reasonably precise correction for the cut size (Napier-Munn et al., 2005).

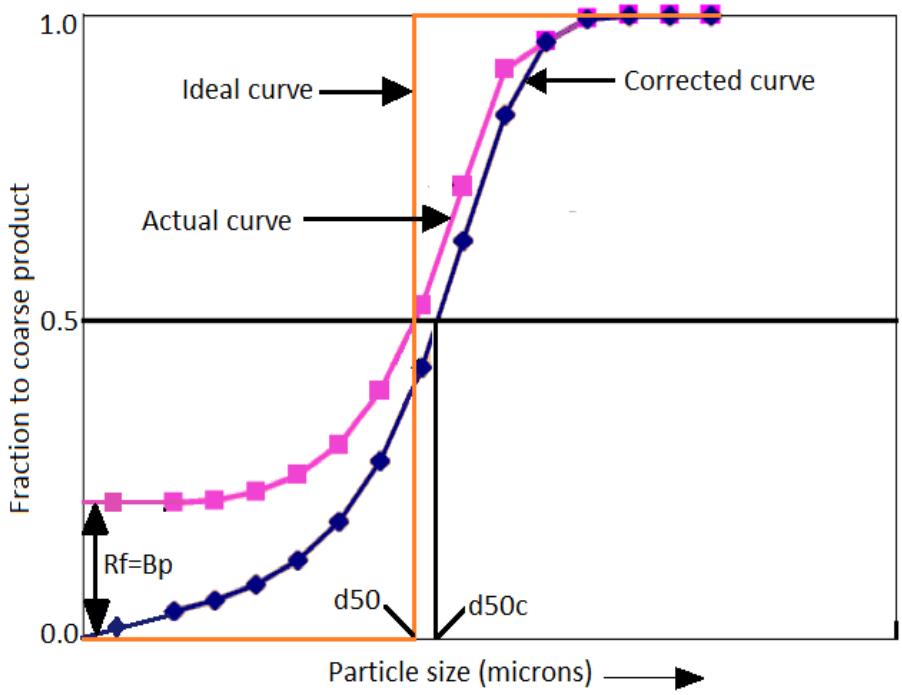

Figure 2-11: Uncorrected and corrected efficiency curves adapted from (Wills & Napier-munn, 2006)

By adjusting each actual efficiency number by an amount equal to the feed water recovered to the coarse product using Equation 2-3, also referred to as Kelsall's formula, the corrected partition number is obtained (Gupta & Yan, 2006). The corrected partition numbers are plotted against the geometric mean size to produce the corrected curve illustrated in Figure 2-11.

$$C_{(i)} = \frac{E_{(i)} - R_f}{1 - R_f}$$

Equation 2-3

Where; $C_{(i)}$ is corrected efficiency to the coarse product, $E_{(i)}$ is the actual (uncorrected) efficiency to the coarse product and R_f is the feed water fraction recovered to the coarse product stream

The corrected efficiency curve can then be normalised by dividing the size axis by the cut size (d_{50c}), making the size axis non-dimensional to form a reduced efficiency curve (Figure 2-12).

The reduced efficiency curve is generally constant for a classifier design and stabilised on bypass and feed size The independency of this curve allows useful empirical models to be formulated (Napier-Munn et al., 2005). Some of the most common empirical models using the exponential form of the reduced efficiency curve have been described in section 2.4.

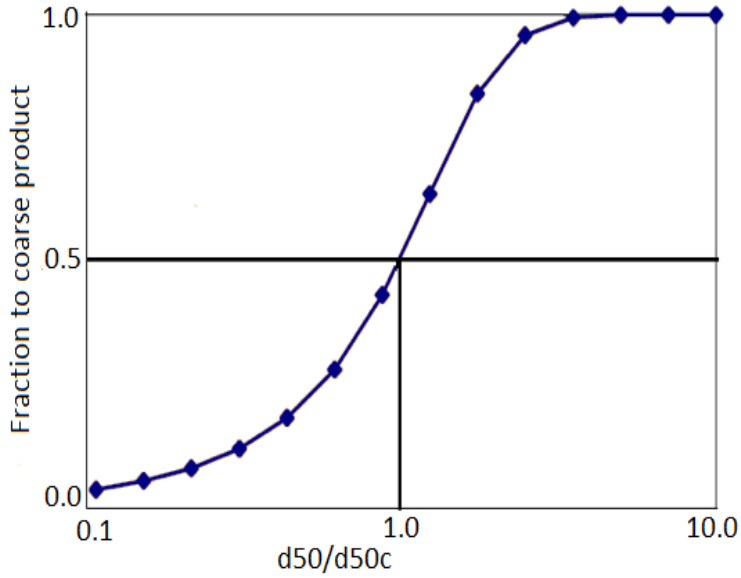

Figure 2-12 Reduced efficiency curve adapted from (Gupta & Yan, 2006)

Whiten (1966) developed a non-linear mathematical model for the reduced curves to the coarse product (Equation 2-4). He later (1996) modified the equation to accommodate the fish-hook effect by introducing a β parameter as shown in Equation 2-5 (Napier-Munn et al., 2005). According to Del villar and Finch, (1992), the fishhook effect is one of the unusual characteristic of a partition curve observed at finer size range. The causes of the fish-hook effect are less clear, even though a number of possible causes attributing to effect have been proposed and reviewed in literature (Laplante & Finch, 1984; Bourgeois & Majumder, 2013; Nageswararao, 2014).

The Whiten efficiency model (Equation 2-4) will be used in this study to fit the experimental data and extract sharpness of separation(α), corrected cut size (d_{50c}) and water split (R_f) values. In cases where the fish-hook effect is observed, β values will also be fitted using Equation 2-5. Note that Equation 2-5 reduces to Equation 2-4, when β is set to zero and β^* to one.

$$C_{(i)} = \frac{\exp(\alpha x) - 1}{\exp(\alpha x) + \exp(\alpha) - 2}$$

Equation 2-4

$$P_{(i)} = C\left\{\frac{(1 + \beta\beta^{*}x)[\exp(\alpha) - 1]}{\exp(\alpha\beta^{*}x) + \exp(\alpha) - 2}\right\}$$

Equation 2-5

Where; $P_{(i)}$ is uncorrected efficiency number of particle size i to the fines product, x is the reduced size (d/d_{50c}), α is sharpness of separation, C is ($1-R_f$), β is a parameter controlling the initial rise at fines and β^{*} can be calculated iteratively.

2.3.1 Efficiency curve properties

The efficiency curve has three key properties used to measure the performance of classifiers. These properties are: corrected cut size ($d50_c$); sharpness of separation (α) and water recovery to the coarse product (R_f). Each property is described below.

Cut size (d_{50})

Cut size, sometimes referred to as classification size is defined as the size for which 50% of the particles in the feed report to the coarse stream, implying that, particles of this size have an equal opportunity to either report with the coarse or fine stream (Svarovsky & Thew, 1992). The cut size (d_{50}) obtained from actual efficiency curve shows the raw operational behavior of the classifier or classification system as it accounts for the bypass effect while the corrected cut size (d_{50c}) is derived from the corrected curve and does not consider bypasses (Heiskanen, 1993). In cyclone operations, cut size is selected based on the process requirements such as the liberation size of the valuable mineral contained in the ore and the solid concentration in the final product to meet the specifications of the subsequent process (Napier-Munn et al., 2005). The required cut size is defined by the selection of the cyclone diameter (Bradley, 1965). Once the diameter has been established, performance can then be improved by changing the apex/spigot and vortex finder openings (Napier-Munn et al., 2005). Whereas, in industrial screen operations cut size is

normally defined by the selection of the aperture size (Wills & Napier-Munn, 2006). The required screen cut size is always less than the selected aperture size and thus, the closer the obtained cut size value to the aperture size, the more efficient is the separation process (Wills & Napier-Munn, 2006; Mabote, 2016).

Sharpness of separation (α)

This is the measure of degree of misplaced particles that ideally should have been in the fine stream but ended up in the coarse and vice versa (Gupta & Yan, 2006). This property is assessed from the steepness of the slope of the central section of the corrected or reduced efficiency curve. The slope is vertical in the case of ideal classification as shown in Figure 2-11; the closer the slope to the vertical, the higher the value of α and the greater the classification efficiency (Wills & Napier-Munn, 2006). Napier-Munn et al. (2005), suggests that one way of maximising α is to minimise the entrainment of fines in the coarse product stream. Most hydrocyclones have the values of α lying in the range of 1.5 to 3.5 (Napier-Munn et al., 2005), and those in a closed-circuit grinding operations have typical values of up to about 2.5 (Tarr Jr., 1985; Gupta & Yan, 2006). The values of α in screen operations are normally high depending on the operational conditions. According to Napier-Munn et al. (2005), α values greater than 4 are common in screen classifiers, implying that efficient separation is normally achieved with screen classifiers.

Water split (R_f)

This is the ratio of volumetric water flow rates of the coarse stream to the feed streams (Kılavuz & Gülsoy, 2011). R_f is usually assessed from the actual efficiency curve. It is the lowest point of the actual efficiency curve (Figure 2-11) and is usually assumed to equal the fines bypass fraction (Kelsall, 1953; Plitt, 1976; Flintoff, Plitt & Turak, 1987). Therefore, the more the recovery of water to the coarse product stream, the lower the efficiency of classification and the more the recovery of water to the fines stream, the greater the efficiency (Wills & Napier-Munn, 2006; Narasimha et al., 2014). R_f can also be fitted using mathematical functions such as the Whiten model described in section 2.3. The effect of bypass is more prominent in conventional cyclone operations treating complex ores such as a dual-density ore (Mainza, Powell & Knopjes, 2004a). Bypass fractions of 0.2 to 0.5 are common for cyclones in closed-circuit grinding operations (Rogers et al., 1981). In, screen operations the bypass fraction is usually low provided

they are running at optimum conditions. Low bypass translates to reduction in circulating load, thus resulting in improved circuit capacity (Valine, Wheeler & Albuquerque, 2009; Dündar et al., 2014; Mainza, 2016).

2.4 Mathematical models – hydrocyclone and fine screen

2.4.1 Hydrocyclone models

Several functions used to predict the performance of cyclones have been derived over the past four decades. These models usually estimate the key relationships between operating and design variables for use in design and optimization purposes (Napier-Munn et al., 2005). The most common type of functions are the empirical models, which are based on regression equations derived from experimental data (Heiskanen, 1993; Wills & Napier-Munn, 2006). Narasimha et al. (2014) urges that these empirical models are limited to the range of conditions used during the derivations and cannot be used outside those ranges. More recently, computational fluid dynamic (CFD) technique has gained tremendous recognition in modelling technology (Narasimha et al., 2014; Vakamalla et al. 2014). This advancement has allowed the usage of appropriate turbulence and multi-phase models to assist in the performance predictions, since the flow inside the cyclone is very complex and turbulent in nature (Wills & Napier-Munn, 2006). The most recent semi-mechanistic model known as the Narasimha/Mainza model was developed by Narasimha and Mainza (Narasimha et al., 2014) and has been described herein, together with the other models used to simulate the performance of cyclones. These models have been discussed with a view to highlighting the variables that affect performance of cyclones. Only the most commonly used models have been reviewed and the most recent model is added to show that even in modern studies similar variables are considered. The effects of the design and operation variables on the performance of cyclones are discussed in section 2.5.

Lynch/ Rao Model (1975)

This was the earliest cyclone model to found wide application in the industry. Lynch and Rao derived empirical functions for a wide range of cyclones using limestone ore described in Lynch (1977). The model shows the relationship between the key performance measures such as cut

size, water split and factors such as cyclone geometry, flowrate and feed solid concentration. The following relationships were established;

$$\log_{10} d_{50c} = K_1 . D_o - K_2 D_u + K_3 D_i + K_4 C_w + K_5 Q_f + K_6$$

Equation 2-6

$$Q_f = K . D_o^{0.73} D_i^{0.86} P^{0.42}$$

K = 6 for limestone

Equation 2-7

$$R_f = K_1 . \frac{D_u}{WF} - \frac{K_2}{WF} + K_3$$

K_1 = 193, K_2 = 271.6, K_3 = 1.61

Equation 2-8

Where; D_o, D_u, D_i are vortex finder, apex and inlet diameters (m) respectively, C_w is feed % solids (wt.), Q_f is feed flowrate (t/h), K_1- K_6 are empirical constants, P is pressure drop (Pa), R_f is water split to underflow (%), WF is mass flowrate of water in feed (t/h).

The authors commended that the model constants can be changed depending on the ore type to be used. However, they did not include the alpha model which is a key performance indicator. Moreover, feed characteristics such as slurry viscosity was not incorporated in their model which is a crucial factor that influences the performance of the cyclone.

Plitt Model (1976)

Plitt model is a semi-empirical model based on experimental results determined from a large database compiled by Plitt from different cyclone sizes ranging from 32mm to 150mm and Lynch and Rao (1976) from cyclone sizes ranging from 150mm to 500mm. The model was

derived to make a complete particle separation process prediction. The equations derived to describe the key performance indicators are presented below;

$$d_{50c} = \frac{F_1 39.7 D_c^{0.46} D_i^{0.6} D_o^{1.21} \mu^{0.5} \exp(0.063 C_v)}{D_u^{0.71} H^{0.38} Q_f^{0.45} \left[\frac{\rho_s - 1}{1.6}\right]^k}$$

Equation 2-9

$$m = F_2 1.94 \left(\frac{D_c^2 H}{Q_f}\right)^{0.15} \exp\left[-\left(\frac{1.58\, R_f}{1 + R_f}\right)\right]$$

Equation 2-10

$$P = \frac{F_3 1.88\, Q_f^{1.8} \exp(0.0055 C_v)}{D_c^{0.37} D_i^{0.94} h^{0.28} (D_u^2 + D_o^2)^{0.87}}$$

Equation 2-11

$$R_f = \frac{F_4 3.29 \rho_p^{0.24} (D_u/D_o)^{3.31} H^{0.54} (D_u^2 + D_o^2)^{0.36} \exp(0.0054 C_v)}{D_c^{1.11} P^{0.24}}$$

Equation 2-12

Where; D_c is cyclone diameter (m), μ is liquid viscosity, C_v is feed % solids (vol.), H is distance between apex and end of vortex finder (m), k is hydrodynamic exponent estimated from the data, m is the efficiency exponent - sharpness of separation, ρ_P is feed slurry density (Kg/m^3) and F_1 – F_4 are empirical constants

Plitt's corrected cut size model incorporates a liquid viscosity term, solid volume concentration and the hydrodynamic exponent. It also considers the feed size effects denoted by the constant F_1. The throughput model included also the effect of solid concentration and feed size (F_3), while the flow split model included the effects of pulp density as well as size feed (F_4). However,

this model does not take into account the fish-hook effect because it depends on the Plitt/Reid function to represent the efficiency curve. Also, according to Napier-Munn et al. (2005) the model does not hold for wide variations in feed particle size.

Nageswararao Model (1995)

This model is a modified form of the Plitt model (1976), consisting of empirical functions for the key performance measures. The model includes terms suggested by dimensional analysis with exponents estimated from a large database obtained by Nageswararao (1978) and Rao (Lynch & Rao, 1975b) using limestone on 102 to 381mm diameter cyclones.

$$\frac{d_{50c}}{D_c} = K_{D1}\left(\frac{D_o}{D_c}\right)^{0.52}\left(\frac{D_u}{D_c}\right)^{-0.47}\lambda^{0.93}\left(\frac{P}{\rho_p g D_c}\right)^{-0.22}\left(\frac{D_i}{D_c}\right)^{-0.5}\left(\frac{L_c}{D_c}\right)^{0.2}\theta^{0.15}$$

Equation 2-13

$$Q_f = K_{Q1}D_c^2\left(\frac{P}{\rho_p}\right)^{0.5}\left(\frac{D_o}{D_c}\right)^{0.68}\left(\frac{D_i}{D_c}\right)^{0.45}\theta^{-0.1}\left(\frac{L_c}{D_c}\right)^{0.2}$$

Equation 2-14

$$R_f = K_{W1}\left(\frac{D_o}{D_c}\right)^{-1.19}\left(\frac{D_u}{D_c}\right)^{2.40}\left(\frac{P}{\rho_p g D_c}\right)^{-0.53}\lambda^{0.27}\left(\frac{D_i}{D_c}\right)^{-0.50}\theta^{-0.24}\left(\frac{L_c}{D_c}\right)^{0.22}$$

Equation 2-15

$$R_v = K_{V1}\left(\frac{D_o}{D_c}\right)^{-0.94}\left(\frac{D_u}{D_c}\right)^{1.83}\left(\frac{P}{\rho_p g D_c}\right)^{-0.31}\left(\frac{D_i}{D_c}\right)^{-0.25}\theta^{-0.24}\left(\frac{L_c}{D_c}\right)^{0.22}$$

Equation 2-16

Where; $K_{D1} = K_{DO}D_c^{-0.65}$, $K_{Q1} = K_{QO}D_c^{-0.1}$, L_c *is cyclone cylindrical section (m),* Θ *is cone angle, g is acceleration due to gravity (9.81 m/s*^{2}*),* R_v *is volumetric recovery of feed slurry to underflow (%),* K_{D1}, K_{W1}, K_{V1} *are constants estimated from data and* λ *is hindered settling correction term.*

Nageswararao considered the pulp density to be a crucial input in all the functions that he derived as well as the feed material constants. He also incorporated a hindered settling factor to account for the feed solids concentrations effects based on the expression suggested by Steinour in 1944 in his cut size and water split models besides the geometrical factors. Nonetheless, the model does not take into account the other factors such as liquid viscosity and particle size which also has a significant effect on slurry viscosity other than the pulp density and hindered settling correction term.

Asomah Model (1997)

This is the first empirical model developed to incorporate the angle of inclination in its functions alongside slurry viscosity, feed size and other design and operating variables of the cyclone. It is also the first model to derive a function that could predict the sharpness of separation (α). However, the model requires many inputs to extract the efficiency parameters. The following relationships have been derived to predict the corrected cut size, separation quality, water recovery to the underflow and the pressure flowrate;

$$d_{50c} = D_c^{0.229}\left[\frac{P_{40}}{D_o}\right]^{-0.457}\left[\frac{D_o}{D_u}\right]^{0.948}\left(1 - V_s^{(1-\theta/180)}\right)^{-2.941}(Re)^{-0.155}(\theta)^{0.719} \times \exp\left[-1.392\frac{i}{180}\right].B1$$

Equation 2-17

$$\alpha = D_c^{-0.148}\left[\frac{D_o}{D_c}\right]^{1.046}\left[\frac{D_u}{D_c}\right]^{-0.161}\left[\frac{\mu_p}{\mu_w}\right]^{-0.854}\left[\frac{\rho_s-\rho_l}{\rho_s}\right]^{-2.182}(Re)^{-0.107}(\theta)^{0.429} \times\exp\left[-0.094\frac{i}{180}\right].B2$$

Equation 2-18

$$R_f = D_c^{0.471}\left[\frac{P_{40}}{D_o}\right]^{0.214}(1-V_s)^{-0.825}\left[\frac{D_o}{D_u}\right]^{-1.806}\left[\frac{L_c}{D_c}\right]^{0.287}(Re)^{-0.175}(\theta)^{-0.478} \times\exp\left[-1.357\frac{i}{180}\right]B3$$

Equation 2-19

$$Q_f = D_c^{0.739}\left[\frac{(D_i.D_o)^{-1.538}.(L_c)^{0.455}.P}{\rho_p.(1-V_s)^{0.435}.(\theta)^{0.246}.\exp\left(-0.113.\frac{i}{180}\right)}\right]^{0.50}.B4$$

Equation 2-20

Where; P_{40} is size 40% feed material passing (cm), V_s is feed volume fraction of solids, Re is the Reynolds number, μ_p is pulp viscosity, μ_w is water viscosity, i is inclination angle, ρ_s and ρ_l are solid and liquid density (Kg/m^3), B1 – B4 are empirical constants.

Narasimha/ Mainza Model (2014)

This Narasimha/ Mainza model is the most recent semi-mechanistic model developed using dimensionless approach based on both the fluid mechanics concepts from Computational Fluid Dynamics simulations and a wide range of industrial cyclone performance data. The separation performance predications of cyclones have been improved, as parameters responsible for fluid and particle flow characteristics such as slurry viscosity are included in the model, besides other key design and operating variables. The following are the relationships derived to predict the key performance measures.

$$\frac{d_{50c}}{D_c} = k_d \left(\frac{D_o}{D_c}\right)^{1.093} \left(\frac{D_u}{D_c}\right)^{-1.00} \left(\frac{(1-fv)^2}{10^{1.82*fv}}\right)^{-0.703} (Re)^{-0.436} \left(\frac{D_i}{D_c}\right)^{-0.936} \times \left(\frac{L_c}{D_c}\right)^{0.187} \left(\frac{1}{Tan(\theta)}\right)^{-0.1988} \left(Cos\left(\frac{i}{2}\right)\right)^{-1.034} \left(\frac{\rho_s - \rho_l}{\rho_l}\right)^{-0.217}$$

Equation 2-21

$$R_f = K_w \left(\frac{D_o}{D_c}\right)^{-1.06787} \left(\frac{D_u}{D_c}\right)^{2.2062} \left(\frac{V_t^2}{R_{max}g}\right)^{-0.20472} \left(\frac{1}{\tan\left(\frac{\theta}{2}\right)}\right)^{0.829} \left(\frac{\mu_p}{\mu_w}\right)^{-0.7118} \times \left(\frac{L_c}{D_c}\right)^{2.424} \left(\frac{V_h}{V_t}\right)^{-0.8843} \left(\frac{(\rho_s - \rho_l)}{\rho_l}\right)^{0.523} \left(Cos\left(\frac{i}{2}\right)\right)^{1.793}$$

Equation 2-22

$$\alpha = K_\alpha \frac{\left(\frac{D_o}{D_c}\right)^{0.27} \left(\frac{V_t^2}{R_{max}g}\right)^{0.016} \left(Cos\left(\frac{i}{180}\right)\right)^{0.868} \left(\left(\frac{(1-fv)^2}{10^{1.82*fv}}\right)^{0.72}\right)}{\left(\frac{D_u}{D_c}\right)^{0.567} \left(\frac{(\rho_s - \rho_p)}{\rho_s}\right)^{1.837} \left(\frac{\mu_p}{\mu_w}\right)^{0.127} \left(\frac{1}{\tan\left(\frac{\theta}{2}\right)}\right)^{0.182} \left(\frac{L_c}{D_c}\right)^{0.2}}$$

Equation 2-23

$$Q_f = K_{QO} \left(\frac{D_i}{D_c}\right)^{0.45} D_c^2 \sqrt{\frac{\rho}{\rho_p}} \left(\frac{D_o}{D_c}\right)^{1.099} \left(\frac{D_u}{D_c}\right)^{0.037} \left(\frac{1}{\tan\left(\frac{\theta}{2}\right)}\right)^{0.405} \left(\frac{L_c}{D_c}\right)^{0.30} \times \left(\frac{V_h}{V_t}\right)^{-0.048} \left(Cos\left(\frac{i}{2}\right)\right)^{-0.092}$$

Equation 2-24

Where; D_o, D_u, D_i are vortex finder, apex and inlet diameters (m) respectively, L_c is cyclone cylindrical section (m), Θ is cone angle, Q_f is feed flowrate (t/h), R_f is water split to underflow, fv is feed volume fraction of solids, α is sharpness of separation, g is acceleration due to gravity,

Re is the Reynolds number, i is inclination angle, μ_p is pulp viscosity, μ_w is water viscosity , ρ_s is solid density and ρ_l is liquid (Kg/m^3), V_h is the particle hindered settling velocity, V_t is terminal velocity, and K_d, K_w, K_α, K_{QO} are constants fitted to each data set.

The advantage of this model is that it can predict the performance of cyclones regardless of the orientation and can be used outside the range of conditions it was developed. The model also illustrates that the same design and operating variables used 40 years ago have been utilised in the derivation of this model, with the inclusion of slurry viscosity and inclination angle. This model has been incorporated in the JKSimMet computer simulator.

2.4.2 Fine screen models

The screen models published in literature can be categorized into four classes which include; probability models - which incorporate the likelihood of a particle passing through the screening surface, kinetic models - which assume that screening is defined by a rate process of a particular order, empirical models – which is based on regression equations derived from experimental data to simulate the partition curve and capacity models- which are used by equipment suppliers in specifying screen design for a particular application (Napier-Munn et al., 2005).

Several authors have used kinetic and/or probabilistic methods to derive the models (Ferrara, Preti & Schena, 1987; Subasinghe, Schaap & Kelly, 1989) and are usually developed for dry and coarse screening greater than 2mm (Ferrara, Preti & Schena, 1987; Subasinghe, Schaap & Kelly, 1989; Trumic & Magdalinovic, 2011). This study is focused on fine wet screening thus; the review is more concerted on fine screen models. More recently, fine screen models have been developed by Mwale (2015) and by Mabote (2016).

Mwale Fine Screen Model (2015)

Mwale (2015), derived a semi-empirical model capable of predicting the performance of a screen as fine as 45μm. The model was based on experimental data compiled by the author from pilot plant tests conducted on a single deck fine screen over a wide range of conditions. The model describes the efficiency curve to the oversize and consists of two terms. The first term describes the efficiency curve when no fish-hook effect is observed and the second term is included, whenever a fish-hook is seen at the finer sizes. The following relationships between the key

efficiency indicators and screen dimensions, and feed conditions such as flowrate, viscosity and solid concentration are presented below;

$$E_i = 100\exp\left[-\frac{f_o K}{Q_f C_w \left(\frac{i}{A}\right)^{\alpha}}\right] + \frac{\beta Q_f}{1 - C_w}\left[\exp\left(-\frac{x}{A}\right)\right]^{\alpha}$$

Equation 2-25

$$\alpha = \left[\frac{F_1\left(\frac{\rho_p^2 Q_f f_o^{2.5}}{\mu M_o^2}\right)}{A^2}\right] f_o$$

Equation 2-26

$$d_{50c} = F_2\left(\frac{\rho_p^2 A Q_f f_o^{2.5}}{\mu M_o^2}\right) + F_3 A$$

Equation 2-27

Where; A is screen aperture (μm), x is particle size, f_o is open area (m^2), K is the kinetic constant ($t/h.m^2$), M_o is the mass flow of fine particles in the feed, F_1, F_2, and F_3 are constants fitted to the data set.

The Mwale model includes the effect of slurry viscosity in both his alpha and cut size models as well as feed material constants. Also, the influence of fractional open area and the screen aperture sizes are incorporated. This model was recently developed, hence has not yet been widely applied in industry. Nonetheless, the model was validated using data that was used in the derivation. Therefore, studies to validate the capability of model to simulate performance outside the range of conditions the model was originally derived has not yet been tested

Mabote Fine Screen Model

Mabote (2016) used the two-parameter Whiten screen model (Equation 2-28) as a basis of modelling jointly, with the experimental data obtained from tests conducted on the fine screen at various feed conditions.

$$E(x) = exp\left[-Nf_o\left(1-\frac{x}{A}\right)^{\sigma}\right]$$

Equation 2-28

Where; E(x) is the fraction of particle x in the feed that reports to the oversize product, N is the efficiency parameter, fo is the fraction screen open area, A is the aperture size and σ is an empirical parameter used for fitting.

The author developed dimensionless terms that included the various main factors affecting the screen efficiency obtained from the experimental data and those reported in literature applying to wet screening operations (Rogers & Brame, 1985; Valine & Wennen, 2002; Napier-Munn et al., 2005) to describe the N and σ parameters in Equation 2-29.

Equation 2-29 and Equation 2-30 were found to be the best substitute for N and σ respectively. In the case when a fishhook is seen at the finer sizes, another dimensionless term represented by the delta function was derived (Equation 2-31).

$$N = K_N\left(\frac{\mu_{sl}A}{m_f}\right)^{-0.78}\left(\frac{m_u}{\rho_p g^{0.5}A^{2.5}}\right)^{-1.25}\left(\frac{A_o}{A^2}\right)^{0.25}$$

Equation 2-29

$$\sigma = K_\sigma\left(\frac{\mu_{sl}A}{m_f}\right)^{0.53}\left(\frac{m_u}{\rho_p g^{0.5}A^{2.5}}\right)^{0.91}\left(\frac{A_o}{A^2}\right)^{-0.16}$$

Equation 2-30

$$\delta = K_\delta \left(\frac{m_u}{\rho_p g^{0.5} A^{2.5}}\right)^{0.35} exp\left[-\left(\frac{\mu_{sl} A}{m_f}\right)^{-0.16} \left(\frac{x}{A}\right)^{1.13}\right]$$

Equation 2-31

Where;μ_{sl} is the feed slurry viscosity, m_f and m_u are the mass flowrate of the feed and undersize particles respectively, ρ_p is the pulp density, g is gravitational acceleration, A_o is the screen open area, K_N, K_σ and K_δ are constants fitted to each data set

Thus, combining Equation 2-28 and Equation 2-31 forms the modified Whiten screen model that incorporates the effect of fish-hook (Equation 2-32). Whenever, the fishhook is not observed at finer sizes, δ is set to zero.

$$E(x) = exp\left[1 - Nf_o\left(1 - \frac{x}{A}\right)^{\sigma}\right] + \delta$$

Equation 2-32

Mabote incorporated the influence of the feed characteristics such as the slurry viscosity. Besides the screen aperture size and open area percentage she also included the effects of pulp density in the efficiency parameter (N), the empirical constant used for fitting as well as the delta function derived for the fishhook effect. The author argues that the modified Whiten screen model fits better at smaller apertures compared to larger openings. Similar to the Mwale model, validation was done using the experimental results used in the derivation of the model. Tests outside the range of conditions it was developed could be best to determine the capability of the model to predict performance.

2.5 Effects of design and operating variables on hydrocyclone and wet fine screen performance

The main parameters influencing the classification performance of the hydrocyclone and wet fine screen are presented in section 2.51 and 2.52 respectively.

2.5.1 Hydrocyclone

Cyclone diameter

The diameter of a cyclone is considered as a principle design variable (Napier-Munn et al., 2005). This is so because the required cut size is determined by the cyclone diameter (Bradley, 1965). Most cyclone models in literature suggest that $d50c \propto Dc^{x}$ (Lynch & Rao, 1975; Nageswararao, 1995; Asomah & Napier-Munn, 1997; Narasimha et al., 2014). The reliance of cut size on cyclone diameter comes from tangential velocities which bring about centrifugal forces driving the separation. Thereby, the smaller the cyclone diameter the finer the cut size (Tarr Jr., 1985; Olson & Turner, 2002; Napier-Munn et al., 2005). Some studies have concluded that the cyclone diameter has no effect on the cut size and that for geometrically similar cyclones the efficiency curve is a function only of the feed material characteristics (Lynch, Rao & Prisbrey, 1974; Lynch, Rao & Bailey, 1975; Rao, Nageswararao & Lynch, 1976) and Plitt, (1976) established that the cyclone diameter has an independent effect on cut size. However, according to the equilibrium orbit theory (Bradley, 1965) the cyclone diameter controls the radius of orbit and hence the centrifugal forces acting on the particle.

Cyclone apertures (apex and vortex finder diameters)

These are the key design variable of a cyclone. The vortex finder opening has a significant effect on both separation and capacity of the cyclone (Tarr Jr., 1985). Smaller vortex finder opening will reduce cyclone capacity but provide a relatively finer separation whereas larger vortex finder opening will have a reverse effect (Olson & Turner, 2002). Likewise, smaller apex opening will reduce the capacity of the cyclone and give a coarser cut because it inhibits a complete discharge of the underflow material, thus allowing some coarse material to be carried out to the overflow while larger apex opening results in excessive dilution of the underflow and

consequently carry away too many fine particles (Kelly & Spottiswood, 1982). Most of the cyclone models depict relationships described above of the corrected cut size and watersplit to the vortex finder and apex opening (Lynch & Rao, 1975a; Nageswararao, 1995; Asomah & Napier-Munn, 1997; Narasimha et al., 2014). Several authors who studied the effect of vortex finder and apex openings on cyclone performance have reported similar findings (Bhaskar et al., 2004; Lusinga, Angombe & Mainza, 2009; Kılavuz & Gülsoy, 2011; Muzanenhamo, 2014)

Cone ratio

Cone ratio as defined by Lusinga et al. (2009) is the ratio of apex diameter to vortex diameter (D_u/D_o). This variable has significant effects the performance of cyclones and is usually considered to be an operating variable rather than a design variable (Napier-Munn et al., 2005). Studies performed to assess the influence of cone ratio on cyclone performance have reported that cut size deceases linearly with increasing cone ratio (Lusinga, Angombe & Mainza, 2009; Kılavuz & Gülsoy, 2011; Muzanenhamo, 2014). Whereas, water recovery to the underflow product increases with increasing cone ratio because the amount of material leaving through the overflow stream is reduced, thus forcing more water to report to the underflow (Lusinga, Angombe & Mainza, 2009; Muzanenhamo, 2014).

Cone ratio also has an influence on the nature of the underflow discharge (Wills & Napier-Munn, 2006). The discharge pattern of the underflow stream provides information about the stability of the cyclone operation (Olson & Turner, 2002). A wide spray pattern is an indication of a dilute underflow and that the cone ratio is too large for the operation. Whereas if the cone ratio is too small, the underflow will ‘rope’ with a very tight narrow discharge. Napier-Munn et al., (2005) urge that a roping discharge should be avoided at all costs, but it is desirable to operate close to roping conditions as possible to obtain the highest possible underflow percent solids in order to minimise the short-circuiting of fine particles (Gupta & Yan, 2006). Concha et al. (1996) have suggested limiting cone ratio values for the transition from spray to roping discharge (Table 2-1**).**

Table 2-1: Transition from spray to roping discharge **(Concha et al., 1996)**

Cone ratio (D_U/D_O)	**Type of condition**
< 0.45	Roping discharge
0.45 – 0.56	Roping or spray
> 0.56	Spray discharge

Feed solid concentration

The feed solid concentration is one of the most important operating variable. Increasing the feed solid concentration increases the cut size value and water recovery to the underflow stream due to the greater resistance to the swirling motion of the slurry inside the cyclone, which in turn reduces the effective pressure drop (Wills & Napier-Munn, 2006). Whereas, cyclone capacity increases to a certain value and then decreases linearly with an increase in solid concentration (Tarr Jr., 1985). Therefore, operating cyclones at high solid concentration reduces the sharpness of separation (Tarr Jr., 1985; Lusinga, Angombe & Mainza, 2009; Muzanenhamo, 2014). In closed grinding circuits, for optimal results cyclones are typically operated with dilute feeds not higher than 60% by weight (Wills & Napier-Munn, 2006). The cyclone models also show a linear relationship between the cut size and feed solid concentration as well as watersplit (Lynch & Rao, 1975a; Plitt, 1976; Nageswararao, 1995; Asomah & Napier-Munn, 1997).

Slurry viscosity

Slurry viscosity is directly related to solid concentration by volume and total surface area of the solids (Olson & Turner, 2002; Wills & Napier-Munn, 2006). Increase in slurry viscosity results in a coarser cut size. Kawatra et al. (1996) investigated the effects of slurry viscosity on cyclone classification and reported that the water recovery to the underflow increased with increasing viscosity and that the corrected cut size was proportional to slurry viscosity with an exponent of 0.35. They commended that the increase in cut size was because of hindered settling and underflow crowding while the increase in water split was attributed to increased fluid drag in the cyclone. Similar results have been reported by other works (Waters, 2012; Muzanenhamo, 2014).

Asomah and Napier-Munn (1997) and Narasimha et al. (2014) have incorporated the slurry viscosity parameter in their models as viscosity is not only affected by solid concentration but can change with feed size distribution. Hence, slurry viscosity must be considered in formulating the cyclone cut size functions.

2.5.2 Wet fine screening

Screen open area and aperture

Open area is the ratio of the net area of the apertures to the whole area of the screening surface (Wills & Napier-Munn, 2006). The higher the open area the greater the percentage of screening surface available to particle passage which in turn results in increased capacity. In addition, the particles will have a higher chance of passage at each presentation resulting in greater efficiency (Kelly & Spottiswood, 1982). Reduction in open area leads to more blinding, thus reducing the screen capacity and efficiency. However, low screen open area is more resistant to breakage and stretching thus gives a longer screen life (Kelly & Spottiswood, 1982). In fine wet screening, typical effective open areas range from 35 to 45% (Albuquerque et al., 2008).

Fowler & Lim (1959) who studied the effect of various variables on screen efficiency identified aperture size as a significant factor in the screening process. Increasing the aperture size increases the separation efficiency and capacity of the screen and similarly, decreasing the screen opening will lead to a reverse effect (Fowler & Lim, 1959; Pryor, 1965; Kelly & Spottiswood, 1982; Valine & Wennen, 2002; Fuerstenau & Han, 2003)

Feed flow rate

Screen feed flow rate is one crucial operating factor affecting the performance and is dependent on the screen capacity. Screen capacity is the optimal feed rate to meet the desired product requirement (Albuquerque et al., 2008). Over feeding the screen will result into misplacement of fine particles to the coarse stream because particles have a lesser chance of seeing the screen opening caused by reduced residence time of the slurry on the screen (Valine & Wennen, 2002). Other studies (Fowler & Lim, 1959; Standish, Bharadwaj & Hariri-Akbari, 1986; Mohanty, Palit & Dube, 2002) also observed that high screen feed rates decreased the separation efficiency. On the contrary, Rogers and Brame (1985) who carried out tests on the derrick screen using coal and

limestone slurries to study the effect of various operating factors on screen efficiency found that the influence of feed flow rate on screen performance is negligible provided that the flow rate did not exceed the maximum required capacity. Despite the findings reported by Rogers and Brame, many authors have shown and proven that feed flow rate is a crucial operating variable in screen operations and if not optimized may lead to detrimental effects.

Feed solids concentration

Feed solid concentration is one dominant factor that affects screening performance. It is also one of the operating factor that can be easily changed simply with water addition (Valine & Wennen, 2002). In wet screening operations, separation efficiency increases with decreasing feed solid concentration because particles smaller than the screen apertures are transported through the opening by the fluid (Valine, Wheeler & Albuquerque, 2009). Once the free water has passed through the screen surface, screen efficiency decreases rapidly (Wills & Napier-Munn, 2006). This is normally rectified by re-pulping using the spray nozzles installed along the screen (Brodzik, 2009). In a study done by Rogers and Brame (1985), they reported that increasing screen feed solids concentration resulted in reduced cut size value and increased water split to the oversize. Similar findings were reported by Firth et al. (1999) who carried out tests on fine coal classification. The decrease in cut size and increase in water split to the oversize could be attributed to the high restriction of the particles through the closely packed bed which in turn reduces the effective screen aperture size and leads to screen feed bypassing to the oversize without being separated (Mabote, 2016).

A practical compromise of the feed solids concentration as reported in (Valine & Wennen, 2002; Albuquerque et al., 2008) is approximately 20% solids by volume for the high frequency screens. They further argue that in order to achieve even better screening performance, the percent solids concentration should be reduced to values as low as 10 to 15% solids by volume. However, operating the screen in closed-circuit grinding with very percent solids concentration will have an adverse effect on the downstream processes, thus a practical compromise should be made.

Feed size distribution

The feed size distribution defines the fraction of undersize, near-mesh and oversize particles in relation to screen aperture size. According to Pryor (1965) near-mesh particle passage is the rate-

determining step in screening processes. Feed size distribution affects both screen capacity and efficiency. Large fractions of near-size particles reduces the capacity and efficiency of the screen because they inhibit the ability of undersize particles to pass through the screen opening caused by blinding problems (Standish, Bharadwaj & Hariri-Akbari, 1986; Valine & Wennen, 2002; Wills & Napier-Munn, 2006). While screen capacity decreases as the fraction of oversize material increases because they influence the load on the surface (Pryor, 1965). Therefore, for effective screen classification to occur, the feed size distribution should be stabilised, preferrably with more undersize material (Lawrence & Beddow, 1968; Matthew, 1985; Soldinger, 2000). However, Lawrence and Beddow (1968) noted that fine particle percentages exceeding 60 % in the feed would result into reduced screening efficiency.

2.6 Circuit configurations

2.6.1 Hydrocyclone circuits

The choice of the hydrocyclone circuit configurations adopted in practice varies depending on the process requirement of a plant. The most common circuit configuration used is the single-stage circuit, where cyclones are typically connected in parallel as shown in Figure 2-7. Cyclones are usually arranged in parallel to increase the material tonnage being processed and in series for better size control (Tarr Jr., 1985; Heiskanen, 1993; Napier-Munn et al., 2005; Wills & Napier-Munn, 2006).

Several studies conducted in the past have demonstrated that classification performance can be improved by employing multi-stage cycloning in closed-circuit grinding. Kelsall et al. (1974) were among the first researchers to study the effect of using multi-stage cycloning on the performance of classification. They used mathematical models to study the performance of the circuit configuration is presented in Figure 2-13.

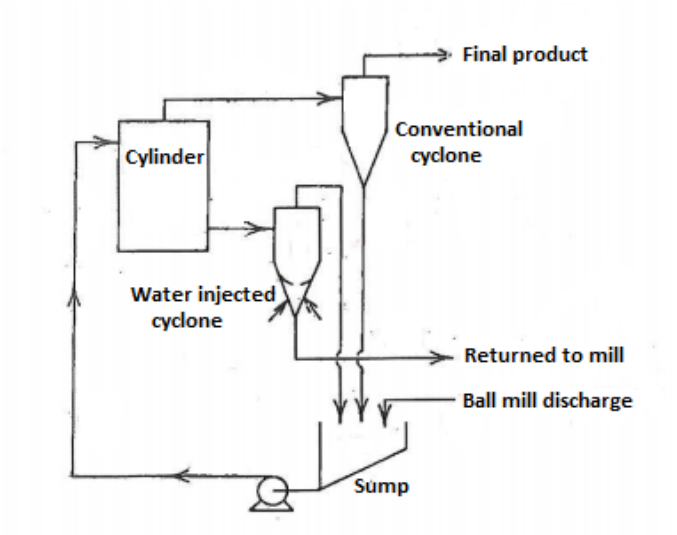

Figure 2-13:Composite cyclone circuit configuration adopted from (Kelsall et al. 1974)

The ball mill discharge was pumped to the cylinder and the cylinder overflow fed to cyclone B whereas, the cylinder underflow was fed to a water injected cyclone B. Test were done on laboratory scale and preliminary full scale to assess the concept. The laboratory tests results showed that the slope of the composite cyclone was steeper than that of a single cyclone as illustrated in Figure 2-14, indicating a sharper classification.

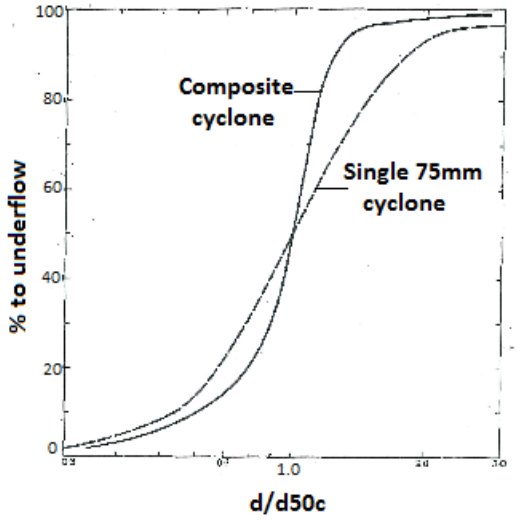

Figure 2-14: Reduced efficiency curves for the laboratory scale composite cyclone and for the single cyclone (Kelsall et al. 1974)

Similarly, the preliminary full scale results of the composite cyclone revealed a sharper classification than the single cyclone, but were not as good as the simulated results particularly in the finer sizes (Figure 2-15).

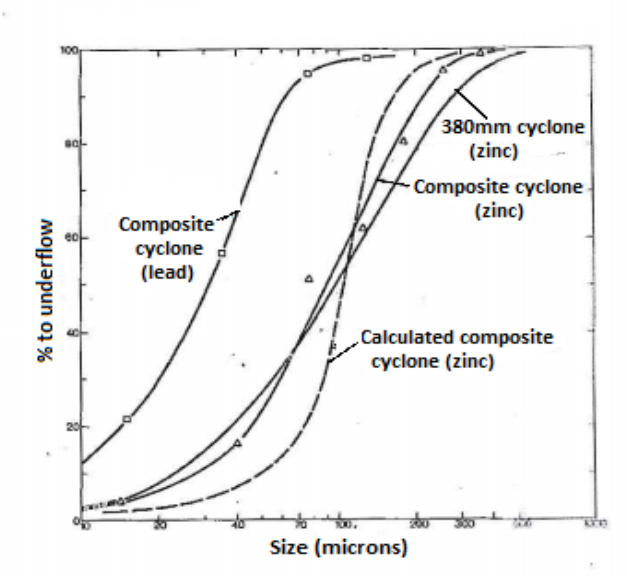

Figure 2-15: Corrected efficiency curves for the preliminary test of the full scale composite (lead and zinc), the calculated composite cyclone (zinc) and single 380mm cyclone (zinc) (Kelsall et al. 1974)

The authors noted that the cylinder used in the primary stage could have limited the overall performance and suggested that perhaps using a conventional cyclone could give better results. From Figure 2-15 the benefit exhibited by using the composite cyclone in comparison with single cyclone (380mm diameter) are very little. Therefore, an economic analysis taking into consideration the cost of additional units should be done to assess the 'real' benefits.

Lynch, (1977) and Luckie and Hogg, (1980) reviewed the fundamental of two-stage cyclone classification and noted that there were four possible cyclone serial configurations for two-stage cyclone in closed-circuit grinding operations shown in Figure 2-16. These configurations were later used by several investigators to assess classification performance (Rogers et al., 1981; Peterson & Herbst, 1984; Dahlstrom & Kam, 1988; Honaker, Boaten & Luttrell, 2007).

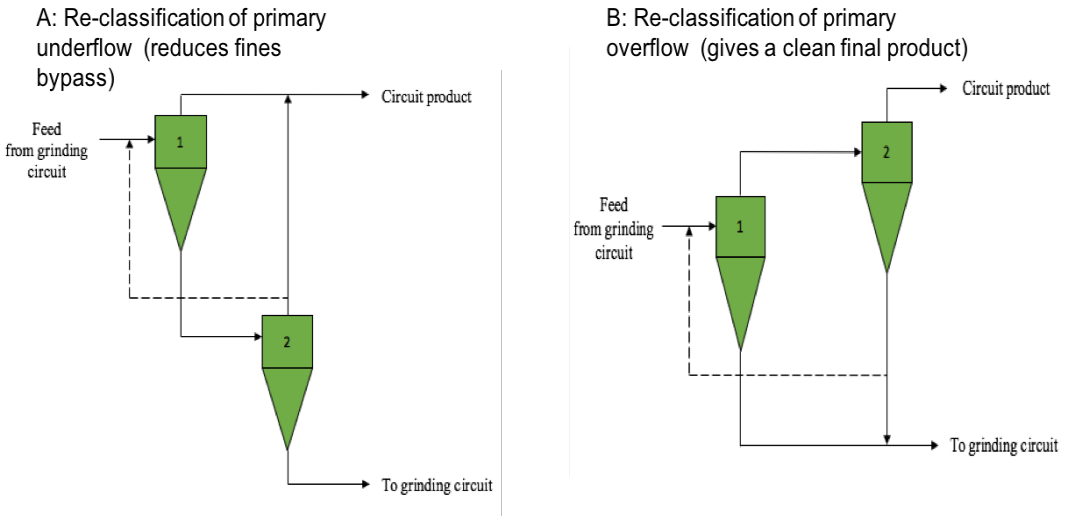

Figure 2-16: Multi-stage cycloning circuit configurations adapted from Lynch (1977).

Other authors also have stuided the effect of serial configuration for three-stage cylone using simulations (Firth & O'Brien, 2003; Honaker, Boaten & Luttrell, 2007) and showed that a much sharper classification could be achieved than the two-stage cyclone configuration. The three-stage and two-stage circuit simulated in the study done by Honaker et al. (2007) is given in Figure 2-17. The results obtained show that the three-stage cyclone had lesser fraction of fines bypass than the two-stage cyclone and single-stage cyclone as shown by the efficiency curves presented in Figure 2-18. However, normally in practice the pumping requirements limits the number of classification stages that can be used in processing plant. Hence, the more the stages of classification the higher the capital and running cost required.

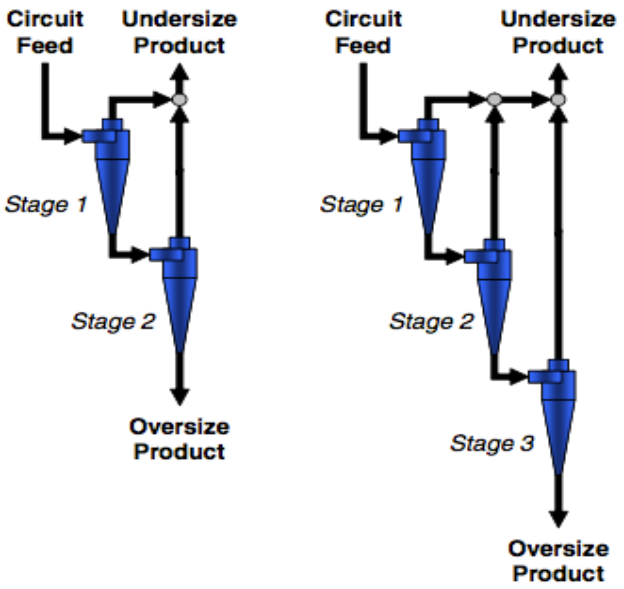

Figure 2-17: Two-stage and three-stage cyclone circuit configurations (Hanoker et al. 2007)

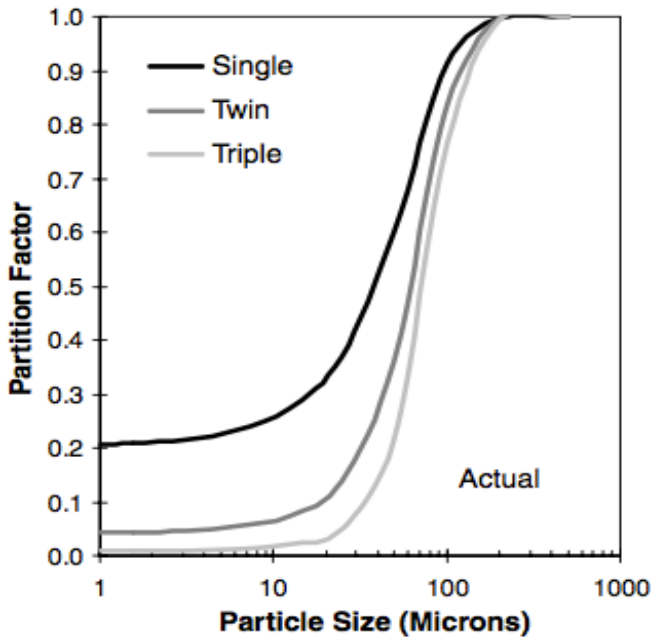

Figure 2-18: Comparison of the actual efficiency curves of a single-stage, two-stage and three-stage cyclone circuit configuration. (Honaker et al. 2007)

The most common configuration studied is the reclassification of primary underflow in the secondary cyclone (Figure 2-16a) with the aim of reducing the fine bypass which in turn would give sharper separation, reduction of energy consumption per unit ton, increased circuit capacity (Heiskanen, 1993; Napier-Munn et al., 2005). However, this type of two-stage cyclone circuit configuration is said to give low percent solids of the final product due to the amount of fresh water added to the system for effective operation (Dahlstrom & Kam, 1988).

The serial configuration given in Figure 2-16b shows the reclassification of the primary overflow in secondary cyclone. Peterson and Herbst (1984) used simulations to investigate the effect of reclassifying the overflow in a secondary stage using the configuration presented in Figure 2-16b. They found that the coarse size in the final product measured by particle size reduced significantly, particle size with less than 1% chance of reporting to the final product stream was reduced from about 140μm in single-stage cyclone to approximately 75μm. However, it was discovered that the two-stage cyclone with overflow reclassification had more fine material bypassing classification compared to a single-stage cyclone, due to the combine bypass material from both stages. These findings are in line with those reported in (Honaker, Boaten & Luttrell, 2007) who also used simulations in their study. Therefore, this type of configuration will have a negative effect on the overall bypass fraction, thus affecting the sharpness of separation but will provide a good quality final product (Napier-Munn et al., 2005).

Cyclones are sometimes mounted incline to the vertical in processing plants. According to Olson and Turner (2002), around 50% of the cyclones installed in the past 20 years on SAG circuits have been mounted at an inclination of 45° from the horizontal. Inclining cyclones is one of the tools used in the minerals industry to increase the concentrator capacity by effectively producing a coarser product and a high underflow solid concentration (Olson & Turner, 2002). This is in agreement with the observations made by Asomah and Napier-Munn (1996) who conducted test on several cyclone diameters ranging from 102 to 508mm at different inclinations. Also, Vakamalla et al. (2014), showed that increasing inclination resulted to a coarser cut and reduced watersplit to the underflow stream. Figure 2-19 shows a picture of the inclined cyclones.

Figure 2-19: Picture showing inclined cyclones in a processing plant.

2.6.2 Fine screen circuits

Advancements in classification technology, has led to many concentrators around the world to replace cyclones with fine wet screens in closed-circuit grinding operations. In the past fine screens were considered inapplicable due to the previous limitations that were associated with fine screening such as low capacity, high wear rate of the screening surface and the tendency of the apertures to blinding (Valine, Wheeler & Albuquerque, 2009). However, these limitations have been minimised in the new screen design. The newly developed fine screen has a 'unique' sack design that allows for high capacity in a small foot print. Figure 2-20 shows a typical stack sizer screen consisting of five individual screen decks stacked one above the other and operated in parallel.

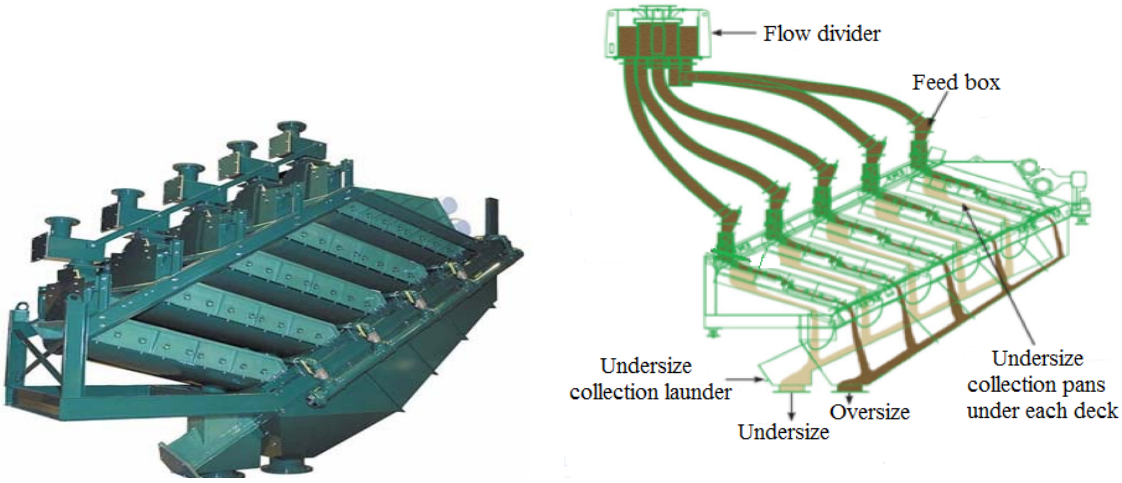

Figure 2-20: Image of a stack sizer screen and its principle of operation (courtesy of Derrick corporation)

Normally, screen classifiers give sharper separations and reduce the circulating load in closed grinding circuits as particle separation is independent of particle density and based on size only (Matthew, 1985; Wills & Napier-Munn, 2006). A number of studies have been done to assess the performance of the newly developed screens. Several authors have document case studies in their reports, demonstrating tremendous improvements such as increase in production, reduced circulating load, reduced overgrinding of valuable minerals, and reduced energy consumption per tonnage (Barrios, 2006; Albuquerque et al., 2008; Valine, Wheeler & Albuquerque, 2009; Dündar et al., 2014; Mainza, 2016). Figure 2-21 shows a typical fine screen circuit consisting of a stack sizer in closed circuit with a ball mill.

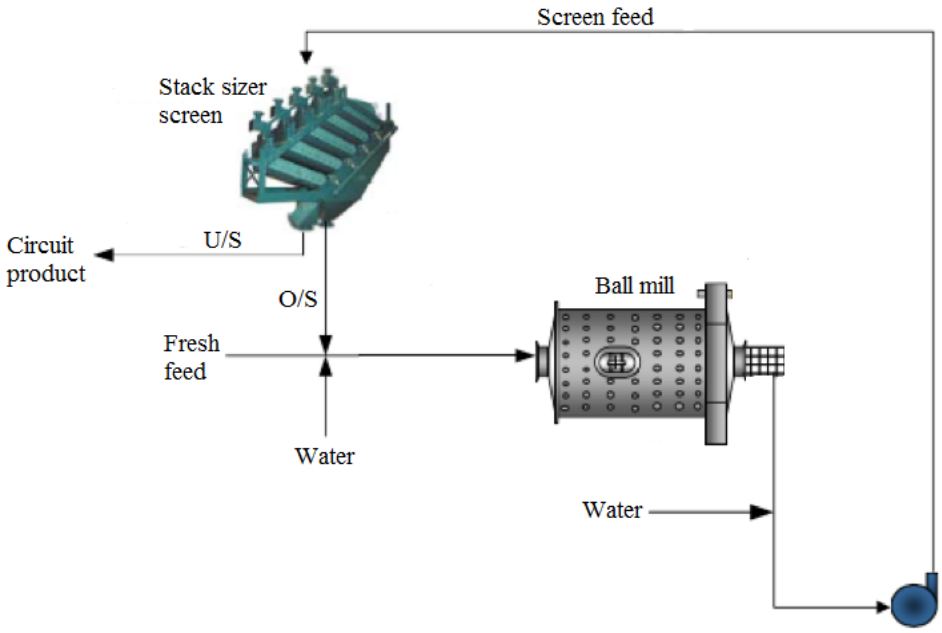

Figure 2-21: A typical fine screen in closed-circuit grinding (Valine et al. 2009)

An example of one of the documented plant operation results in a report by (Valine, Wheeler & Albuquerque, 2009) are those from Mineral Cerro Lindo (Peru). The concentrator treats a polymetallic ore to produce copper, zinc and lead concentrates. The cyclone clusters originally installed at the concentrator where replaced with stack sizer screens. The results showed that circulating load reduced from 244% to 108% and circuit throughput increased by 13.6%. Table 2-2 highlights some of the benefits of the change to screen classification and Figure 2-22 shows

the actual efficiency curves of the fine screens and cyclones.

Table 2-2: Comparison of performance between cyclones and screens at Mineral Cerro Lindo

Parameter	With Hydrocyclones	With Screens
Capacity (t/h)	242	275
Circulating load (%)	244	108
Steel consumption (g/kwh)	778	696
Mill discharge particle size (% minus 75 µm)	24	30
Mill solids (%)	83	79
Flotation feed particle size (% minus 75 µm)	55	47
Flotation feed P_{80} (µm)	141	160

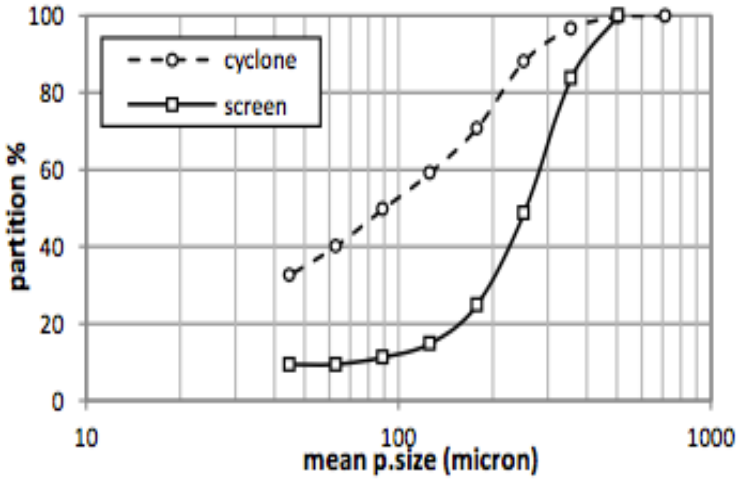

Figure 2-22: Actual efficiency curves for cyclones and screens in the grinding circuit at Mineral Cerro Lindo concentrator

Similarly, in another case study reported in (Mainza, 2016), done at a platinum processing plant in South Africa, where cyclones were replaced with fine screens. The results showed that the circuit throughput increased by 14% and energy savings was made due to the reduced fines bypass in the circulating load. Also, a study documented in Dündar et al. (2014) conducted at Catalina Huanca Mine in Peru, replaced cyclones with fine screens in closed-circuit grinding. The results revealed that the circuit with the fine screens had better efficiency curves, reduced circulating load and the breakage rates in the mills increased.

2.6.3 Hybrid hydrocyclone-fine screen circuits

There is little information available in literature regarding hybrid cyclone-fine screen circuits. However, the concept of combining the cyclones and fine screens was long initiated by Hukki, (1975). Hukki suggested that by applying a two-step classification consisting of a hydrocyclone in the primary stage and a fine screen in the secondary stage reclassifying the cyclone underflow stream (Figure 2-23a) would give a sharper separation compared to a single-stage cyclone. But, Hukki's suggestion was not tested at the time because fine screening in closed-circuit grinding was considered inapplicable. Also, studies by (Mainza, Powell & Knopjes, 2004a; Becker et al., 2008) investigated the dense media effect using a 600mm diameter three-product cyclone, postulated that the middling particles reporting to the additional vortex finder could be processed on a fine screen. By so doing, unliberated material containing the minerals of interest could be screened out and sent back to the mill for size reduction. Figure 2-23b shows the a three-product hydrocyclone-fine screen system postulated by (Mainza, Powell & Knopjes, 2004a).

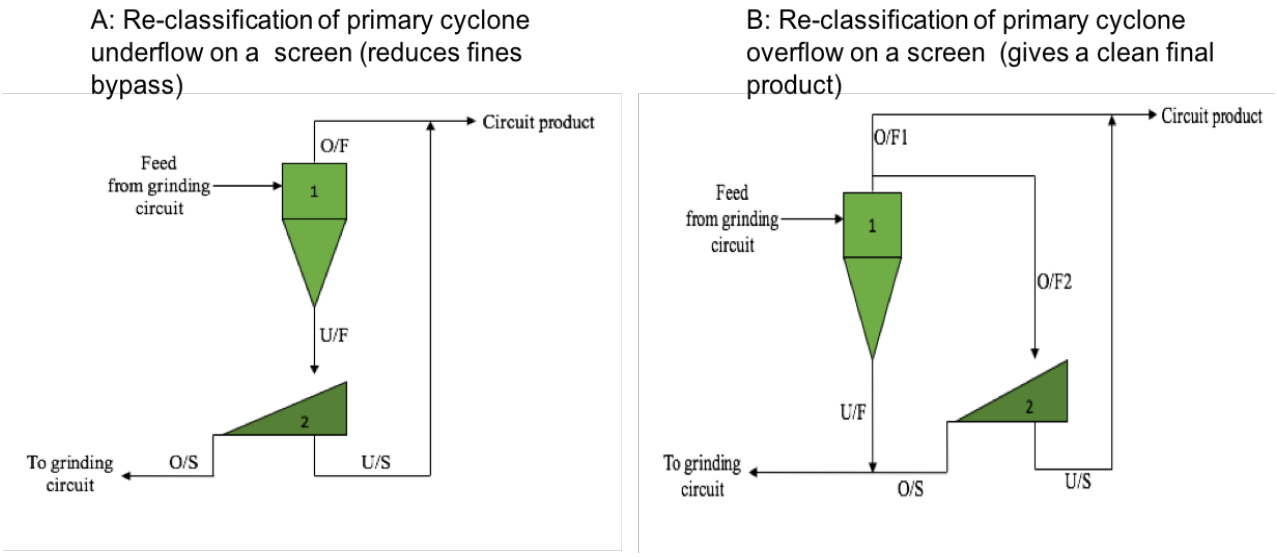

Figure 2-23: Schematics showing the possible cyclone-fine screen hybrid configurations

In 2013, Jankovic and Valery investigated the classification efficiency of three configurations using mathematical models. One of the configurations tested was a hybrid cyclone-fine screen similar to the circuit illustrated in Figure 2-23a. They found that high classification efficiencies ranging from 75% to 95% could be realised compared to single-stage cyclone whose typical efficiency is about 50%. Consequently, showing an increase in circuit capacity potentially by 20

to 25%. And more recently, a case study reported in (Brodzik, 2009) conducted at James River Coal company in the United State of America, where a stack sizer screen fitted with 75μm panels was placed on a 152mm diameter cyclone underflow stream. This study was aimed at reducing the ash content in the clean coal hydrocyclone circuit. The results showed that the total ash content (-75μm) was reduced from approximately 36% in cyclone underflow stream to 14% in the screen oversize stream. These results indicate that the fines bypass fraction could be reduced significantly by employing hybrid cyclone-fine screen configurations to close grinding circuits.

2.6.4 Summary

Inappropriate classification circuit configuration can significantly impair the performance of the grinding circuit and the whole plant at large. In the minerals industry, cyclone circuits are the most utilised configurations in closed-circuit grinding operations. The different types of cyclone configurations and design modifications have been discussed in section 2.6.1 and 2.2.1, respectively. In an effort to minimise the challenge predominantly faced in single-stage cyclone circuits, several investigators have demonstrated that multi-stage cycloning could improve the efficiency of classification. However, even with the encouraging results taking into consideration the additional units required will result into little improvements. Furthermore, since cyclones are inherently inefficient units due to the hydraulic entrainment, the same problem encountered in the prior stage of classification will occur in the subsequent stage. This implies that the fines bypass of the prior cyclone will also have a higher chance of reporting to the secondary cyclone underflow stream thus, only partially resolving the problem. While, most modified cyclones have not found wide application in the mineral processing plants due to practical limitations related to control and unstable operations

Fine screens have found wide use in closed-circuit grinding operations due to the improved design and screening surface media. Generally, screens are efficient classifying units as shown in section 2.6.2. However, screen capacity and efficiency decreases rapidly as the aperture size becomes smaller. In addition, the capital and running costs of fine screens are quite high thus operations processing large tonnages of ore will require a larger number of screening units.

The hybrid cyclone-fine screen configurations have been suggested to effectively remedy the classification challenges of both cyclone and screen circuit configurations in closed-circuit grinding operations. The hybrid configuration takes advantage of the high capacity performance offered by cyclones and the high precision classification characteristics of screening. It is evident from literature that most of the investigations on the study of the performance of hybrid cyclone-fine screen configurations have been based on computer simulations. While other studies have only postulated the performance outcome of these circuits based on literature Therefore, there is a gap in literature about the performance of hybrid cyclone-fine screen circuits based on full scale experimental tests. Normally, simulations are idealistic in some way, thus the results will differ with full scale tests.

3 THREE: EXPERIMENTAL APPARATUS

3.1 Introduction

This chapter describes the experimental apparatus used in performing the investigations of this study. The experimental work was carried out at Black Mountain Mine (BMM) concentrator. The BMM concentrator process is outlined briefly followed by a detailed description of the current classification circuit configuration including the revised circuit configurations that include the inclined cyclone and fine screen. The specifications of the process equipment employed in the various circuits are discussed and the sampling points considered are indicated on key streams in the flowsheet of the configurations tested.

3.2 Black Mountain Mine (BMM) process description

Black mountain Mine (BMM) is a South African registered company owned by Vedanta Resources Plc. (74%) and Exxaro Resources Ltd (26%). The mine consists of a concentrator, which services two underground mines (Deeps and Swartberg orebodies) and an open-pit mine (Gamsberg orebody) currently under development. The operation is situated about 113km west of Springbok, in the Northern Cape province of South Africa.

The concentrator treats a polymetallic ore to produce three concentrates namely; zinc, lead and copper. Silver is also produced as a by-product during the processing of lead and copper. The concentrator is made up of five sections, which include: crushing; grinding / milling; aeration; flotation; and thickening and filtering. A schematic diagram of the processes is shown in Figure 3-1.

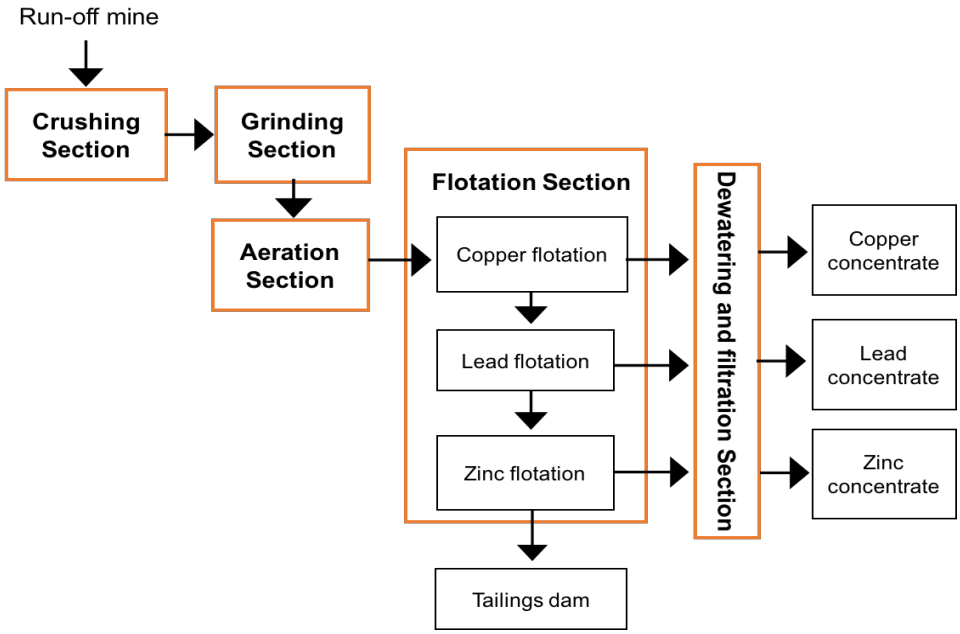

Figure 3-1:Process block flow diagram at Black Mountain Mine concentrator

The run-of-mine (ROM) ore undergoes primary crushing underground using a gyratory crusher, before it is transported to the concentrator for further size reduction. At the concentrator, the pre-crushed ore undergoes secondary and tertiary crushing, using cone crushers. The final size product of the crushing section is approximately 80% sub 12mm.

The minus 12mm material from the mill bin is weighed by the Inflo weightometer before being fed to the 3.2m × 5.05m Allis Chalmer rod mill (charged with 4.8m mill rods) at 190 to 250 t/h. The rod mill discharge is pumped to the primary hydrocyclone cluster. The underflow of the primary hydrocyclone streams is then fed to the secondary hydrocyclone cluster. The secondary cluster underflow stream is fed to the 4.88m × 5.13m Allis Chalmer ball mill (charged with 50mm mill balls), forming a closed circuit. The overflow streams from both the primary and secondary clusters proceed to the aeration section. During the process of aeration, copper is activated and lead is depressed by addition of suitable reagents, then transferred to the flotation section. The slurry undergoes three stages of flotation, where copper is floated out first, followed by the flotation of lead from copper tails and finally zinc is floated out from the lead tails. The final zinc tails are then transported to the tailings dam. The final section is the thickening and filtration. During thickening, dewatering process take place, the thickener overflow containing

mostly water is transferred to the water pond and is recycled to the plant. The thickened underflow concentrate goes through filtration process forming filter cakes with moisture content between 6% - 8%. Figure 3-2 shows the general flowsheet of the comminution circuit.

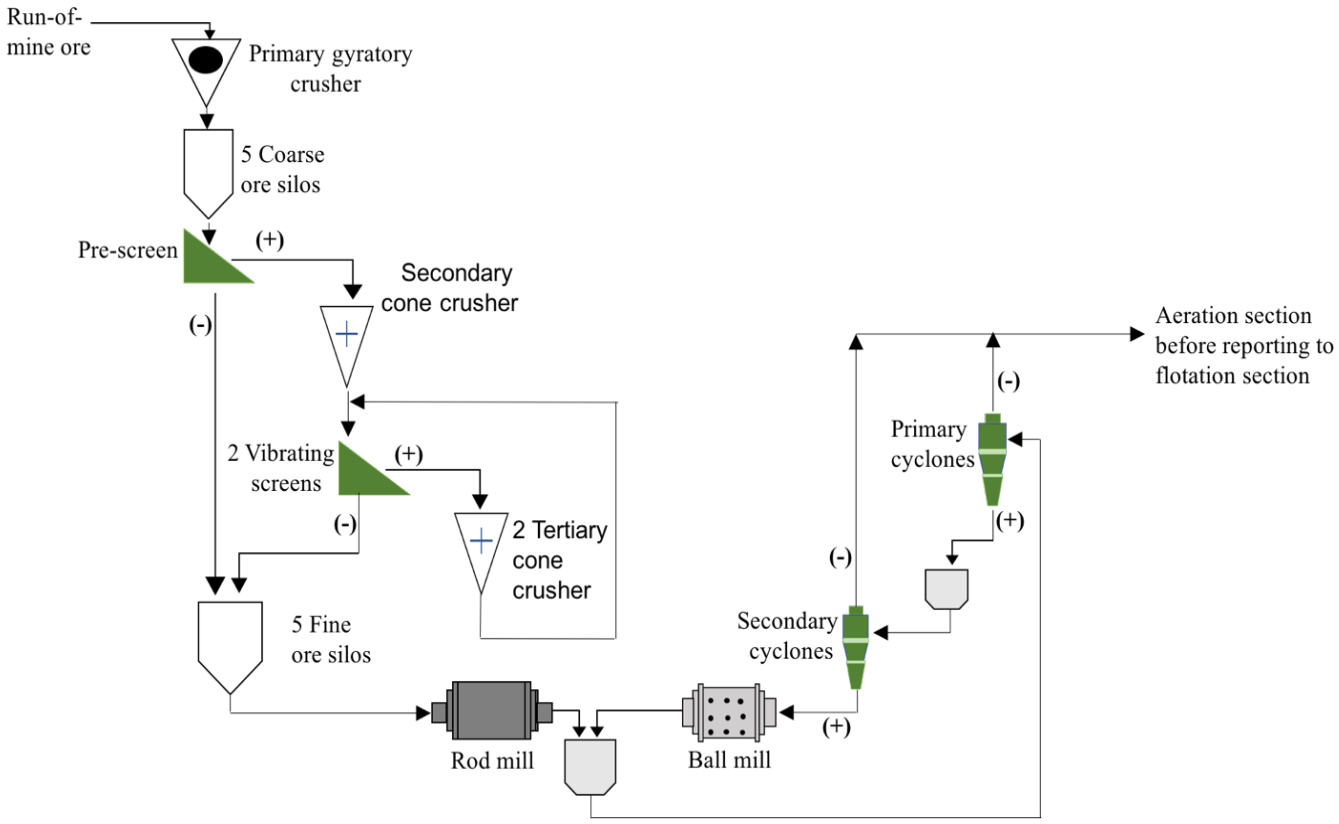

Figure 3-2: Schematic of the comminution circuit flowsheet at BMM concentrator

3.2.1 Current classification circuit configuration

The surveys were focused on the classification stage in the grinding circuit. Figure 3-3 shows a flowsheet of the current classification configuration employed at the BMM concentrator. The rod mill discharge combined with the ball mill discharge is fed to the primary cyclones. The primary cyclone underflow product is diluted with fresh water to feed secondary hydrocyclones and the secondary cyclone underflow product is sent back to the ball mill for further size reduction. Both primary and secondary cyclones overflow streams gravitate to aeration section before reporting to the flotation section. The target grind size is 65% sub 75µm.

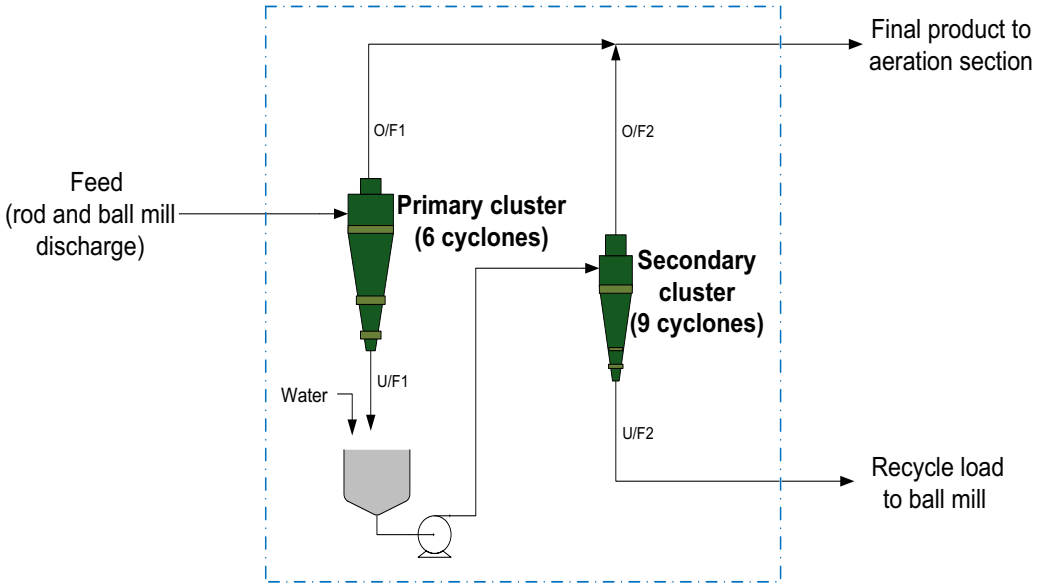

Figure 3-3: Schematic flow sheet of the current classification circuit at BMM concentrator before modifications

3.2.2 Classification circuits after inclusion of an inclined hydrocyclone and single deck screen

Alterations to the current circuit configuration employed at BMM concentrator were made by incorporating an inclined cyclone and a single deck fine screen. Figure 3-4 to Figure 3-7 show the different configurations generated after the inclusion of an inclined cyclone in the primary stage and a fine screen in the primary, secondary and tertiary stages of classification.

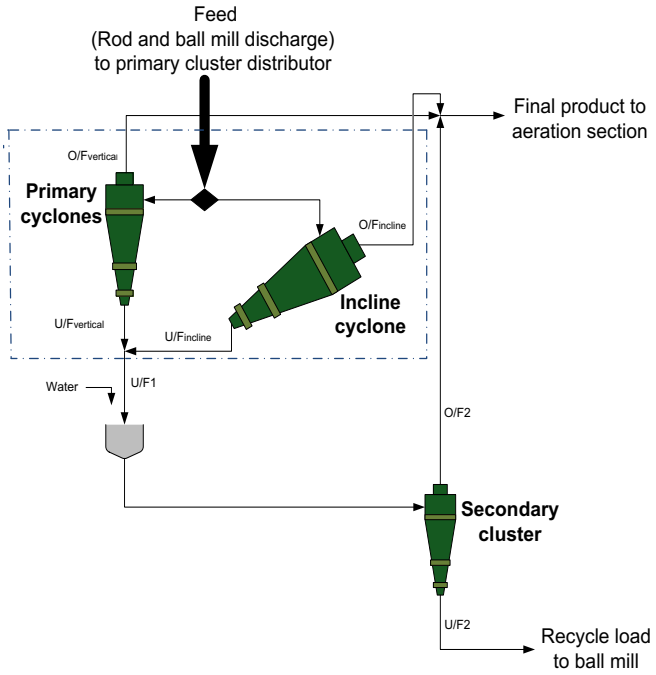

Figure 3-4: Schematic of the classification circuit post incline hydrocyclone inclusion in the primary stage at BMM concentrator

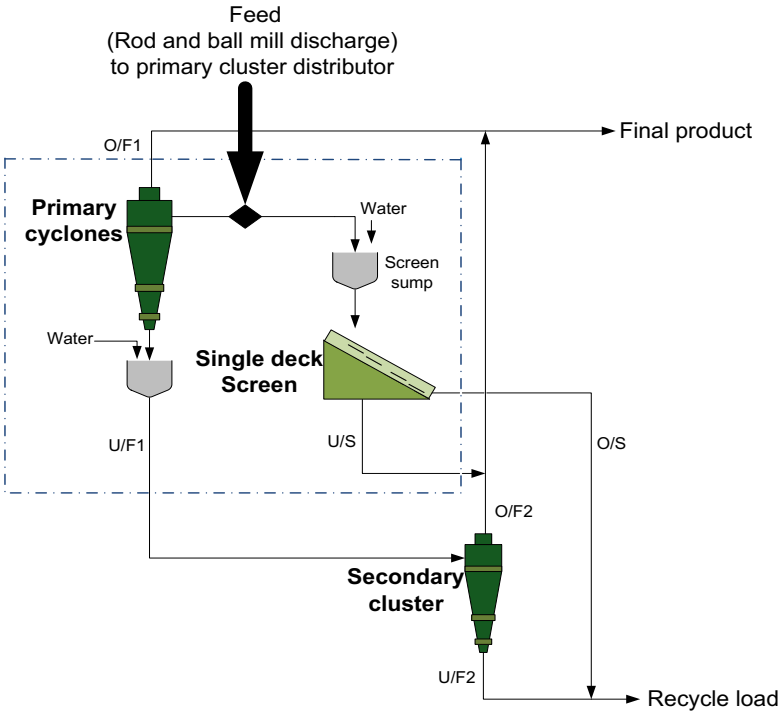

Figure 3-5: Schematic of the classification circuit post fine screen inclusion in the primary stage at BMM concentrator

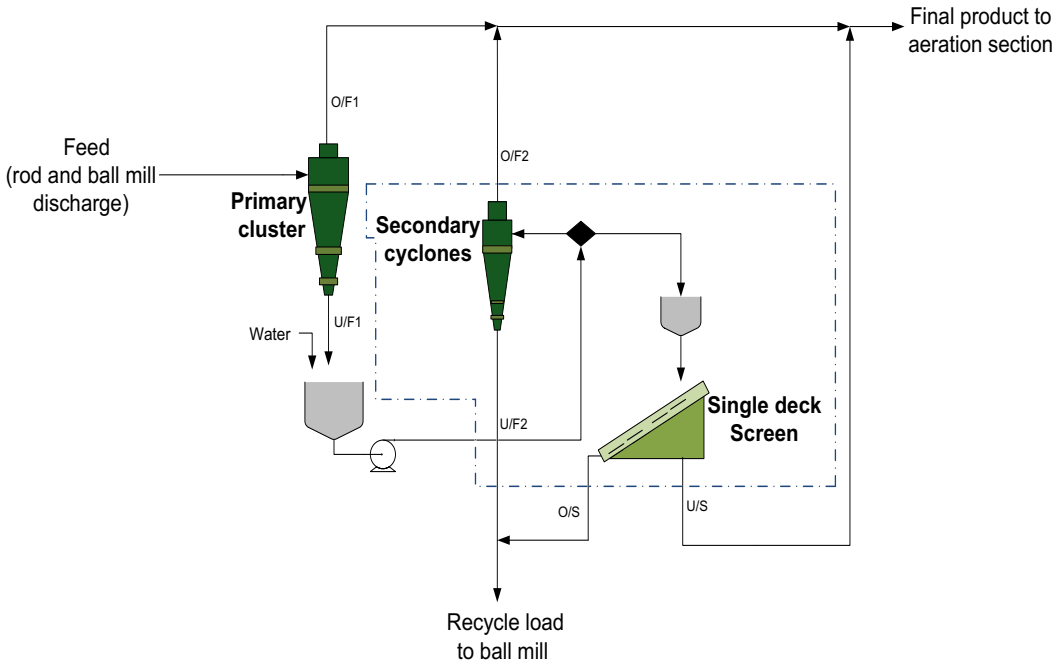

Figure 3-6: Schematic of the classification circuit post fine screen inclusion in the secondary stage at BMM concentrator

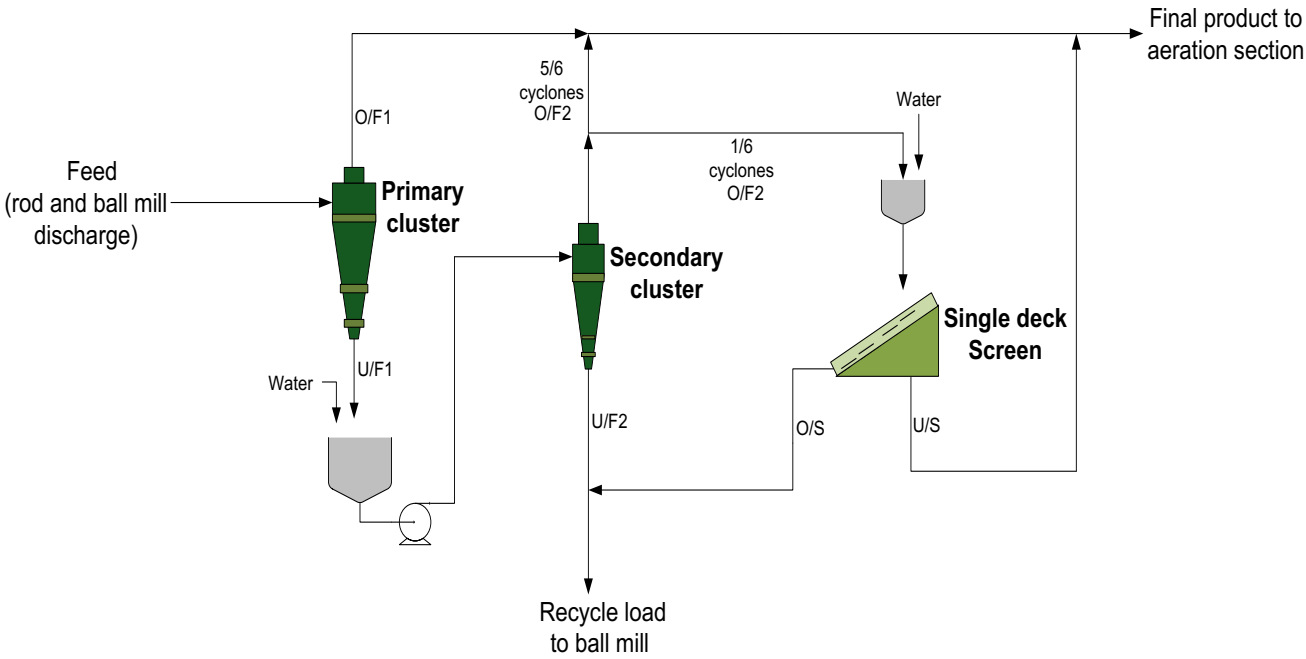

Figure 3-7: Schematic of the classification circuit post fine screen inclusion in the tertiary (third) stage at BMM concentrator

The pictures showing the inclined cyclone incorporated in the primary cyclone cluster and a fine screen in the secondary stage are presented in Figure 3-8 and Figure 3-9, respectively.

Figure 3-8: Picture showing an inclined cyclone in the primary stage of classification at BMM concentrator

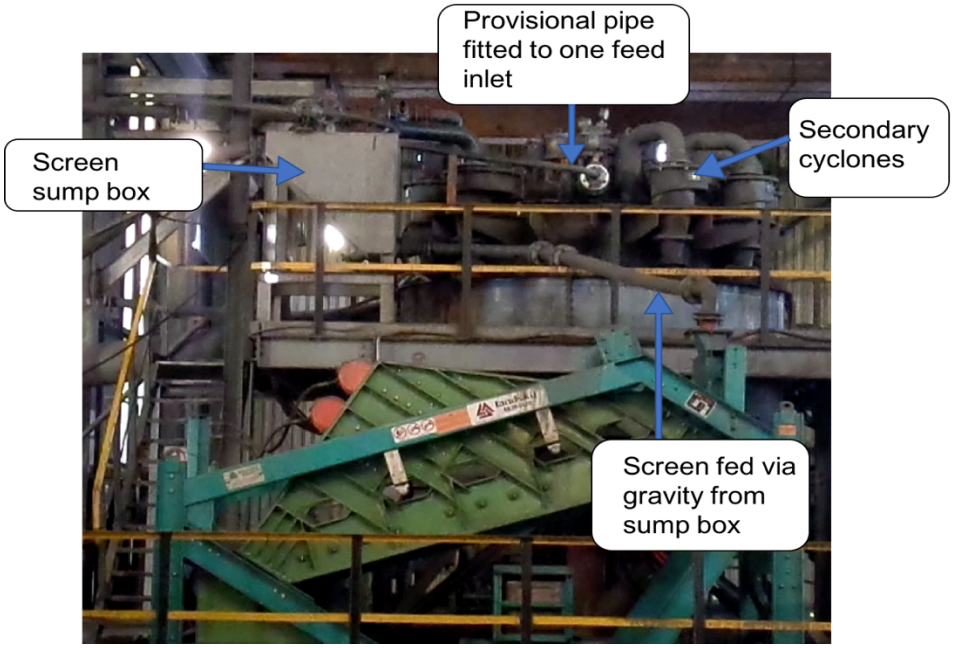

Figure 3-9: Picture showing of a single deck fine screen integrated in the secondary stage of classification at BMM concentrator

3.2.3 Process equipment

Hydrocyclones

The vertically mounted cyclones in the primary and secondary clusters shown in Figure 3-10 were manufactured by Krebs. The diameter of each cyclone in the primary cluster is 381mm and those in the secondary cluster is 254mm. Normally, four out of the six cyclones in the primary cluster and six out of the nine cyclones in the second cluster are in use while the others are on standby. The inclined cyclone incorporated in the primary stage of classification after the alteration the classification circuit at BMM was manufactured by Multotec. Figure 3-11 shows the installation of the inclined cyclone. The specifications of the cyclones are summarised in Table 3-1.

Table 3-1: Specifications of hydrocyclones used during tests at BMM concentrator

Design parameter	**Primary cyclones**	**Secondary cyclones**	**Interim cyclone**
Make	Krebs (Gmax)	Krebs (Gmax)	Multotec
Orientation	Vertical	Vertical	Inclined
Inclination angle (°) from horizontal position	90	90	20
Number in cluster	6	9	-
Cyclone diameter - Dc (mm)	381	254	500
Vortex finder diameter - Do (mm)	171.45	95.25	225
Apex diameter – Du (mm)	90	75	130

Primary cyclones

Secondary cyclones

Figure 3-10: Pictures showing the primary and secondary cyclone clusters amounted at 90° from the horizontal at BMM concentrator

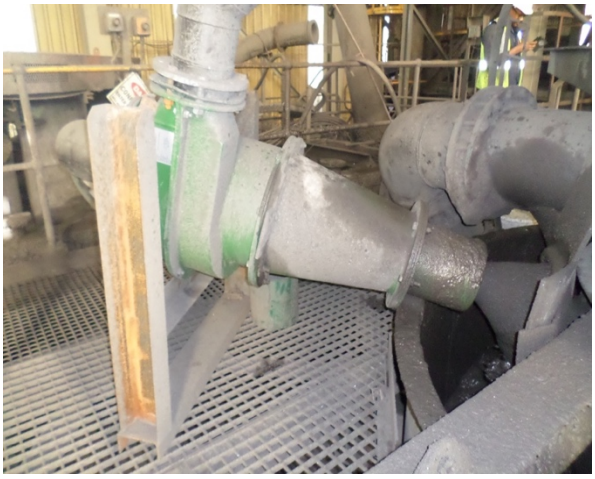

Figure 3-11: Picture of the interim incline cyclone amounted at 20° from horizontal position in the primary cluster at BMM concentrator

Fine screen

The specifications of the fine screen are given in Table 3-2. The screen was supplied by Landsky. It is a single deck screen fitted with a polyurethane screening surface. The screen has a fractional open area of 35.8%; three screening panels; and is equipped with spray nozzles through which water is introduced into a re-pulping trough that is positioned between the panels. Figure 3-12 presents a picture of the single deck fine screen.

Table 3-2: Specifications of the fine screen

Make	Landsky
Number of decks	1
Panel number	3
Length (m)	2.4
Width (m)	1.2
Angle of inclination (°)	17.5
Aperture (um)	100
Open area (%)	35.8

a. Screen panels fitted with 100µm polyurethane screening surface

b. Outer frame of the single deck fine screen

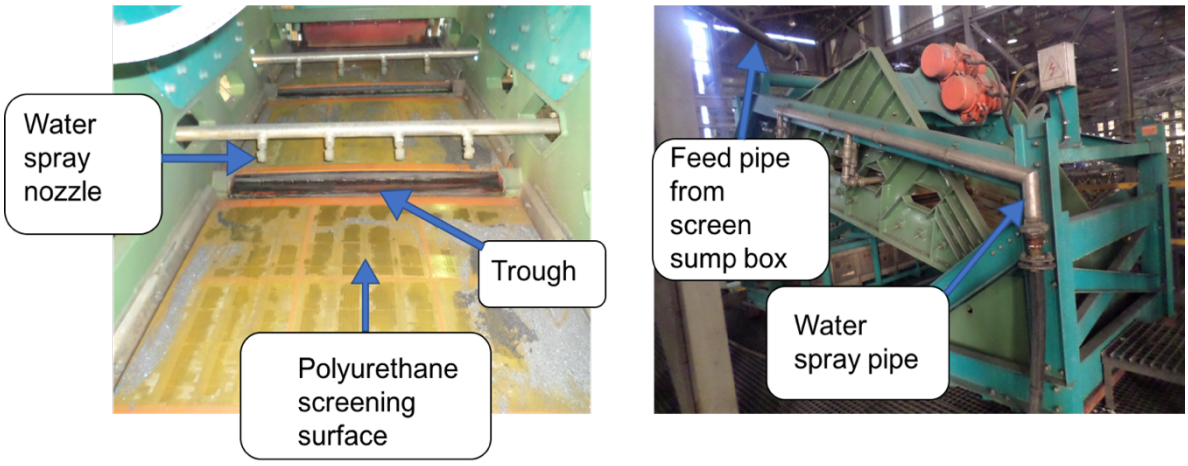

Figure 3-12: Pictures showing various components of the Landsky screen

3.3 Sampling points for each classification configuration

Five different classification configurations were tested and these were: a two-stage cyclone circuit; an inclined cyclone circuit; a fine screen circuit; a hybrid cyclone-fine screen circuit; and a hybrid two cyclones-fine screen circuit. Figure 3-13 to Figure 3-17 show the circuit configurations tested highlighted by the dashed boxes and the positions where samples were collected.

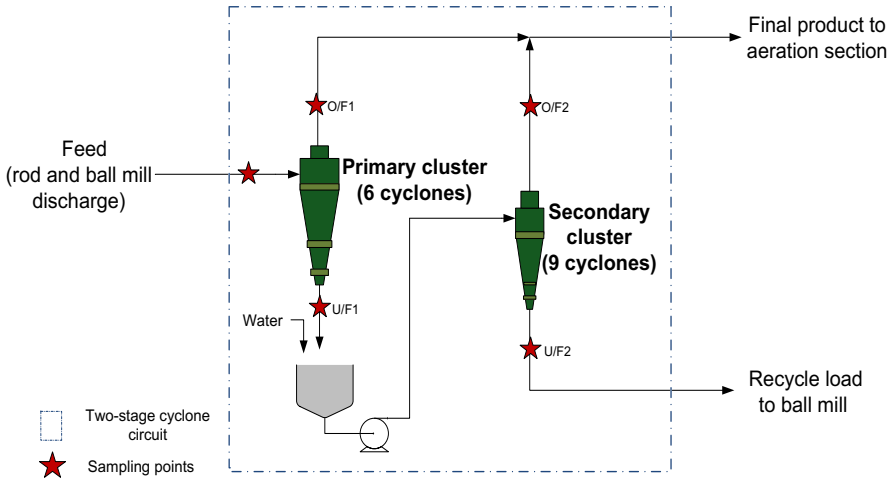

Figure 3-13: Schematic showing the sampling points around the two-stage cyclone circuit configuration

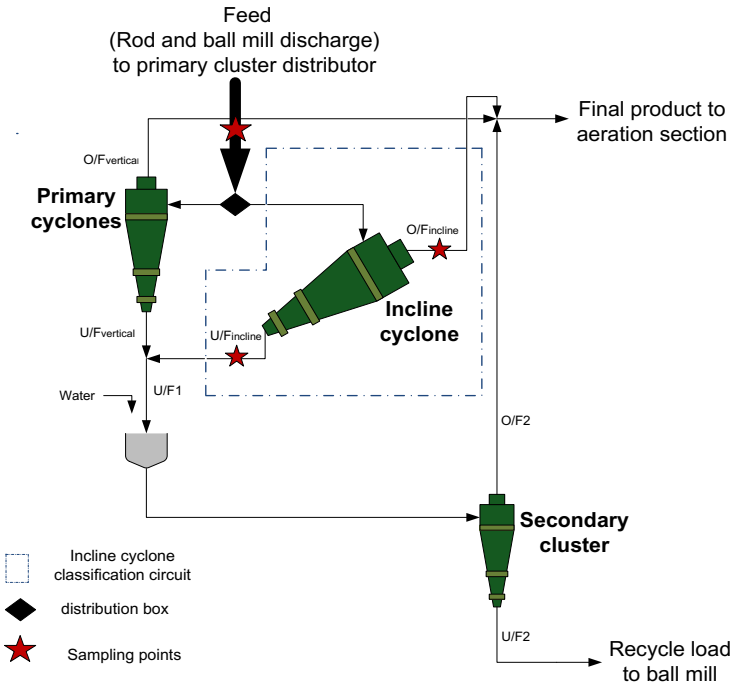

Figure 3-14: Schematic showing the sampling points around the modified inclined cyclone circuit configuration

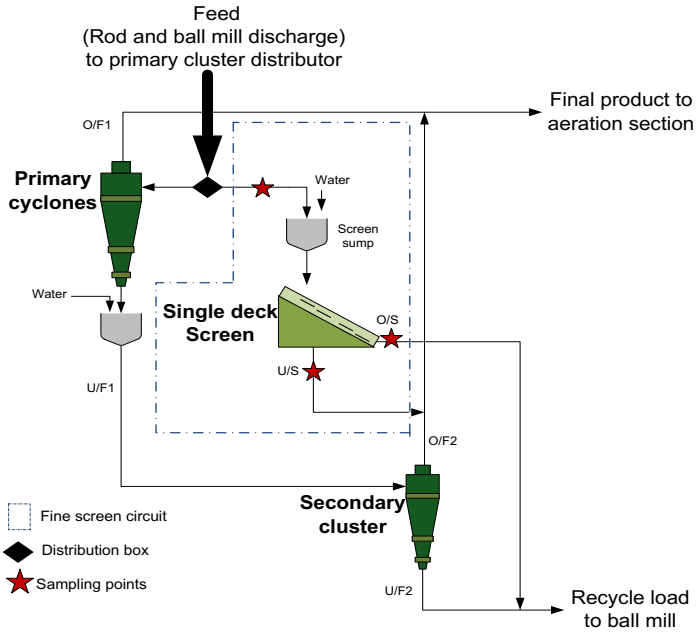

Figure 3-15: Schematic showing the sampling points around the modified fine screen circuit configuration

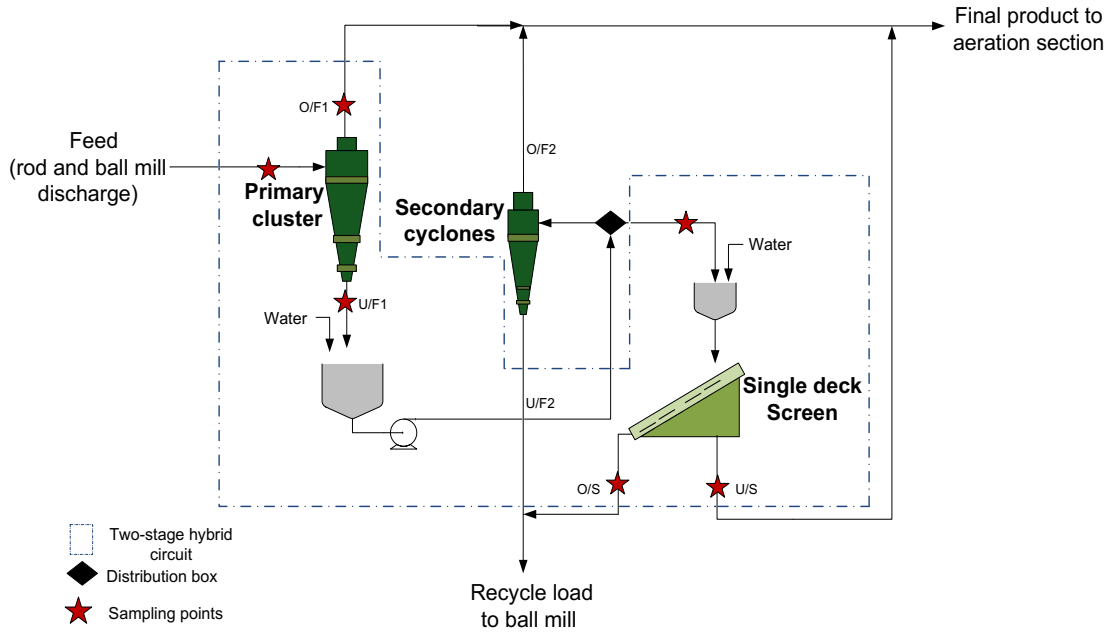

Figure 3-16: Schematic showing the sampling points around the modified hybrid cyclone- fine screen circuit configuration

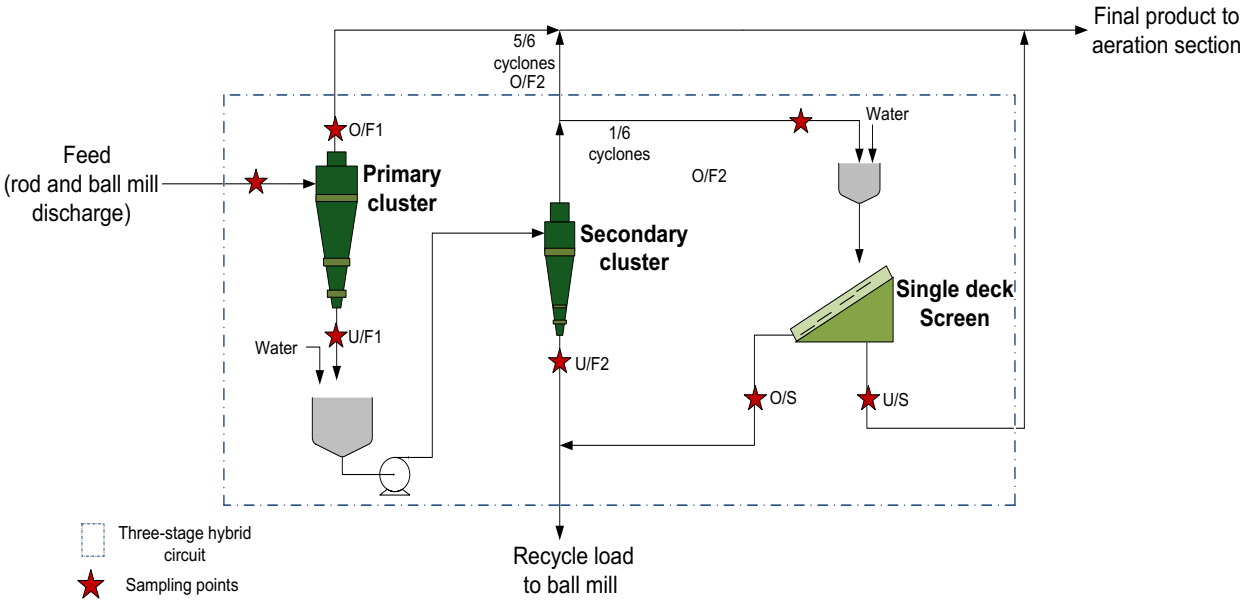

Figure 3-17:Schematic showing the sampling points around the modified three-stages hybrid with two cyclones in series followed by a fine screen circuit configuration

4 CHAPTER FOUR: EXPERIMENTAL METHODOLOGY

4.1 Introduction

This chapter describes the survey procedures of the circuit configurations tested. The pre-survey planning, sampling and post-survey tests are presented. Thereafter, the sample processing methods used at the Centre for Minerals Research Laboratory are described. The feed conditions at which each classification circuit configuration test was conducted are presented and discussed. Finally, the mass balancing method used in assessing the integrity of the experimental results is explained.

4.2 Surveys

Surveys were performed on the BMM circuits operating under five different classification configurations. The tests were confined to the classification section of the plant only because of production commitments which did not allow plant stoppage required if the mills were included in the testwork. Therefore, the scope of the testwork was the classification section of the circuit. Section 4.2.1 to 4.2.5 describes the survey procedure of each configuration tested

4.2.1 Two-stage cyclone circuit configuration – reclassification of primary cyclone underflow

Four cyclones were running in the primary cluster when the survey was conducted. The feed stream was sampled from the bleed pipe above the distributor and the overflow and underflow samples were collected from three of the four working cyclones in the cluster at each sampling interval. Six cyclones were operating in the secondary cluster. The feed stream to the secondary cyclone cluster was inaccessible for representation sampling. However, the feed particle size distribution and percent solids was reconstituted from the overflow and underflow particle size determinants. The overflow and underflow samples were obtained from three operating cyclones in the secondary cluster. Figure 4-1 shows the underflow stream sampling points.

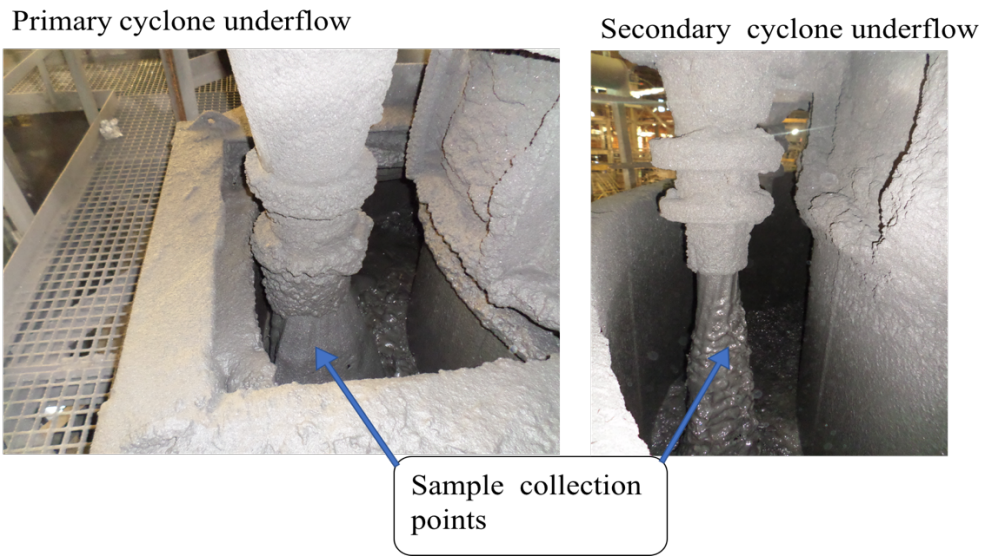

Figure 4-1: Picture showing the points were sample were collected in underflow streams of both primary and secondary cyclones

4.2.2 Inclined cyclone circuit configuration

Three cyclones were operating in the primary cluster including the inclined cyclone during the survey. Samples were only taken from the inclined cyclone overflow and underflow streams. The feed sample to this configuration was taken from the bleed pipe before entering the primary cyclone cluster distribution box. Figure 4-2 shows the underflow and overflow streams of the inclined cyclone sampling was accessed.

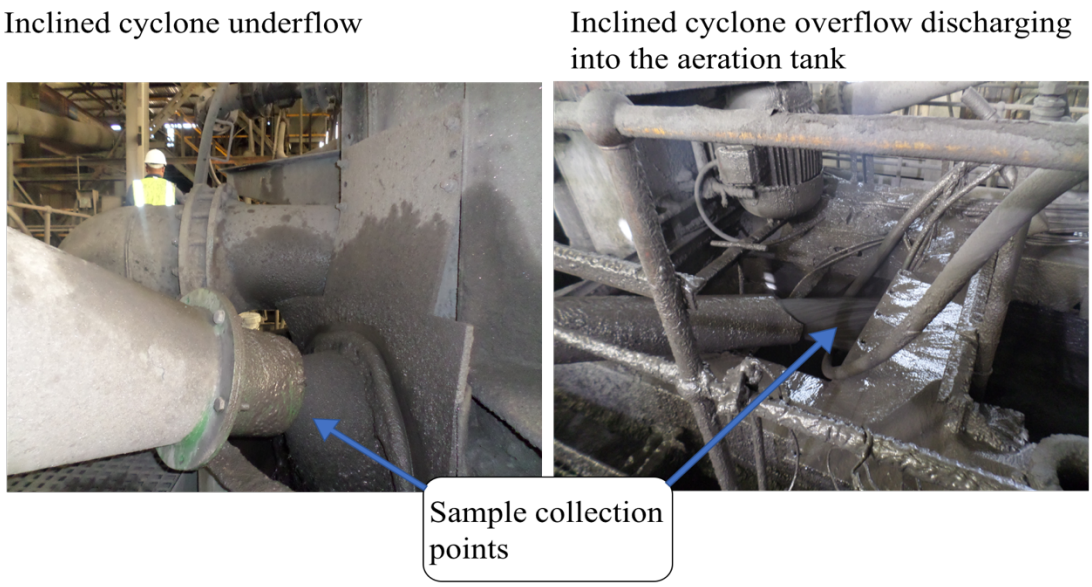

Figure 4-2: Picture showing the locations where samples of the underflow and overflow were taken from the inclined cyclone.

4.2.3 Fine screen circuit configuration

Three primary cyclones were running during the survey. The feed to the screen was obtained from the primary cyclone distribution box through a retro-fitted flexible pipe. The screen feed sample was taken at the discharge end of the flexible pipe shown in Figure 4-3. Fresh water was added to the sump to assist with slurry conveyance by agitating the slurry body, though the sump was no equipped with an agitator. Consequently, the pipe feeding the screen from the sump was prone to blockage due to the accumulations of solids at the bottom of the sump. The screen oversize sample was taken as the oversize material was being discharged into the ball mill feeder. The undersize samples were taken as the undersize product into the launder that transports the final product of both the primary and secondary cyclones to the aeration section.

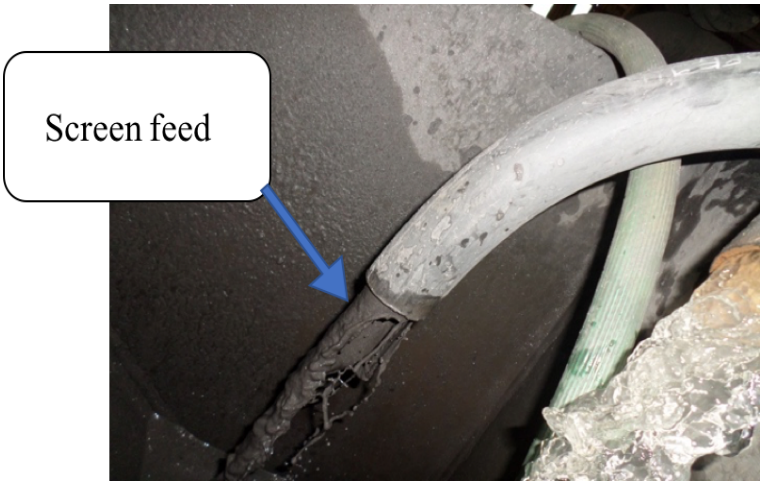

Figure 4-3: Picture showing where screen feed samples were as was slurry being discharged into the sump

4.2.4 Hybrid cyclone-fine screen circuit configuration - reclassification of primary cyclone underflow

Four cyclones were operating in the primary cluster at the time of the survey and the samples were taken from three cyclones. Because the feed to the screen was the underflow product of the primary cluster, one cyclone in the secondary cluster was detached and fitted with a provisional pipe conveying slurry into the screen feed sump. The feed sample to the screen was taken at the discharge to the sump as shown in Figure 4-3.

4.2.5 Hybrid two cyclones-fine screen circuit configuration – reclassification of primary cyclone underflow and secondary cyclone overflow

Four primary cyclones and six secondary cyclones were operating during the survey. The overflow and underflow product samples were taken from three working cyclones in the primary cyclone cluster. In the secondary stage the stream product samples were taken from the cyclone overflow stream feeding the screen sump. The screen feed sample was taken at the provisional pipe discharge to the screen feed sump (Figure 4-3).

4.3 Pre-survey planning, sampling and post-survey tests

Prior to each survey, two labelled and pre-weighed buckets, A for processing and B for back-up were placed at each sampling point. The circuit was monitored at least two hours before starting

to take samples from the selected streams for its stability. This was done by monitoring the feed flowrates of the rod mill, primary and secondary cyclones from the control room to ensure that there were minimal variations. Once it was determined that the circuit was stable, sampling was done for an hour at intervals of 15 minutes. The samples collected from each stream were used for particle sizing and percent solid analysis described. Sample cutters specifically designed for classification surveys were used to collect samples shown in Figure 4-4.

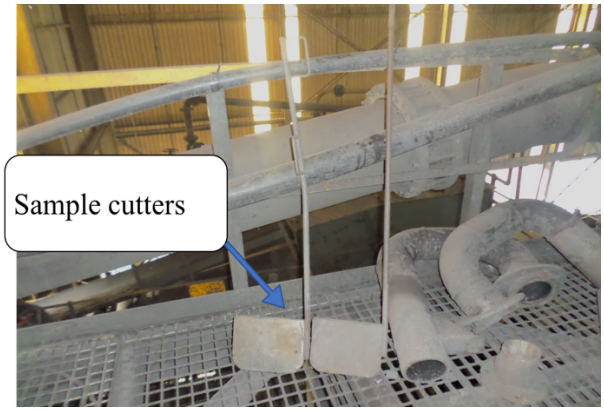

Figure 4-4: Picture showing the sample cutters used for cutting samples

The cutter opening was held perpendicular to the flow of the stream and passed across the flow at an even speed ensuring a full coverage of the stream then back again. Afterward the collected sample was carefully discharged into the processing bucket labelled A. The second sample was then cut and emptied into the back-up holding bucket labelled B. During the emptying of the samples the cutter was tapped upside down to ensure that all the solids were removed from the cutter. In instances when the sample accidently spilt or full stream coverage was not collected the sample was dumped and another one was taken.

After the sampling processing, measurements of the flowrates were done immediately at sampling points where there were no online flowmeters installed, such as the feed and product streams of the fine screen classifier. The basic method that was used for measuring the flowrates was the bucket and stop watch, where a bucket of known mass was placed under a stream and the time taken to fill the bucket to was recorded. Then the bucket containing slurry was weighted and the mass of the slurry was calculated from the difference between the bucket mass and the

mass of the bucket plus slurry mass. The measurements gave the slurry flowrate in tph, from which the solid flowrate (F_s) was calculated (Equation 4-1). To improve the accuracy of this method, three duplications were done for each flowrate measurements to reduce the standard error.

$$F_s(tph) = \%\ \text{solids} \times \text{slurry flowrate}\ (tph)$$

Equation 4-1

4.4 Sample processing

The process and back-up samples collected were weighed immediately after each survey to get the wet masses, thereafter filtered using press filters and dried in the oven overnight at 80°. After drying, the samples were removed from the oven to cool and dry weights were recorded. The percent solids of the samples were then calculated from the wet and dry masses of the samples. The dried samples were de-lumped using the 1mm screen in preparation for splitting. Sample splitting was done at the Metallurgy laboratory at BMM concentrator and the split representative sub-samples were packed in plastic bags for the analysis of particle sizing which was performed at the Centre for Mineral Research (CMR) laboratories. The splitting and particle sizing process procedure adopted at the UCT CMR laboratory was followed. A total of twenty-nine samples were collected from all the tests conducted. Section 4.4.1 and 4.4.2 describes the splitting and size analysis methods respectively.

4.4.1 Procedure of splitting the bulk samples into sub-samples

The dried de-lumped samples were split into small representative samples for easy handling using the rotary splitter (Figure 4-5). Prior to the splitting process, the splitter and the cups were cleaned. The sample was then introduced slowly into the cone of the splitter and the motor was started, then the feeder vibration was set to a minimum. At the end of the first split, cups opposite to each other were combined and the sample was put back into the cone for further splitting until a sub-sample weighing between 250 to 350g was obtained. Two sub-samples were collected which included; a screening sample and a back-up sample.

Figure 4-5: Picture of the rotary splitter at the BMM Metallurgy laboratory

4.4.2 Wet and dry screening procedure

Screen analysis was carried out down to 25µm and the process was done in two stages. The first stage was wet screening were a pre-weighed representative sub-sample was introduced on a 25µm screen, which was placed onto the ring of the screen shaker and below the screen was an empty bucket. Thereafter, water was introduced on the screen to wet the whole sample and the shaker was started up. Continuous addition of water was done at a controlled rate until clear water was being discharged into the bucket. The 25µm screen was then removed from the shaker. A 106µm screen was placed on the ring of the screen shaker and a clean empty bucket was place under the screen. All the solids retained on the 25µm screen was transferred on to the 106µm screen and the shaker was started. Controlled amounts water was added on the screen until clear water was being discharged into the bucket. The material retained on the 106µm was transferred onto the laboratory dish, ensuring that all the solids were removed from the screen to the dish. The sample was dried overnight in the oven at 80°. The procedure was repeated for 75, 53, 37 and 25µm screens. The material passing 25µm from the first and second screening were combined, then filtered and dried. Masses of all the dry samples retained on each screen were recorded.

The dry sample retained on the 106µm was placed on the top screen for the dry screening process, which consisted of stack of screens arranged in a descending order of screen aperture size starting with the largest opening down to the smallest opening. The following screen series was used for dry screening; 2.8mm, 2mm, 1.4mm, 1.0mm, 850µm, 600µm, 420µm, 300µm, 212µm, 150 µm and 106µm. The stack was placed on the screen shaker with the pan at the

bottom of the screen shaker. The material retained on a 106µm screen was placed on the top screen and the lid was clamped tightly on the shaker. Then the shaker was switched on and allowed to vibrate for 25mins. At completion, the screens were emptied and each size fraction was weighed separately, each time cleaning the screen with the brush. The mass of material retained on the pan was added to the material retained on the 75µm screen.

4.5 Experimental variables

The operating and design conditions of all the classification circuit configurations investigated in the study were not varied. They were limited to the plant practice during the period at which the survey was conducted as changing either the operating or design conditions would have affected the plant operational requirements and downstream processes. It was crucial that the feed operating conditions of all the circuit configurations were as similar as possible

The flowrates of the streams with the online flowmeters such as those for the primary cyclones and secondary cyclones, where retrieved from the plant Supervisory Control and Data Acquisition (SCADA) system after each survey. The bucket and stop watch method was used to obtain feed and product flowrates of the screen and the percent solids were calculated from the wet and dry masses of the samples collected. Table 4-1 shows the feed flowrates and percent solids by weight obtained for all the configurations tested.

Table 4-1: Operating conditions of the feed stream recorded during the survey campaigns

Circuit configuration	Stage	Solids flowrate (t/h)	% solids
Two-stage cyclone	primary	1287	69
	secondary	1098	74
Inclined cyclone	primary	404	69
Fine screen	primary	3	13
Hybrid cyclone-fine screen	primary	1498	68
	secondary	9	32
Three-stage hybrid with two cyclones in series-fine screen	primary	1424	68
	secondary	1209	68
	tertiary	10	31

4.6 Mass balancing

Mass balancing is a method of assessing the quality of data obtained during plant surveys. Normally, during the process of mass balancing steady state conditions are assumed, for example the mass flow rate leaving a circuit or unit is equal to the new feed flowrate. Furthermore, to conduct a mass balance, one stream is assumed accurate (Napier-Munn et al. 2005). In the case of in this study, the flowrates of the feed for each configuration were considered accurate.

A computer program known as JKMBal incorporated in JKSimMet software, was used to mass-balance the experimental data collected such as; particle size distributions, solid concentrations and flowrates. Basically, the program offers estimates of all experimental data with accuracies and an adjusted set of self-consistent results. JKMBal uses the least-square method based on the minimization of the sum of weighted squared error, presented in Equation 4-2 below:

$$\mathrm{SSQ} = \sum_{j=1}^{N} . \sum_{i=1}^{L} \left(\frac{X_{ij} - x_{ij}}{\sigma_{ij}} \right)^2 + \sum_{i=1}^{L} \left(\frac{A_i - a_i}{\sigma_i} \right)^2$$

Equation 4-2

Where; N is number of measurements, L is number of streams, X is the measurement i.e. % solids, assay, size, x is the adjusted measurement, A is the measured flow, a is adjusted flow and σ_{ij} *and* σ_I *am the weights or standard deviations (SD) for the measurements and flows respectively.*

There are various ways of interpreting the quality of results obtained from JKMBal. The program displays values of the estimated SSQ, which can be used as a guide to explain if the balance is of good or poor quality. Normally, low values in the estimated SSQ fields imply a good data quality while large values indicate a poor balance. Also, by comparing the size of the stream SD's with that of the related flow value, when the SD is small compared with the value, it means that the flowrate is of good quality but if the SD is large then the flowrate is said to be poorly determined.

The most common way used to assess the success of a balance is by plotting experimental and adjusted size values on the same graph. If the values are in line with each other, then the experimental size values are of good quality. A detailed description of this program can be found in (Napier-Munn et al. 2005)

5 CHAPTER FIVE: RESULTS AND DISCUSSIONS

5.1 Introduction

This chapter presents the results obtained from the testwork conducted in this study. Five different classification circuit configurations were tested and these included; a two-stage cyclone, an inclined cyclone, a fine screen, a hybrid cyclone-fine screen (2 stage) and a hybrid two cyclones-fine screen (3 stage). Firstly, the stability of the operational data retrieved from the online device (SCADA) during the period of the surveys are discussed as well as the sampling consistency. Thereafter, mass-balancing of experimental data to validate the integrity of the data obtained is discussed. Particle size distribution data of all the streams sampled in each circuit configuration is presented, followed by the efficiency curves to quantify the performance of each circuit. Comparisons of the total efficiencies of all the classification circuit configurations tested are thereby discussed and finally a summary of the results is presented.

5.2 Survey operational conditions

An indication of the degree of steady state can be established from the consistency of the operational data during which the tests were conducted. It is difficult to attain true steady state conditions in operations such as the one investigated in this study (Napier-Munn et al., 2005). An example is given in Figure 5-1 showing the time series graph of the operational data three hours before and one hour after the survey. The survey period is highlighted by the dashed box. The operating data which included: rod mill feed flowrate; primary cyclone cluster flowrate and inlet pressure; and secondary cyclone cluster flowrate and inlet pressure were retrieved from the SCADA system.

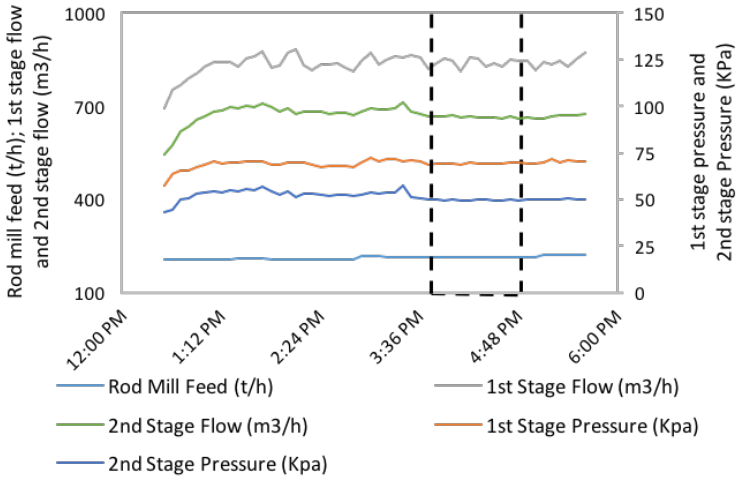

Figure 5-1: Operational data logged online during survey 1 (two-stage cyclone circuit)

Minor deviations in the operational data logged were realised as shown in Figure 5-1. This is typical in industrial scale operations because of large slurry flows (Napier-Munn et al., 2005). The slight deviations are usually regarded insignificant in such operations and as such the survey was deemed to have been conducted at steady state. Similar time series graphs were achieved for survey 4 and 5, presented in the section 8.1. Except for survey 2 were in the first hour of the three hours before the start of the survey the plant was down as can be seen from the rod mill curve. Also, just before the start of the survey was a slight pressure drop. This was due to the inclusion of the inclined cyclone which had a larger diameter than the usual vertical cyclones in the primary cluster, thus causing the pressure to drop. After realizing that the inlet pressure had reduced, the feed inlet valve to one of the cyclones was closed, triggering the sudden increase in pressure as shown in Figure 5-2. Immediately after the survey, the feed inlet valve to the inclined cyclone was closed and that to the vertical cyclone initially closed was opened, causing the pressure to drop back to its normal operational value.

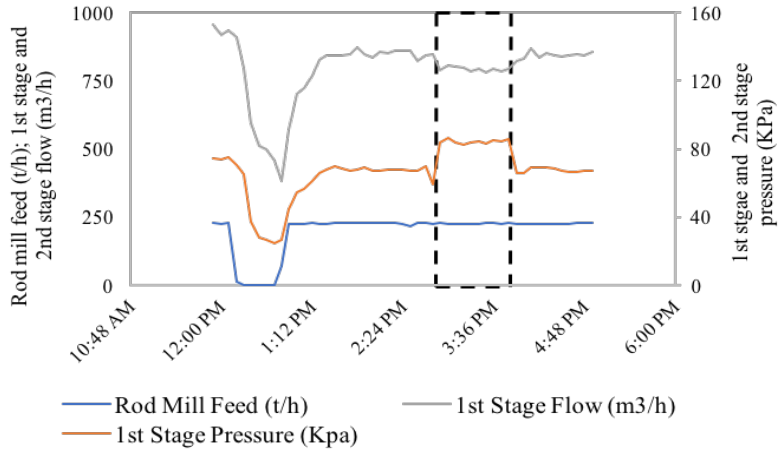

Figure 5-2: Operational data logged during survey 2 (inclined cyclone circuit)

In the case of survey 3, there was an abrupt drop in all the operational variables as shown in Figure 5-3. This was due to the plant being shut down after the survey was completed.

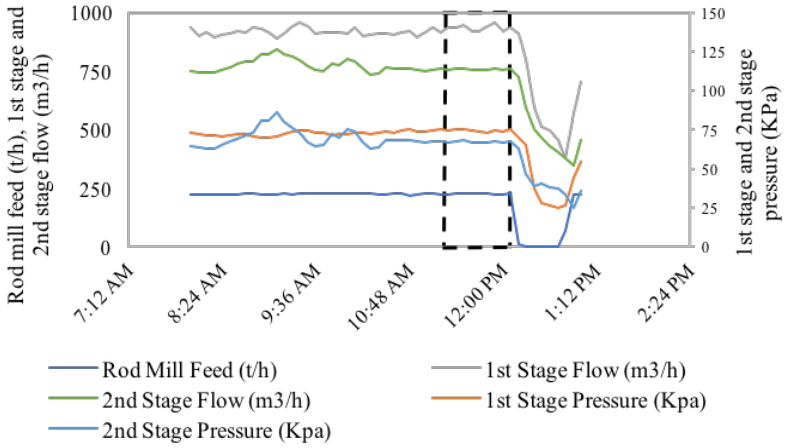

Figure 5-3: Operational data logged during survey 3 (fine screen circuit)

The averages and standard deviations of the logged operational data over the survey period for all the surveys conducted are shown in Table 5-1. It should be noted that survey 1, 2, 3, 4 and 5 denote two-stage cyclone, inclined cyclone, fine screen, hybrid cyclone-fine screen and hybrid two cyclones-fine screen circuits, respectively.

Table 5-1: Summary of averages and standard deviations of operational data recorded online during the one hour period of the survey

Operational parameter	Survey 1		Survey 2		Survey 3		Survey 4		Survey 5	
	Av.	Std. dev.	Av.	Std. dev.	Av.	Std. dev.	Av.	Std. dev.	Av.	Std. dev.
Rod mill feed (t/h)	215	0.41	225	0.64	226	1.56	214	2.73	224	0.54
1st stage flow (m^3/h)	841	16.86	796	11.85	931	14.06	957	22.21	939	20.87
Pressure 1 (KPa)	69	0.82	83	5.63	74	0.78	74	4.36	80	1.08
Slurry S.G 1	2.2	0.01	2.2	0.01	2.3	0.004	2.3	0.01	2.3	0.01
2nd stage flow (m^3/h)	605	5.59	-	-	756	3.6	810	18.89	792	13.71
Pressure 2 (KPa)	50	0.52	-	-	67	0.49	60	2.59	65	1.82
Slurry S.G 2	2.5	0.01	-	-	2.6	0.01	2.6	0.03	2.6	0.01

From Table 5-1, the standard deviations of the logged operational data were relatively low for all the surveys. Therefore, the deviations of data from the average values were not significant, of which the highest deviation was about 7%, indicating that the surveys were representative.

5.3 Consistency of sampling

To assess the consistency of sampling and sample preparation, the solids content obtained from the process samples and back-up samples of the feed and product streams of the various stages in all the circuit configurations tested were compared. Table 5-2 shows the percent solids by weight for the primary and back-up (A and B) samples from all the streams sampled. The results indicate that the relative errors were not significant with the highest being 10.6% for the screen feed sample obtained during survey 3. The percent solids results have shown that the solids content obtained were consistent and reproducible, thus the process of sampling was consistent.

Table 5-2: Comparison of solids content per stream obtained from processing and back-up samples for the five surveys carried out at BMM concentrator

Streams	Survey 1			Survey 2			Survey 3			Survey 4			Survey 5		
	A	B	Rel. Diff %	A	B	Rel. Diff %	A	B	Rel. Diff %	A	B	Rel. Diff %	A	B	Rel. Diff %
Primary cyclone feed	68.8	66.4	3.5	69.5	68.6	1.3	-	-	-	67.8	68.4	0.9	68.3	67.5	1.2
Primary cyclone underflow	80.6	80.3	0.4	81.5	82.0	0.6	-	-	-	81.4	88.8	9.1	82.1	82.3	0.2
Primary cyclone overflow	36.4	37.3	2.5	51.3	50.5	1.6	-	-	-	35.0	34.5	1.4	34.5	32.7	5.2
Secondary cyclone feed	74.0	74.3	0.4	-	-	-	-	-	-	-	-	-	68.5	69.6	1.6
Secondary cyclone underflow	81.2	82.3	1.4	-	-	-	-	-	-	-	-	-	77.6	81.1	4.5
Secondary cyclone overflow	42.4	41.8	1.4	-	-	-	-	-	-	-	-	-	43.0	41.2	4.2
Screen feed	-	-	-	-	-	-	13.2	14.6	10.6	32.4	33.6	3.7	31.3	31.1	0.6
Screen oversize	-	-	-	-	-	-	22.9	22.8	0.4	40.3	40.9	1.5	33.7	33.5	0.6
Screen undersize	-	-	-	-	-	-	4.9	5.2	6.1	11.3	10.9	3.5	19.4	18.2	6.2

Another significant observation that was made from the percent solid data presented in Table 5-2, was that the feed solids concentration for both primary and secondary cyclones was generally high all above 65% with the highest being the secondary cyclone at 74% in survey 1. Jankovic and Valery (2012) reported that cyclones are operated with typical feed densities of 55 to 65% by weight in modern mill circuits to achieve a product P80 in the range of 100µm - 200µm. Most of the cyclone underflow streams exhibited high solid concentrations above 80% and in mineral processing norms 75% is thought to be ideal.

5.4 Mass balancing of experimental data

Mass balancing is a method used to assess the integrity and consistency of data obtained by sampling in a processing plant or circuit and to supply missing data such as flowrates that could not be measured during the experiment (Napier-Munn et al., 2005). Ideally, the purpose of sampling is to collect representative stream data, but this is rarely achieved in practice as in any sampling exercise, errors are inevitable. These errors are typically introduced because of plant dynamics, analytical errors, random errors or even human errors. The experimental data obtained from the surveys performed included: particle size distribution; water flowrate; solids flowrate;

and solid concentration of the feed and product streams. Mass balancing was performed for data from each test using a program called JKMBal incorporated in JKSimMet software described in section 4.6.

A summary of the mass balanced output comparing the experimental and balanced data for two-stage cyclone circuit configuration is illustrated in Table 5-3 and the particle size distribution data is given in section 5.5.

Table 5-3: Experimental and mass balanced data for the two-stage cyclone circuit configuration

Stream properties	Cyclone 1 feed		Cyclone 1 underflow		Cyclone 1 overflow		Cyclone 2 feed		Cyclone 2 underflow		Cyclone 2 overflow		Cyclone 1 overflow + Cyclone 2 overflow	
	Exp.	**Bal.**	**Exp.**	**Bal.**	**Exp.**	**Bal.**	**Exp.**	**Bal.**	**Exp.**	**Bal.**	**Exp.**	**Bal.**	**Exp.**	**Bal.**
TPH Solids	1287	1287	1098	1098	189	188	1098	1098	980	980	118	118	307	307
TPH Water	584	591	265	261	330	329	386	386	227	225	161	161	487	491
% Solids	69	69	81	81	36	36	74	74	81	81	42	42	39	38
% -75 (um)	24	24	16	16	71	70	16	16	12	12	44	44	60	60
P80 (mm)	0.288	0.292	0.319	0.319	0.097	0.097	0.319	0.319	0.338	0.333	0.178	0.178	0.130	0.131

5.5 Stream particle size distribution

The mass balanced data in Figure 5-4 to Figure 5-8 are represented by the line and the experimental data by the marker for each stream that was analysed in the two-stage cyclone, inclined cyclone, fine screen, hybrid cyclone-fine screen and hybrid two cyclones-fine screen circuit configurations, respectively. It can be seen that the mass balanced data matched the experimental data well indicating that the sampling campaigns were successfully conducted and the data collected was of acceptable quality. However, in Figure 5-8 minor variations were observed in the screen feed and oversize stream of the hybrid two cyclones-fine screen circuit. This could be due to errors introduced during sampling and sample preparation.

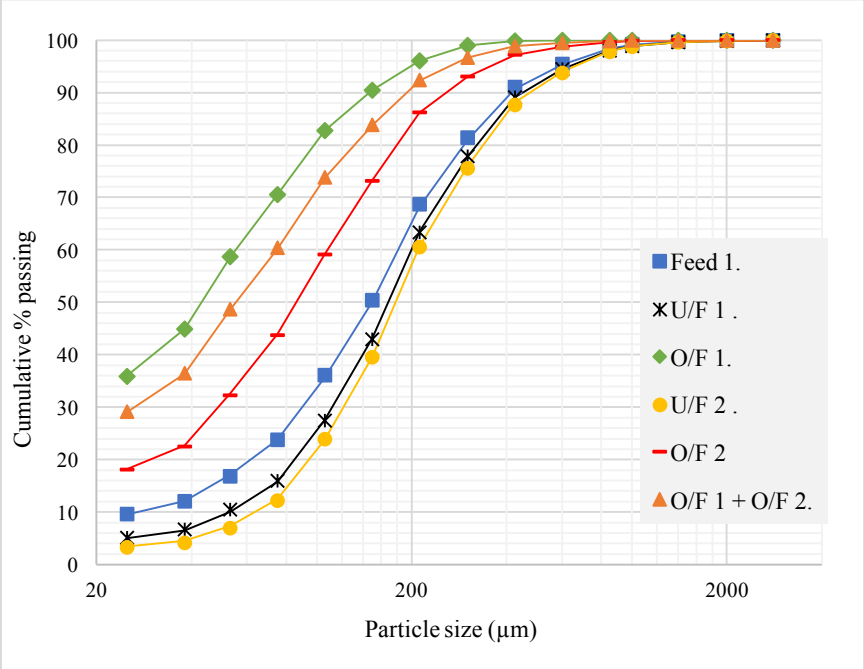

Figure 5-4: Comparison of mass balanced data (line) against experimental data (marker) of the particle size distribution for two-stage cyclone circuit configuration

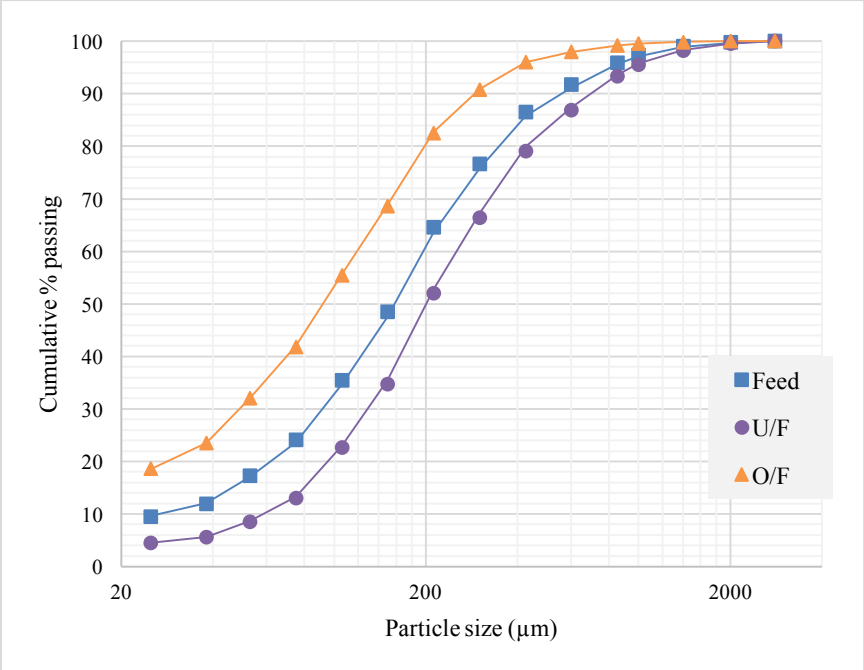

Figure 5-5: Comparison of mass balanced data (line) against experimental results (marker) of the particle size distribution for inclined cyclone circuit configuration

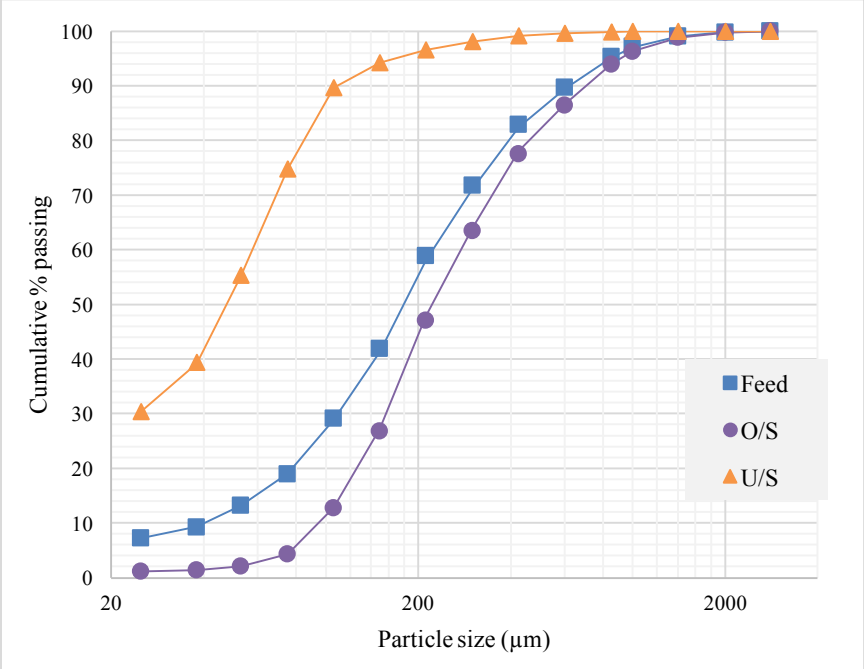

Figure 5-6: Comparison of mass balanced data (line) against experimental results (marker) of the particle size distribution for fine screen circuit configuration

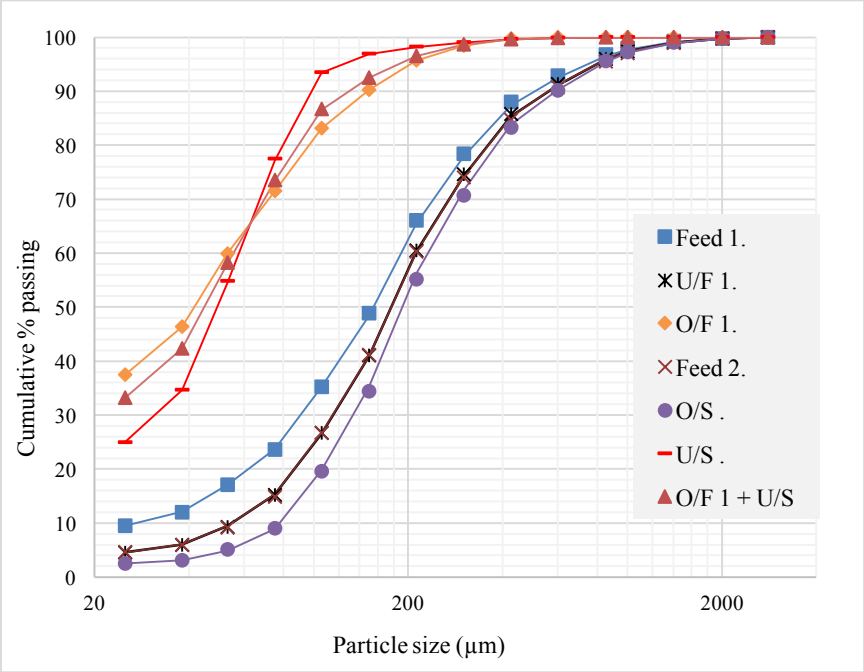

Figure 5-7: Comparison of mass balanced data (line) against experimental results (marker) of the particle size distribution for hybrid cyclone-fine screen circuit configuration

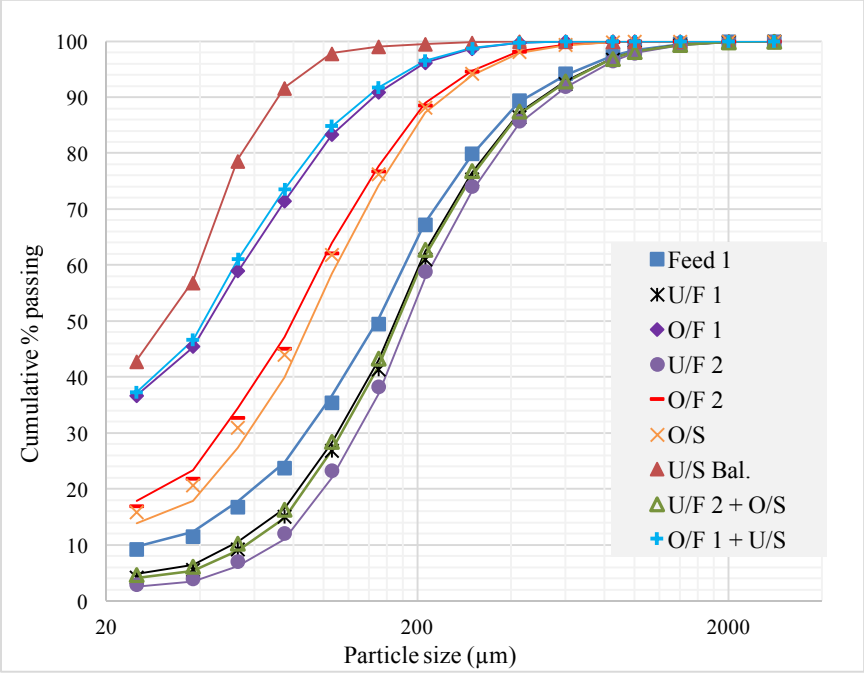

Figure 5-8: Comparison of mass balanced data (line) against experimental results (marker) of the particle size distribution for hybrid two cyclones-fine screen circuit configuration

According to Drzymala (2007), evaluation of particle separation based on the size distribution curve is achieved by comparing the shape of the product curves with the curve for the feed. In the case when separation does not occur, the distribution curves for the products are the same as for the feed. Also, Wills and Napier-Munn, (2006) state that normally the distribution curves are S-shaped, resulting in crowded plots at finer particle sizes. Thus, the summary of particle size distributions obtained for all configurations tested show that the streams follow the expected trends as described above.

5.5.1 Comparison of circuit product size distribution

The circuit feed and final product size distribution data of all the circuit configurations tested are presented in Figure 5-9 and Figure 5-10, respectively.

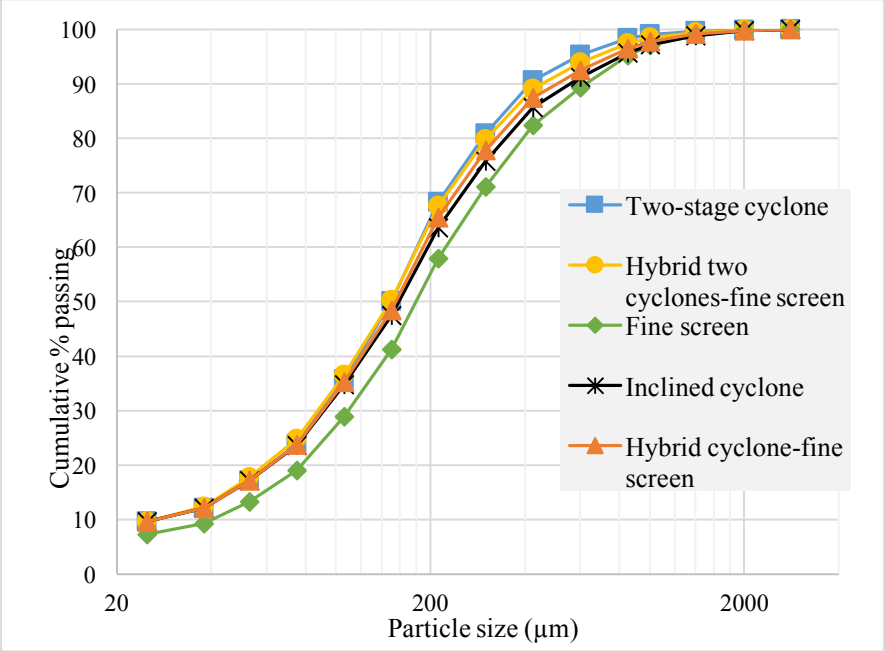

Figure 5-9: Feed particle size distribution data of the classification circuit configurations tested

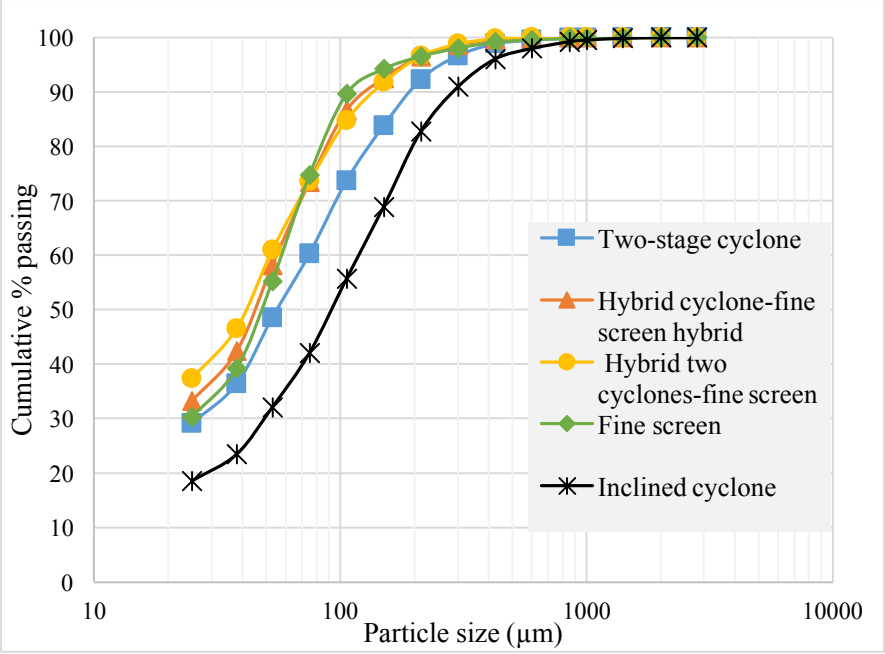

Figure 5-10: Final product particle size distribution data of the classification circuit configurations tested

A shift of the size distribution curve to the right indicates a coarser grind whereas, to the left a finer grind. Figure 5-9 shows that the feed size distribution for all the configurations tested had were similar, thus for comparison purposes, the feed appeared quite consistent even though the fine screen configuration revealed a slightly coarser feed which is not unusual in industrial based studies. This could be due to the plant dynamics as it is not possible to have a constant feed. But, the difference was minimal, thus the effect was considered insignificant.

The particle size distributions of the final product streams of all circuit configurations tested (Figure 5-10) showed that the inclined cyclone configuration had the coarsest grind size of 41.84% sub 75µm material while the two-stage cyclone exhibited a product size of 60.40% sub 75µm material. In comparison with the target grind size of the plant of 65% sub 75µm, the inclined cyclone and two-stage cyclone configurations yielded coarser products. The fine screen, hybrid cyclone-fine screen and hybrid two cyclones-fine screen configurations gave finer product grind sizes of 74.8%, 72.3% and 71.8% sub 75µm, respectively. It was also observed that the hybrid two cyclones-fine screen circuit had more fine particles at very fine sizes (40% sub 25µm) compared to the other circuits. This could be because of the effect of reclassifying the cyclone overflow stream in a separate classifier unit. For this reason substantial amounts of fine material were recovered in the final product stream. (Peterson & Herbst, 1984; Napier-Munn et al., 2005).

5.6 Efficiency curves

Efficiency curves were used to assess the performance of the different classification systems used in this work. The curves were generated from the particle size distribution data and the solid flowrates of the feed and product streams of the classifier for individual stages and the feed and product streams of the classification system for overall performance. Efficiency curve properties such as sharpness of separation, assessed from the slope of the corrected and reduced curves; water split to the coarse product, which is the lowest point of the actual curve; and corrected cut size obtained from the corrected curve are used as performance indicators.

The overall performance of configurations comprising of multi-stages of classification were calculated using Equation 5-1 and Equation 5-2 suggested by Luckie & Austine (1973). Equation 5-1 was used when evaluating the overall performance of circuit configurations with classifiers connected in series when the coarse stream of the classifier was reclassified in a separate unit whereas, Equation 5-2 was applied when a fine stream was being reclassified in another unit.

$$E_T = E_1 \times E_2$$

Equation 5-1

$$(1 - E_T) = (1 - E_1)(1 - E_2)$$

Equation 5-2

The actual, corrected and reduced efficiency curves developed from the experimental work for each of the classification configurations tested are presented in Section 5.6.1 to 5.6.3.

5.6.1 Actual efficiency curve

The actual efficiency curve is plotted to obtain the actual cut size and bypass fraction as discussed in section 2.3. Figure 5-11 to Figure 5-15 shows the actual efficiency curves of the individual stages and overall classification systems for the configurations tested.

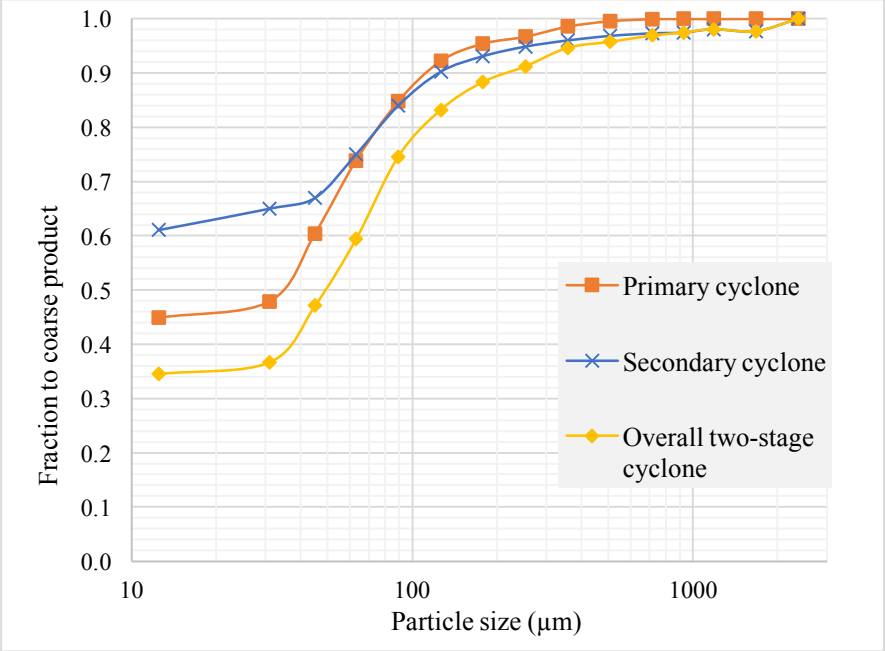

Figure 5-11: Actual efficiency curves of the individual classification stages and overall two-stage cyclone circuit configuration

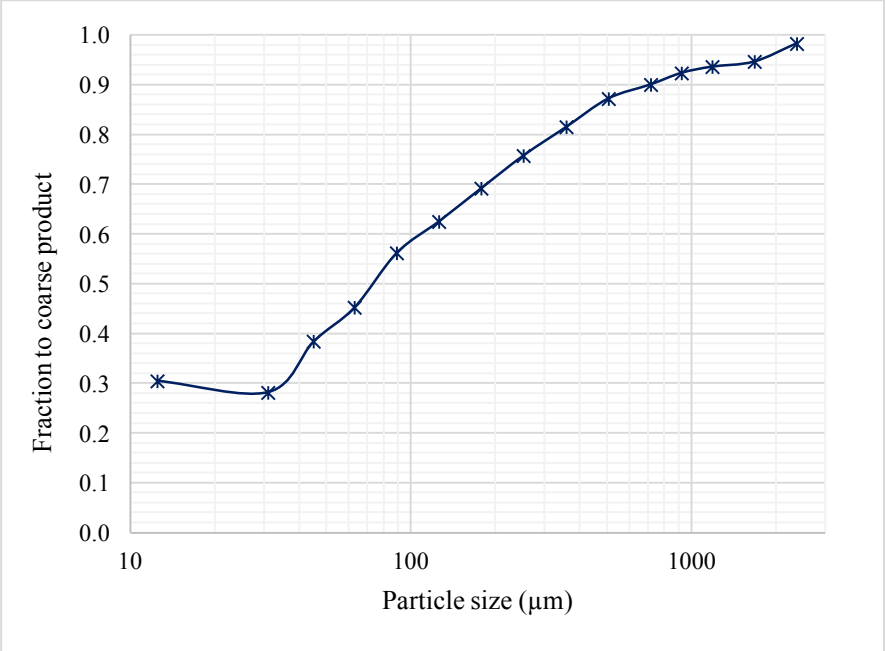

Figure 5-12: Actual efficiency of the inclined cyclone circuit configuration

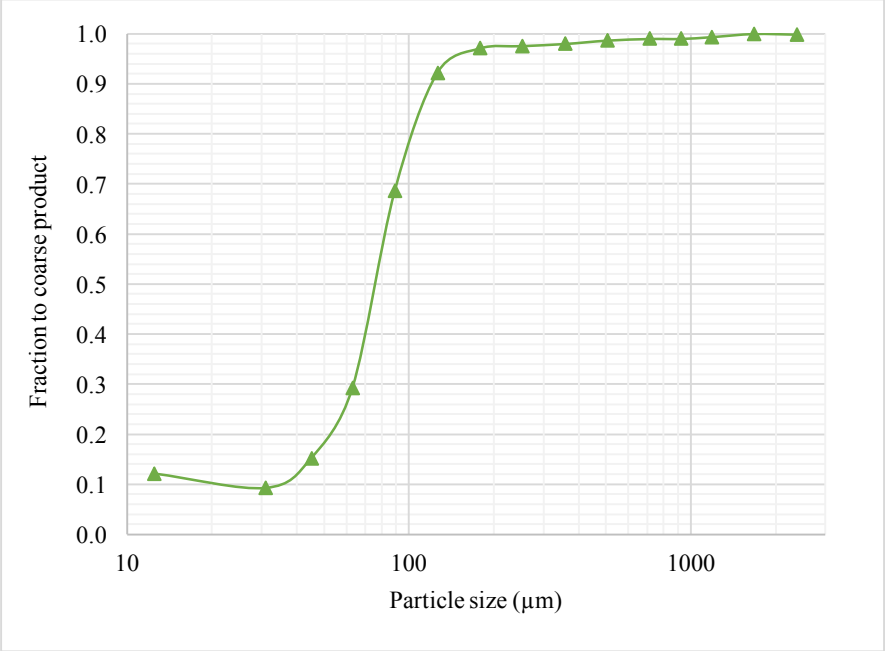

Figure 5-13: Actual efficiency of the fine screen circuit configuration

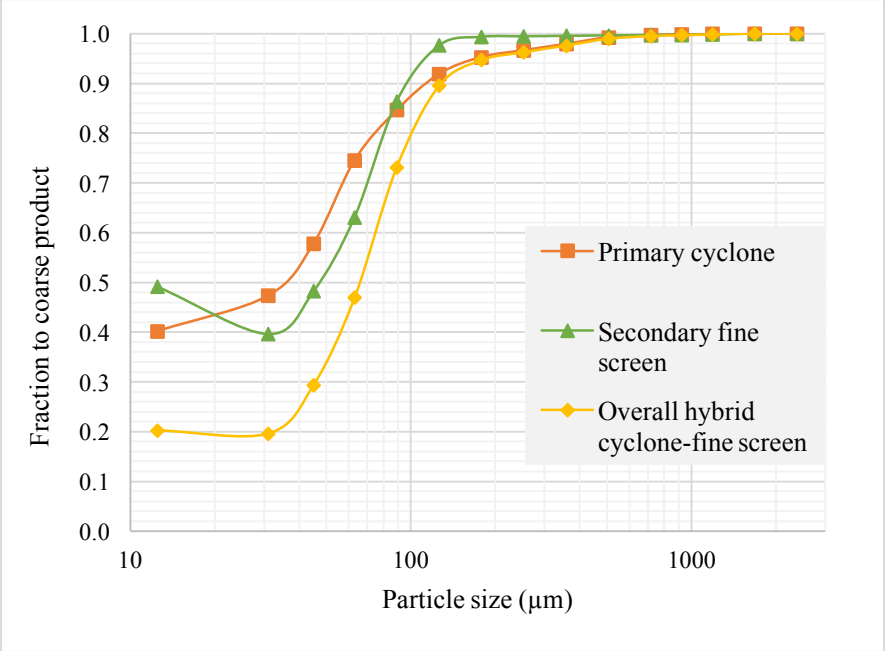

Figure 5-14: Actual efficiency curves of the individual classification stages and overall hybrid cyclone-fine screen circuit configuration

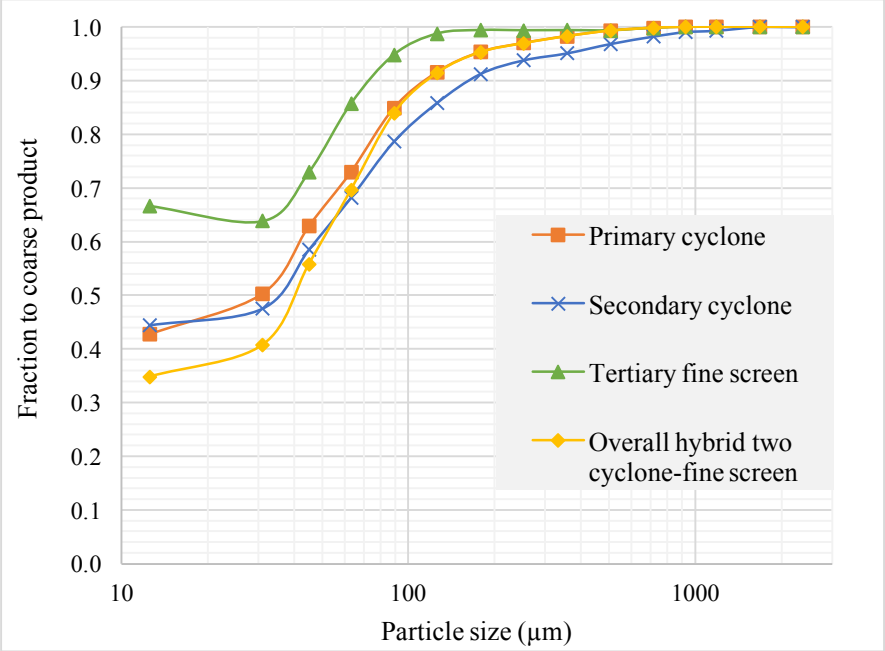

Figure 5-15: Actual efficiency curves of the individual classification stages and overall hybrid two cyclones-fine screen circuit configuration

The actual efficiency curves of the primary cyclone, secondary cyclone and the overall two-stage cyclone system are shown in Figure 5-11. It was found that the secondary cyclone had excessive amounts of feed water reporting to the underflow of approximately 65%. This could be attributed to high solids concentration in the secondary cyclone feed which was about 74%. High solids concentration increases the effective slurry viscosity as well as the degree of hindered settling (Wills & Napier-Munn, 2006). A study by Kawatra et al. (1996) investigated the effect of slurry viscosity on performance using a 102mm diameter cyclone and found that water recovery to the underflow increased with increasing slurry viscosity. This is in agreement with the findings by Wills and Napier-Munn (2006) who noted that high feed solids concentration in cyclones leads to great resistance of slurry to the swirling motion inside the cyclone, which in turn reduces the effective pressure drop, consequently causing most of the feed slurry to report to the underflow stream. Similarly, relatively high feed water of approximately 45% was seen in the primary cyclone underflow stream. Rogers et al. (1981) have reported that water recovery to the underflow of about 20 to 50% is common in cyclone operations. A case study by Dündar et al. (2014) conducted at Catalina Huanca mine treating a Cu-Zn-Pb ore with feed rates of 396t/h and

569t/h produced bypass percentages of 39% and 51%, respectively. This supports the view that cyclones generally have high water recovery to underflow stream possibly due to hydrodynamic effects, especially in mineral processing plants treating multi-density ores such as the Cu-Zn-Pb ore used in this study. However, Napier-Munn et al. (2005) commends that it is desirable to limit the fraction of water reporting to cyclone underflow to less than about 40% in order to give reasonable efficiency. The overall two-stage cyclone showed a lower bypass fraction of approximately 34%. The decrease in fines bypass could be attributed to the application of multiple stages of classification. Reclassification of the primary underflow in a secondary cyclone will reduce the overall fines bypass of a circuit. This is because any fine particle that short-circuits the primary cyclone will have a second chance through another cyclone, resulting in a lower bypass fraction. This is in line with the observations made by Rogers et al. (1981) who, through computer simulations, found that the bypass reduced from 30% in a single cyclone to about 9% in two-stage cycloning. Also, Dahlstrom & Kam (1988) using simulations, showed that energy saving of about 6 to 30% could be achieved with the use of two-stage cycloning due to reduced fines bypass recirculating to the mills. Other researchers who also used simulations have reported similar findings (Kelsall, Stewart & Restarick, 1974b; Luckie, Hogg & Schaller, 1980; Peterson & Herbst, 1984; Honaker, Boaten & Luttrell, 2007).

The actual efficiency curve of the inclined cyclone configuration is illustrated in Figure 5-12. Approximately 30% of the cyclone feed water was recovered to the underflow. Napier-Munn et al. (2005) concluded that 30 to 40% water to the cyclone underflow gives reasonable efficiency. The resulting relatively low water split to the underflow could be attributed to the effect of inclination at constant pressure which increases the axial velocity flow (Vakamalla et al., 2014). Asomah & Napier-Munn (1996) performed experiments at low pressures on various sizes of cyclones ranging from 102 to 508mm at different inclinations. They found that mounting cyclones at 45° or more to the vertical would reduce the water recovery to the underflow and consequently produce denser underflows. Vakamalla et al. (2014) performed tests on a 75mm diameter cyclone at 0°, 30°, 45° and 60° inclinations to the vertical and confirmed the findings reported by Asomah & Napier-Munn (1996).

The fine screen circuit had low fines bypass fraction to the oversize of about 12% as shown in Figure 5-13. This is typical in screen operations because classification of particles is based on size only, unlike cyclone operations in which both particle size and density are considered. According to Dündar et al. (2014) and Mainza (2016) reduction of fine material short-circuiting to the oversize translates to a sharper separation and reduces the circulating load in the circuit, thus resulting in increased capacity. Several case studies (Albuquerque et al., 2008; Brodzik, 2009; Valine, Wheeler & Albuquerque, 2009; Dündar et al., 2014; Mainza, 2016) where cyclones were replaced with fine screens agrees with the findings of this study.

In Figure 5-14, the actual efficiency curves to the coarse product for the primary cyclone, fine screen in the secondary stage and overall hybrid cyclone-screen fine circuit are illustrated. The primary cyclone had a relatively high bypass percentage of 40% which could be attributed to the density effect as discussed earlier. The fine screen in the secondary stage reclassifying the cyclone underflow stream showed a higher water split to the oversize percentage of about 49%. The unusual high water split could be due to excessive water addition on the screen for re-pulping via the nozzle sprays installed along the screen consequently, increasing the slurry flowrate on the screen surface and causing a more dilute slurry. As much as screening operations favors dilute slurries (Valine & Wennen, 2002), a high slurry flowrate on the screening surfaces reduces the chance of fine particles from accessing the screen openings because of reduced residence time which will result in most of the screen feed reporting to the oversize. According to Matthew (1985), the benefit of using spray waters can only be realised if the correct amount of water is added. Nonetheless, the overall two-stage cyclone-fine screen hybrid circuit significantly reduced the water split to the coarse product to approximately 20%. This could be due to the application of multi-stages of classification as alluded to earlier. In Comparison with the overall two-stage cyclone, the results showed 14% lower water split to the coarse product. This was because in the hybrid circuit the fine screen classifier was used to reclassify the primary underflow, thus classifying particles on the basis of size only. Unlike in the two-stage cyclone circuit where the secondary stage of classification had the cyclone classifier which takes into account both particle size and density.

Approximately 43% and 44% feed water recovery to the underflow streams for the primary and secondary cyclones, respectively, were observed in the hybrid two cyclones-fine screen circuit as shown in Figure 5-15. The percentages found in this study are within the typical cyclone range of 20 to 50% as reported by Rogers et al. (1981). More than 65% of feed water reported to the screen oversize for the tertiary stage of classification. This could be attributed to a high slurry flowrate on the screen, which in turn reduced the residence time thus forcing a significant fraction of the feed material to report to the oversize. However, the overall water split to the coarse product of the circuit was found to have reduced to about 35% due to multi-stage classification. The overall circuit showed the highest water split to the coarse product compared to the other configurations.

5.6.2 Corrected efficiency curve

To remove the influence of the bypass, the actual efficiency curves are corrected. Thus, the corrected curve expresses efficiency of separation by true classification only. The slope and the size of separation also known as cut size of the corrected curve are used to assess the performance of a classifier. The steeper the slope of the curve the greater the separation efficiency. Figure 5-16 to Figure 5-20 shows the corrected efficiency curve of the individual stages and overall classification circuits for the configurations tested.

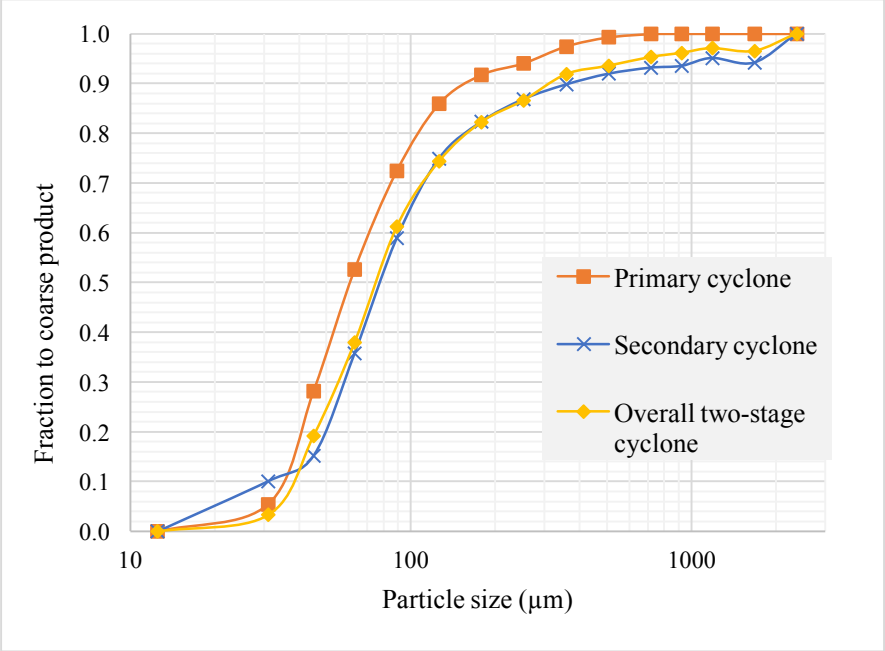

Figure 5-16: Corrected efficiency curves of the individual classification stages and overall two-stage cyclone circuit configuration

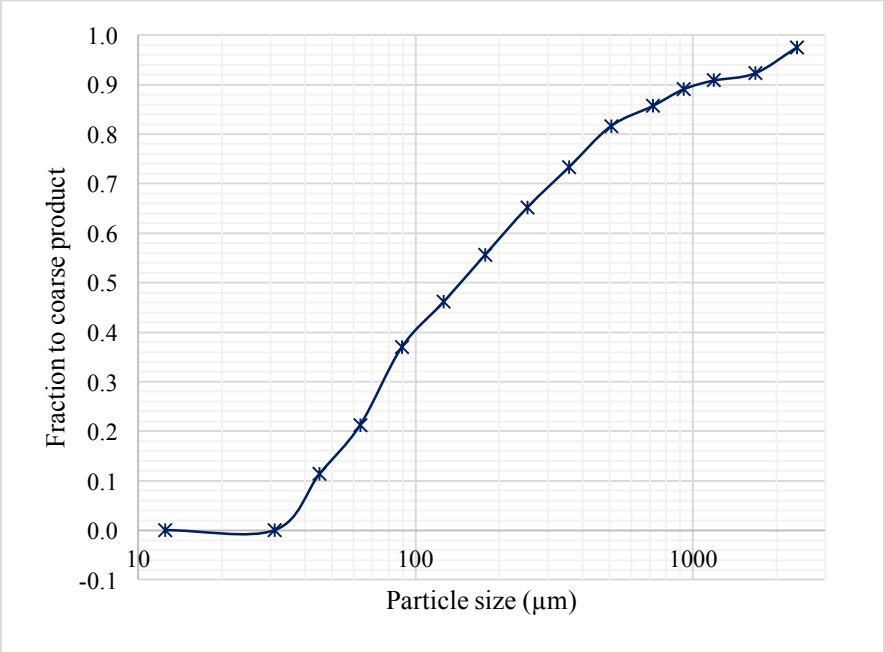

Figure 5-17: Corrected efficiency curves of the inclined cyclone circuit configuration

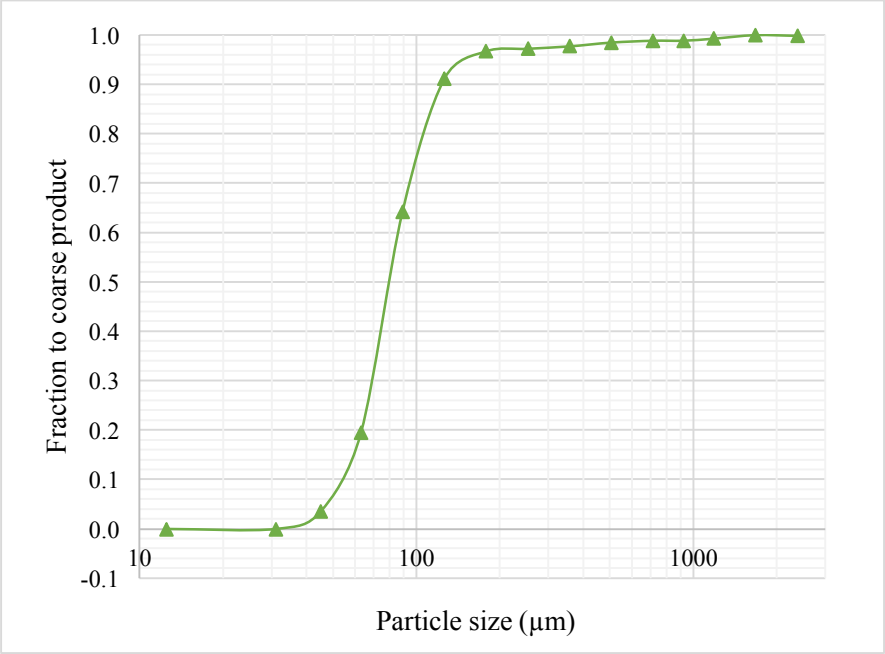

Figure 5-18: Corrected efficiency curves of the fine screen circuit configuration

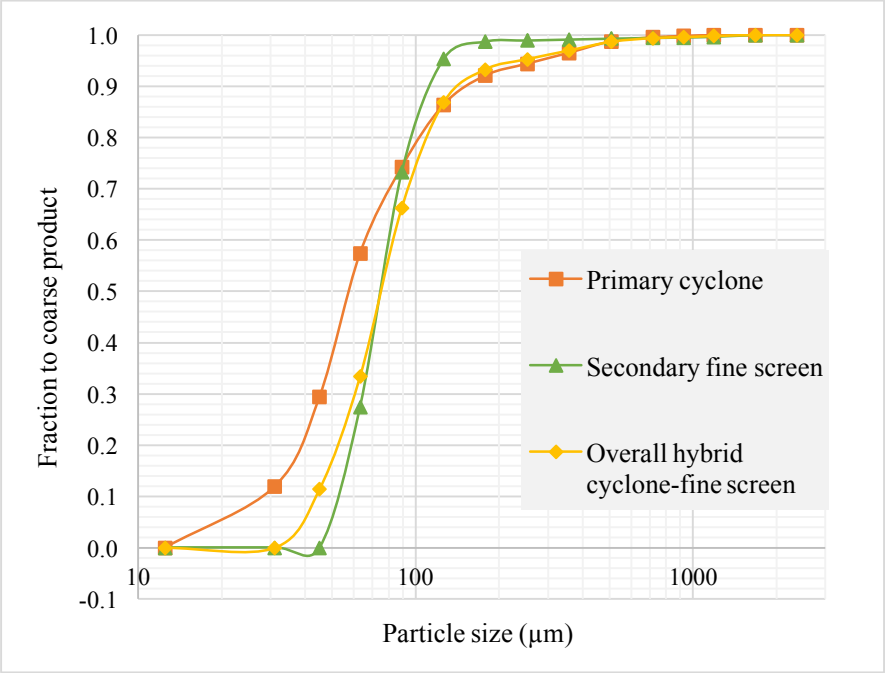

Figure 5-19: Corrected efficiency curves of the individual classification stages and overall hybrid cyclone-fine screen circuit configuration

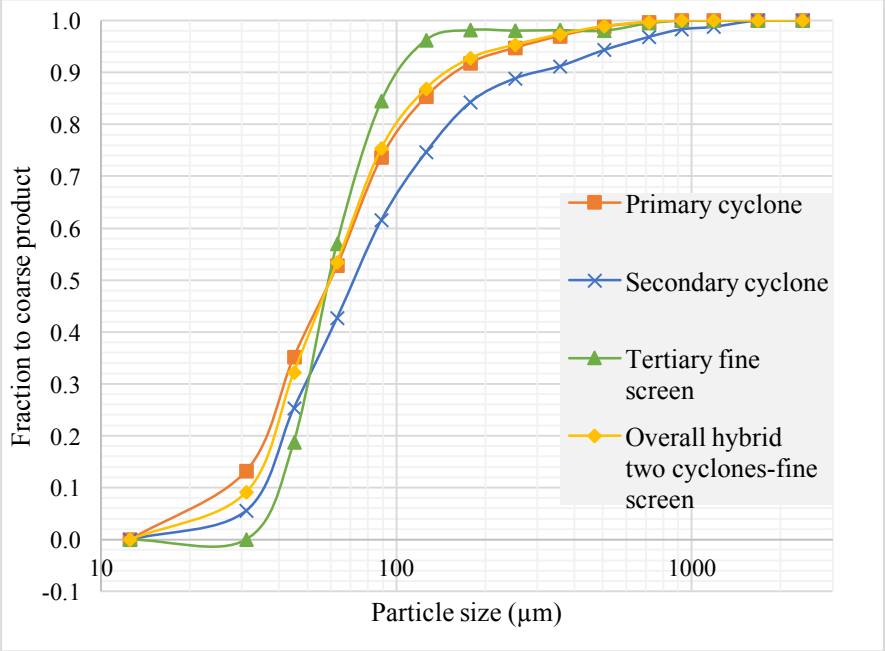

Figure 5-20: Corrected efficiency curves of the individual classification stages and overall hybrid two cyclones-fine screen circuit configuration

Table 5-4 shows the solid mass flowrates of the feed and product streams of individual stages in the circuits and the overall classification configurations. However, it should be noted that the feed flowrate of the inclined cyclone circuit, fine screen circuit, secondary fine screen in the hybrid cyclone-fine screen circuit, and the tertiary fine screen in the hybrid two cyclones-fine screen circuit were scaled-up to represent the nominal feed rate to the individual stages recorded on the SCADA system during the period of the surveys. The flowrates of the product streams were then calculated from the feed flowrate ratio of the actual and the value obtained from the SCADA system. Though the flowrates were scaled-up, the separation efficiency was assumed constant as the number of units can be increased to cope with the increase in the tonnage.

Table 5-4: Summary of solids mass flowrates of individual stages of classification in each circuit configuration tested

Circuit configuration	Stages	Feed (tph)		Coarse (tph)		Fines (tph)	
		Actual	Scaled-up	Actual	Scaled-up	Actual	Scaled-up
Two-stage cyclone	Primary cyclone	1287	-	1098	-	189	-
	Secondary cyclone	1098	-	980	-	118	-
Inclined cyclone	Inclined cyclone	405	1214	258	772	147	442
Fine screen	Fine screen	3.2	798	2.5	631	0.7	167
Hybrid cyclone-fine screen	Primary cyclone	1498	-	1272	-	227	-
	Secondary fine screen	9	1272	8.2	1153	0.8	118
Hybrid two cyclones-fine screen	Primary cyclone	1424		1209		215	
	Secondary cyclone	1209		1027		182	
	Tertiary fine screen	9.9	182	8.5	157	1.4	25

Figure 5-16 shows the corrected efficiency curves of the primary cyclone, secondary cyclone and overall two-stage cyclone circuit. It was observed that the primary cyclone exhibited a finer cut compared to the secondary cyclone and overall two-stage cyclone circuit. This was due to the secondary cyclone feed being coarser than the primary cyclone feed. The overall two-stage cyclone curve revealed a trend similar to the secondary cyclone curve except at the coarser and finer sizes. This was because the split in the primary cyclone was substantially high at approximately 1098tph to the underflow which was then reclassified in the secondary cyclone as shown in Table 5-4. The primary cyclone exhibited an efficiency curve with a steeper slope than the secondary cyclone and the overall was an average of the two classification stages.

The inclined cyclone corrected efficiency curve shown in Figure 5-17 had a flatter efficiency curve, implying the separation was not sharp. Also, a coarser separation was realised which could have been due to the short-circuiting of the coarse particles to the overflow. This is in line with Asomah & Napier-Munn (1996) who noted that inclining large cyclones typically cut coarser.

A steeper efficiency curve was observed for the fine screen circuit as illustrated in Figure 5-18. This could be attributed to the screens ability to allow most undersize particles to pass through the openings and retain the oversize particles, thus minimises the fines carryover to the oversize product resulting in reduced circulating load. This has been demonstrated in case studies where the application of fine screens in closed-circuit grinding operations reduced the bypass from approximately 35% with cyclones to about 10%, consequently reducing the circulating load from 244% to 108% (Valine, Wheeler & Albuquerque, 2009; Dündar et al., 2014).

The efficiency curves of the primary cyclone, secondary fine screen and overall hybrid cyclone-fine screen circuit are presented in Figure 5-19. The secondary fine screen revealed a sharper curve compared to the primary cyclone, which is as expected because the use of screens in closed-circuit grinding operations normally results in reduced circulating load by minimising the misplacement of fine particles in oversize. Several studies have shown that there is a significant reduction in the circulating load where fine screens were applied (Albuquerque et al., 2008; Brodzik, 2009; Mainza, 2016).

Figure 5-20 shows the efficiency curves of the primary cyclone, secondary cyclone, tertiary fine screen and the overall hybrid two cyclones-fine screen circuit. Again, the tertiary stage comprising of a fine screen exhibited a steeper curve than both the primary and secondary cyclones. This is attributed to the screen separation being based on particle size only, thus permitting particles smaller than the screen opening to pass through and those larger to be retained on the screen surface.

5.6.3 Whiten efficiency model fitting to experimental data

The Whiten model was graphically fit to the efficiency curves established from the experimental data for each of the classification configuration tested. The corrected efficiency curves from the experimental data (marker) fitted with the Whiten model (line) for individual stages and overall system of the all the classification configurations tested are shown in Figure 5-21 to Figure 5-25. The parameters for the efficiency properties used to assess the performance are presented in Table 5-5 to Table 5-10.

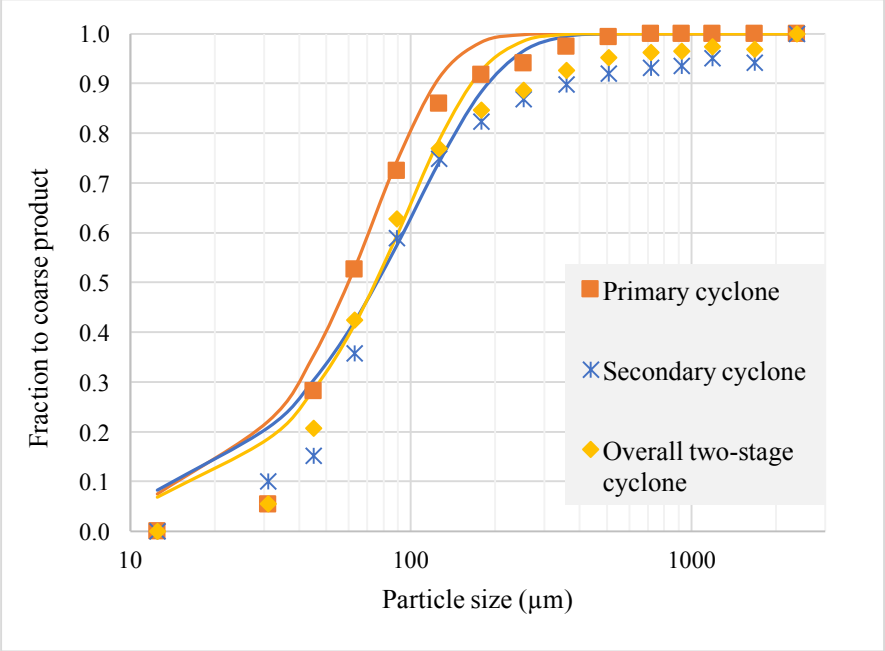

Figure 5-21: Corrected efficiency curves fitted to the Whiten model (line) of the primary cyclone, secondary cyclone and the overall two-stage cyclone circuit configuration

Table 5-5: Efficiency parameter values of individual stages and the overall two-stage cyclone circuit configuration

Efficiency parameter	Efficiency values		
	Primary cyclone	**Secondary cyclone**	**Overall two-stage cyclone**
Sharpness of separation (α)	2.0	1.4	1.7
Water recovery to coarse product (Rf)	0.45	0.61	0.34
Corrected cut size - µm (d50c)	60	76	75
Beta (β)	0.00	0.00	0.00

From Table 5-5, it can be seen that the primary cyclone performed relatively better than the secondary cyclone and the overall classification system. The values of α obtained were 2.0, 1.4 and 1.7 for primary cyclone, secondary cyclone and overall system, respectively. According to Tarr Jr. (1985) and Gupta and Yan (2006), an α value of about 2.5 is common for most cyclones in closed-circuit grinding operations and the higher the α value the sharper the separation. Thus, the primary cyclone had a sharper classification than the secondary cyclone and the overall was in between the two stages of classification.

The water recovery to the underflow for both primary and secondary cyclones were substantially high, with the secondary cyclone having more than 60% whereas the primary cyclone showed a percentage of about 46%. These results imply that there were significant amounts of fines bypassing the process of classification in both stages. Kelsall (1953) proposed that the fraction of feed water reporting to the underflow is directly proportional to the fraction of fines misplaced in the underflow stream. Therefore, the lower the value of R_f the higher the efficiency of classification. However, the overall two-stage cyclone revealed a lower value of R_f of 34%. This is because the fines particles that bypassed the primary cyclone had a second pass in a separate cyclone, thus reducing the fines bypass in the overall two-stage cyclone. Computer simulation studies done by Rogers et al. (1981) and Peterson & Herbst (1984) showed that fines bypass was reduced from about 30% and 42% in a single cyclone to around 9% and 19% in overall two-stage cyclone circuit, respectively. It is also worth noting that in these studies the primary cyclone was considered as the single-cyclone and the performance of the secondary cyclones were not shown in the articles, thus their efficiencies are not known. However, even though the results found in this work show a sharp reduction in the fines bypass, the α value for the overall two-stage cyclone was slightly lower than that of the primary cyclone implying that the single cyclone gave a slightly sharper classification. This could be due to the poor performance of the secondary cyclone, whose feed was comprised of the primary cyclone underflow and fed at high solids concentration as illustrated in Table 5-6. Svarovsky (1984) notes that classifying slurry containing substantial amounts of coarse particles is by existence difficult to handle in cyclone classifiers because particles will settle readily on entry into a ribbon of solids on the wall, swirling into the underflow carrying most of the feed material. Table 5-6 illustrates that most of the feed water reported to the underflow of the secondary cyclone, implying that significant fines bypassed the cyclone.

Table 5-6: Solids and water flowrate mass balance of the feed and product streams of the two-stage cyclone circuit configuration

Stream properties	Cyclone 1 feed		Cyclone 1 U/F		Cyclone 1 O/F		Cyclone 2 feed		Cyclone 2 U/F		Cyclone 2 O/F		Cyclone 1 O/F + Cyclone 2 O/F	
	Exp.	**Bal.**	**Exp.**	**Bal.**	**Exp.**	**Bal.**	**Exp.**	**Bal.**	**Exp.**	**Bal.**	**Exp.**	**Bal.**	**Exp.**	**Bal.**
Solids (tph)	1287	1287	1098	1098	189	188	1098	1098	980	980	118	118	307	307
Water (tph)	584	591	265	261	330	329	386	386	227	225	161	161	487	491

The corrected cut size of both stages and the overall two-stage cyclone circuit were found to be relatively fine, thus the assumption that most of the particles recovered to the final product were fully liberated although supporting mineralogy data to validate this was not available.

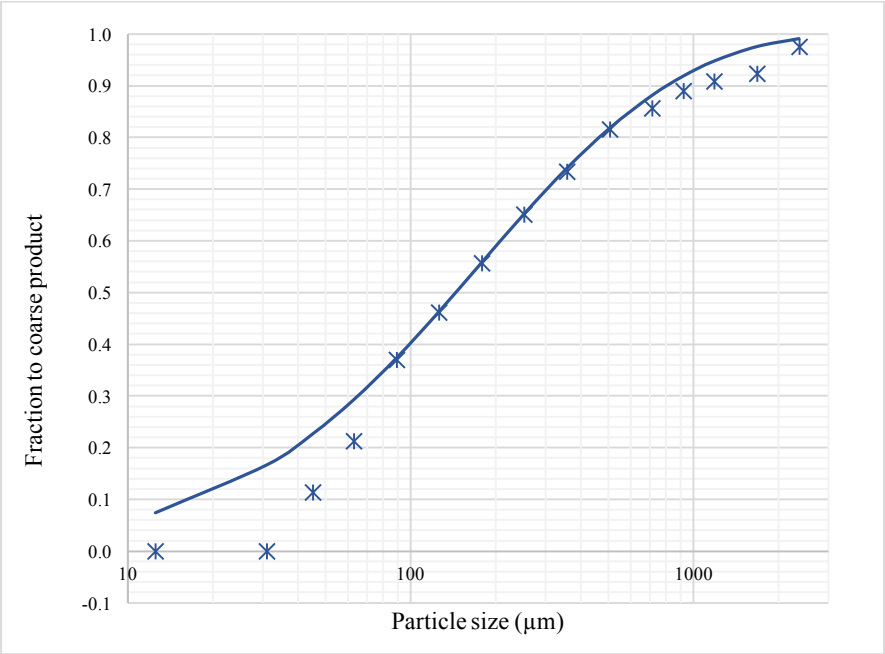

Figure 5-22: Corrected efficiency curve of the inclined cyclone circuit configuration fitted with Whiten model (line)

Table 5-7: Efficiency parameter values of the inclined cyclone circuit configuration

Efficiency parameters	Value
Sharpness of separation (α)	0.54
Corrected cut size - µm (d50c)	147
Water recovery to coarse product (Rf)	0.30
Beta (β)	0.03

The corrected efficiency curve fitted with the Whiten model for the incline cyclone circuit is shown in Figure 5-22 and its parameter values extracted from the model are presented in Table 5-7. A fish-hook was seen at the finer sizes of the actual efficiency curve (Figure 5-12) and thus the beta parameter was also fitted. The α value was found to be 0.54. This is low and is indicative of a poor sharpness of separation. This could be because of the coarser cut of 147µm obtained, which implies that there was short-circuiting of coarse particles to the overflow. Vakamalla et al. (2014) and Asomah and Napier-Munn (1996) also observed coarser cut sizes in inclined cyclones compared to vertically mounted cyclones.

The water recovery to the underflow was found to be 30% and is indicative of a good operating range according to Napier-Munn et al. (2005). The lower value of R_f could be attributed to the inclination effect which results in increased axial velocity flow, leading to lower amounts of feed water reporting to the underflow stream. Similar findings have been reported by Asomah & Napier-Munn (1996) and Vakamalla et al. (2014).

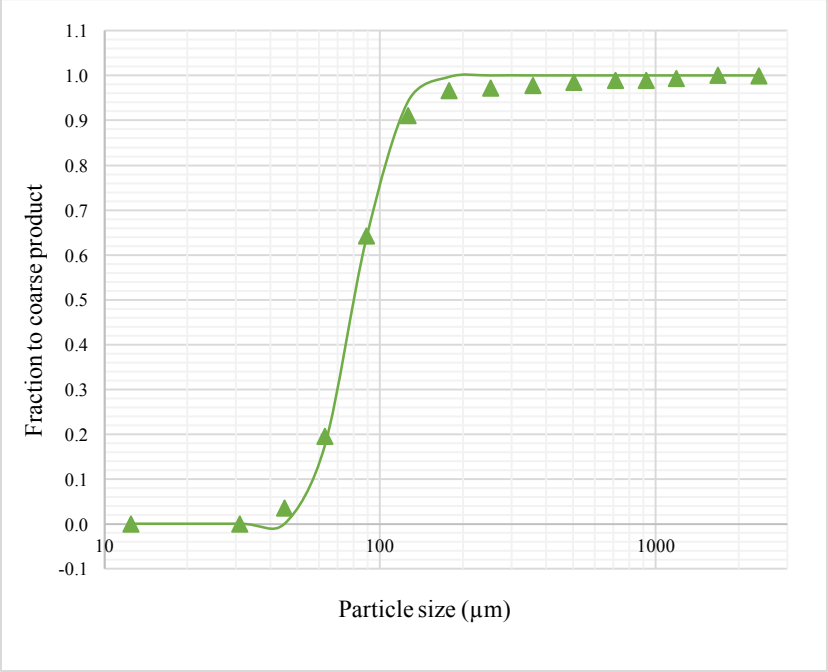

Figure 5-23: Corrected efficiency curve of the fine screen circuit fitted with Whiten model (line)

Table 5-8: Efficiency parameter values of the fine screen circuit configuration

Efficiency parameters	Value
Sharpness of separation (α)	4.1
Corrected cut size - µm (d50c)	79
Water recovery to coarse product (Rf)	0.17
Beta (β)	0.43

Figure 5-23 and Table 5-8 present the corrected efficiency curve fitted with the Whiten model and the extracted parameter values from the model of the fine screen circuit configuration, respectively. Generally, the performance of the fine screen system was good. A high value of α of more than 4 was achieved, which according to Napier-Munn et al. (2005) suggests that the process of classification was efficient. Additionally, the amount of water recovered to the coarse product was considerably low, indicating minimal misplacement of fine particles to the oversize stream, thus maximising sharpness of separation. Performance based on corrected cut size was assessed from the closeness of the determined cut size to the selected screen aperture size, which in the case of this work was 100µm. The closer the $d50_c$ value is to the aperture size, the greater the separation efficiency. Therefore, the obtained cut size of 79µm was close to the 100µm screen aperture size, thus giving a sharper cut. In screen operations, particles smaller than the aperture opening will pass through whereas particles larger will be retained, thus the cut size is always smaller than the aperture size (Wills & Napier-Munn, 2006; Drzymala, 2007).

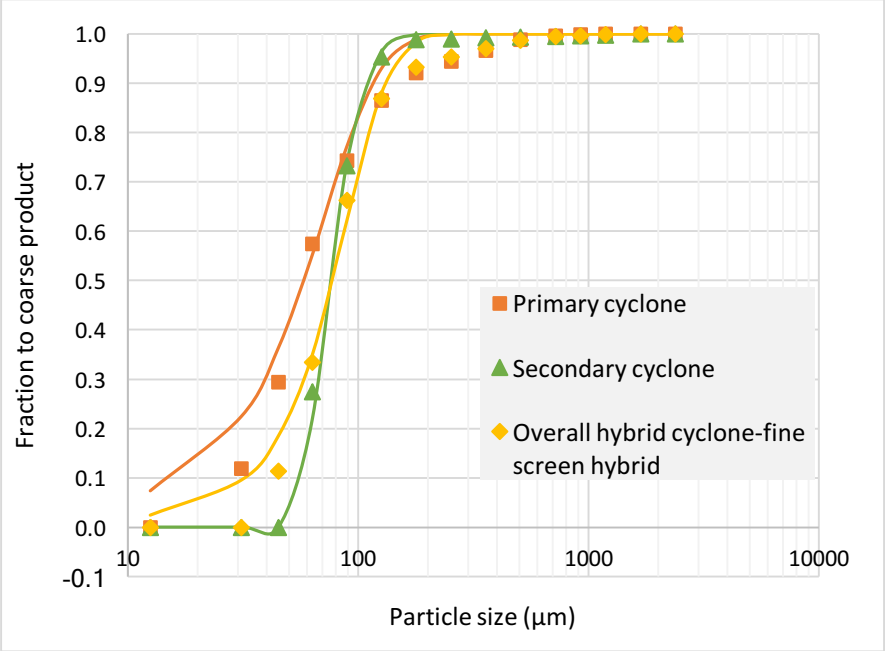

Figure 5-24: Corrected efficiency curves fitted to the Whiten model (line) of the primary cyclone, secondary fine screen and the overall hybrid circuit configuration

Table 5-9: Efficiency parameter values of the individual stages and the overall two-stage cyclone-fine screen hybrid circuit configuration

Efficiency parameters	Efficiency values		
	Primary cyclone	**Secondary fine screen**	**Overall hybrid circuit**
Sharpness of separation (α)	2.1	3.2	3.0
Corrected cut size - µm (d50c)	58	75	75
Water recovery to coarse product (Rf)	0.40	0.55	0.20
Beta (β)	0.00	0.50	0.05

The main aim of this thesis is to test the potential of applying cyclone-fine screen hybrid circuit closed-circuit grinding operations, with the idea of making relative improvements to the classification circuits. The hybrid cyclone-fine screen configuration in this study has the fine screen reclassifying the primary cyclone underflow. A detailed description of the circuit configuration is presented in chapter three. Figure 5-24 presents a summary of the corrected efficiency curves fitted with the Whiten model for the primary cyclone, secondary fine screen and the overall two-stage hybrid circuit. Table 5-9 shows the summary of the parameter values extracted from the model. From the efficiency curves presented in Figure 5-24, the fine screen in

the secondary stage exhibited a much steeper curve than both the primary cyclone and the overall hybrid circuit, indicating that the second stage of classification was the most efficient step. Normally, screens are better classifying units compared to cyclones, even though throughput is limited for fine screening technologies. This is in agreement with the observations made by Valine & Wennen (2002), Barrios (2006), Albuquerque et al. (2008) and Dündar et al. (2014).

From Table 5-9, the $d50_c$ values for the individual stages in the circuit as well as the overall circuit were quite reasonable as they were fine enough for the flotation process. A high value of R_f of over 50% was observed for the secondary fine screen, which could be due to the excessive water addition onto the screen surface through the spray water thus causing increased slurry flowrate which in turn reduces the chance of the particles from accessing the screening surface and are carried over to the oversize. About 40% of the feed water was found to report to the underflow stream for the primary cyclone. However, the overall hybrid cyclone-fine screen circuit revealed a sharp decrease in R_f of approximately 20%. This could be attributed to the effect of applying two stages of classification where the misplaced fines in the primary cyclone have another chance to be classified in the secondary stage (Luckie, Hogg & Schaller, 1980; Rogers et al., 1981; Peterson & Herbst, 1984; Dahlstrom & Kam, 1988; Honaker, Boaten & Luttrell, 2007). The β value of 0.5 was obtained for the secondary fine screen and thus, the fish hook effect was also observed in the overall hybrid system but at a lower value of 0.05.

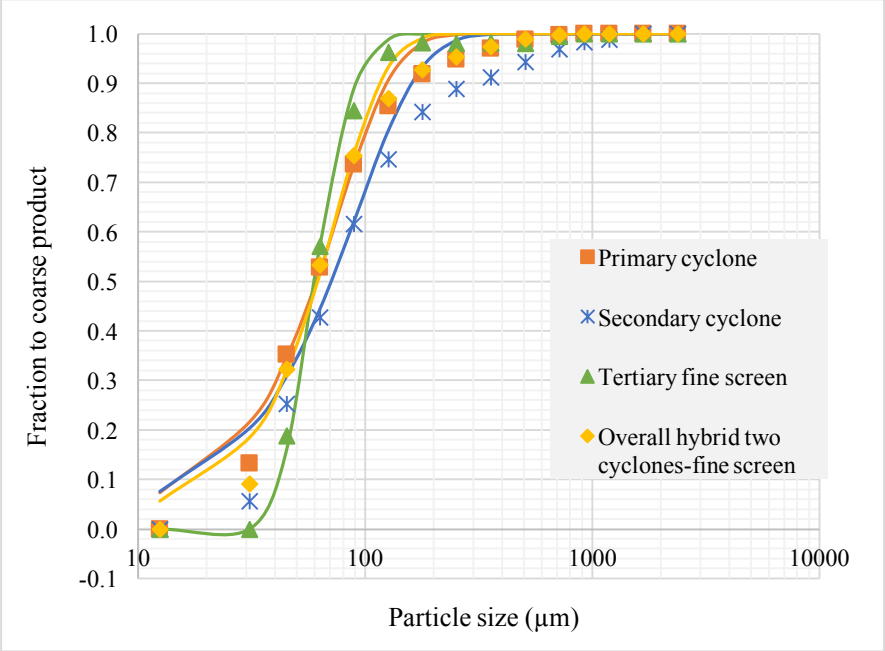

Figure 5-25: Corrected efficiency curves fitted to the Whiten model of the primary cyclone, secondary cyclone, tertiary fine screen and the overall hybrid circuit configuration

The hybrid two cyclones-fine screen hybrid configuration had the first two classification stages consisting of cyclones and then the tertiary stage a fine screen. A detailed description of the process flow of this configuration is presented in chapter three. Figure 5-25 shows the corrected efficiency curves for the primary cyclone, secondary cyclones, tertiary fine screen and the overall three-stage hybrid. From the curves, it can be seen that the tertiary stage consisting of the fine screen had a steeper curve. The fitted efficiency parameter values of the individual stages and the overall circuit are shown in Table 5-10.

Table 5-10: Efficiency parameter values for individual stages and the overall hybrid circuit

Efficiency parameters	**Efficiency values**			
	Primary cyclone	**Secondary cyclone**	**Tertiary fine screen**	**Overall hybrid circuit**
Sharpness of separation (α)	2.0	1.6	2.8	2.4
Corrected cut size - µm (d50c)	61	71	60	61
Water recovery to coarse product (Rf)	0.43	0.44	0.67	0.35
Beta (β)	0.00	0.00	0.60	0.02

From Table 5-10 the values of the corrected cut size obtained for all the three stages as well as the overall hybrid circuit yielded fine cut sizes, thus reasonably good separations were realized. More than 60% of the feed water was recovered to the oversize stream for the tertiary fine screen stage. This could be attributed to poor operational control of water additions through the water sprays onto the screen. However, the overall hybrid circuit revealed a reduced fraction of R_f of approximately 35%. Thus, operating the screen at its optimum could lead to even greater improvements in the overall circuit. Furthermore, the value of α appeared to have increased in the overall hybrid circuit compared to the primary cyclone circuit due to the inclusion of the fine screen. The fine screen showed the highest α value due to its ability to separate particles on the basis of size only (Matthew, 1985). A finer cut of 61% was realised by virtual of reclassifying the cyclone overflow, thus reducing the coarse particles from short-circuiting to the undersize. Peterson and Herbst (1984) showed that reclassifying the cyclone overflow in a separate classifier could reduce the fraction of coarse particles misplaced to the final product. They found that the coarse size in the final product measured by particle size reduced significantly, particle size with less than 1% chance of reporting to the final product stream was reduced from about 140μm in single cyclone to approximately 75μm. The β values of 0.6 and 0.02 were obtained for tertiary fine screen stage and the overall hybrid circuit, respectively.

5.6.4 Comparisons of circuit configurations tested – the overall classification circuit performance

Table 5-11shows a summary of the efficiency parameter values extracted from the Whiten model of the overall performance of all the classification circuit configurations tested

Table 5-11: Efficiency parameter values extracted from the Whiten model of the overall circuit performance of each configuration

Efficiency parameters	Two-stage cyclone	Inclined cyclone	fine screen	Hybrid cyclone-fine screen	Hybrid two cyclones-fine screen
Alpha (α)	1.70	0.54	4.10	3.00	2.40
Corrected cut size (d50c)	75	147	79	75	61
Watersplit (Rf)	0.34	0.30	0.17	0.20	0.35
Beta (B)	0.00	0.03	0.43	0.05	0.02

From Table 5-11, it can be seen that the fine screen configuration had the highest α value and the lowest was exhibited in the inclined cyclone configuration. The two hybrid circuit configurations revealed relatively higher values of α compared to configurations with cyclones only such as the two-stage cyclone and inclined cyclone, which agrees with the first hypothesis of this study. The relative improvements in the sharpness of separation in the hybrid circuits could be attributed to the inclusion of the fine screen in the configurations. Fine screens are independent of particle density thus classification is based on size only. Unlike cyclones, particle separation takes into consideration both the size and specific gravity, consequently leading to higher circulating loads and low classification efficiency (Barkhuysen, 2009; Valine, Wheeler & Albuquerque, 2009; Dündar et al., 2014; Mainza, 2016). Fine screening is considered expensive in closed-circuit grinding operations due to the associated capital and maintenance costs. However, the application of hybrid circuits would reduce these challenges as the tonnage of material to be handled by the screen is reduced by the prior cyclone classification step. Thus, lesser screen units would be required resulting in reduced capital and running costs and providing relatively sharper classification.

Water recovery to the coarse product as defined by Kilavuz and Gülsoy (2011) is the ratio of the volumetric water flowrates of the coarse stream to the feed stream. Plitt (1976) and Flintoff et al. (1987) have reported that water recovery to the coarse stream is directly proportional to the fraction of fine particles that bypasses classification forces. Higher values of R_f are undesirable because the classification efficiency reduces (Napier-Munn et al., 2005). The results revealed that the hybrid two cyclone-fine screen circuit had the highest fraction of feed water reporting to the recycle stream. This could be due to the high fines bypass exhibited in the secondary cyclone which happened to be one of the streams that formed the final recycle stream returned to the ball mill. Generally, the cyclone overflow stream reclassification would have a negative effect in terms of the overall bypass fraction but could yield finer separations according to Peterson & Herbst (1984). On the other hand, the hybrid cyclone-fine screen circuit revealed a relatively lower value of R_f, this is due to reclassifying the cyclone underflow on the separate fine screen which then correctly placed the misdirected fines to the undersize, resulting in a sharper classification for the overall circuit. The two-stage cyclone and inclined cyclone configurations also revealed relatively low values of R_f. Whereas, the fine screen configuration had the lowest

fraction of feed water reporting to the oversize is expected than the other circuit configurations tested in this work, providing the sharpest classification.

Generally, cut size is selected based on the liberation size of the minerals of interest in the ore and the particular solid concentration of the final product to meet the specifications of the subsequent process. It was revealed that the inclined cyclone circuit had the highest $d50_c$ value of 147μm. This meant that particles of 147μm had a 50% chance of reporting to the circuit final product stream, thus sending unliberated particles to the subsequent process which could result in poor recoveries of the valuable minerals in the flotation process. Asomah and Napier-Munn (1996) also found that inclining the cyclone to the vertical results in a coarser cut. The other configurations showed relatively good overall $d50_c$ values, implying finer cut sizes were realized.

The beta parameter is associated with the effect of fish-hook. A fish-hook is an inflexion in the efficiency curve showing a dip at the finer size (Nageswararao, 2000). Several causes of this effect have been proposed in literature (Finch, 1983; Frachon & Cilliers, 1999) however, there has been no definite explanation to the existence of the fish-hook phenomenon. The beta values in this study were extracted from the Whiten efficiency function reported in Napier-Munn et al. (2005). In the case where no fish-hook was observed, the beta value was set to zero. The results showed that the fine screen circuit had a higher value of β, implying that more particles were entrained at the fine sizes. While the inclined cyclone, hybrid cyclone-fine screen and hybrid two cyclones-fine screen circuits revealed lower β values of 0.03, 0.05 and 0.02, respectively. The two-stage cyclone circuit did not exhibit a fish-hook, thus β was zero. The fish-hook effect observed in the overall hybrid circuits were as a result of the fish-hook exhibited by the fine screen incorporated in the configurations. However, the effect appeared to have reduced in the overall hybrid circuits.

5.6.5 Reduced efficiency curves

Reduced efficiency curves were used to qualitatively compare the overall performance of the classification circuit configuration tested as they are deemed constant for the given classifier design and feed characteristics. Therefore, the overall net separation effect of each configuration

was measured using reduced curves. Figure 5-26 shows the reduced efficiency curves of the overall circuit configurations tested in this study.

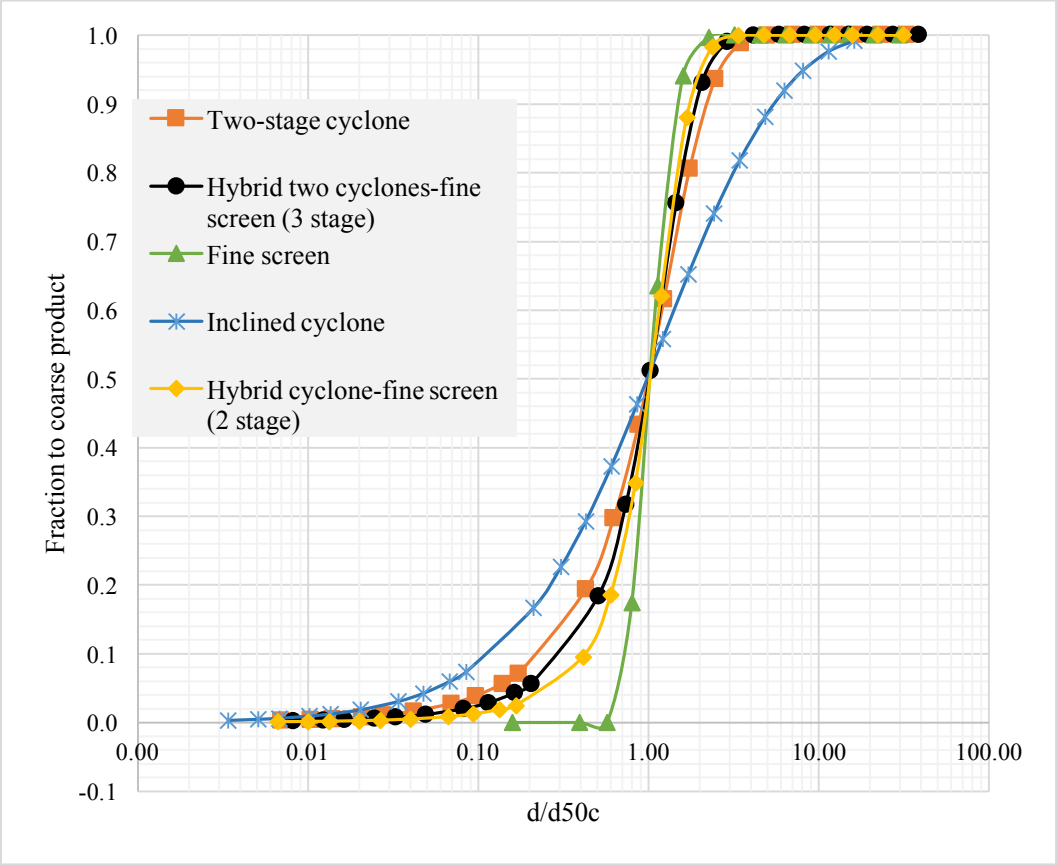

Figure 5-26: Reduced efficiency curves of the circuit configurations tested

The concept of sharpness of separation was applied to determine the most efficient configuration. The circuit configuration with a curve that had the steepest slope was deemed the most effective whereas the one with a shallow slope performed poorly. From Figure 5-26 the order of efficiency from most efficient configuration to the least is: fine screen; hybrid cyclone-fine screen (2 stage); hybrid two cyclones-fine screen (3 stage); two-stage cyclone; and finally, inclined cyclone.

5.7 Summary

The performance of the individual stages of classification and the overall circuit investigated in this study have been evaluated using efficiency curves. The evaluation of the results was based on the sharpness of separation (α), water split to the coarse product (R_f), corrected cut size ($d50_c$) and beta (β) extracted from the Whiten efficiency model fitted to the experimental data. The results showed that stage of classification incorporating the fine screen exhibited higher α values than the stage with cyclones. The fine screen configuration showed the lowest water split fraction as expected however, the fine screen included in the two hybrid configuration tested revealed excessively high water split fractions. This was attributed to the increased slurry flows which resulted in most of the feed material to be carried over to the oversize stream. Nonetheless, the overall hybrid circuits showed sharp reduction in the feed water reporting to the final recycle stream. The inclined cyclone and the overall two-stage cyclone configurations also revealed reasonably low water split fractions. A coarser separation was realised in the inclined cyclone configuration and the other four configurations revealed relatively finer corrected cut sizes. The fish-hook effect was observed in all the configurations that incorporated the fine screen and the inclined cyclone.

Comparisons of the overall performance of the different configurations tested revealed that the fine screen configuration had the sharpest separation whereas the inclined cyclone configuration gave a poorer separation. The two hybrid circuit configurations exhibited sharper separations compared to the circuit configurations with cyclones only which agrees with the first hypothesis of this study. The results also showed that reclassifying the primary underflow in a separate unit could reduce the overall fines bypass of the circuit agreeing with the second hypothesis. However, the magnitude of fines bypass reduction depends on the type of configuration. In the case of this study the hybrid cyclone-fine screen circuit showed a bypass fraction of 0.2 whereas 0.34 was obtained for the two-stage cyclone circuit.

The hybrid cyclone-fine screen circuits documented in literature based on computer simulations have shown that improved classification could be achieved and the experimental tests conducted in this study have confirmed the computational results. One exceptional aspect of a hybrid cyclone-fine screen classification is the capability of employing a fine screen in the classification

stage prior to cyclone classification, consequently reducing the tonnage of material to be treated by the fine screen. This allows for effective screening with lesser screen units required compared to using fine screens only which would require substantial capital and running costs. Furthermore, the use of screen classifiers requires significant water additions, which will result in a more dilute classification product thus having an adverse effect on the downstream process. In order to assess the full potential of applying hybrid circuit configurations in closed-circuit grinding operations, an economic analysis of the additional costs for installing and operating the fine screens as well as the additional water needed, should be done.

6 CHAPTER SIX: CONCLUSIONS AND RECOMMENDATIONS

6.1 Introduction

This chapter presents a summary of the main findings obtained from the test work performed to assess the potential of applying hybrid classification configurations containing hydrocyclone(s) and a fine screen in closed-circuit grinding operations with the aim of improving the classification efficiency of the circuit. This was achieved by comparing the performance of the hybrid configuration with: (i) a fine screen circuit; (ii) a two-stage cyclone circuit; and (iii) an inclined cyclone circuit. The conclusions drawn from this work are presented here as well as the recommendations for future work to be done.

6.2 Key observations

The key observations that were made from the classification tests of the different configurations investigated include the following:

- The hybrid configurations containing cyclone(s) and a screen gave relatively higher classification performances measured in terms of the sharpness of separation than configurations with hydrocyclones only. The overall sharpness of separation values obtained for the two-stage and three-stage hybrid circuits were 3 and 2.4, respectively. The two-stage cyclone and inclined cyclone circuits showed sharpness of separation values of 1.7 and 0.54, respectively.

- The bypass percentage of 20% was obtained for the hybrid cyclone-fine screen (2 stage) configuration while 35% was calculated for the hybrid two cyclone-fine screen (3 stage) configuration. However, a finer corrected cut size of 61μm was achieved in the three-stage hybrid compared to 75μm for the two-stage hybrid configuration.

- The secondary cyclones in the two-stage cyclone and three-stage hybrid configurations showed poorer classification performances than the primary cyclones. The sharpness of separation values obtained for the secondary cyclones in the two-stage cyclone and three-

stage hybrid circuits were 1.4 and 1.6, respectively whereas, the primary cyclones achieved values of 2 for both configurations.

- The fine screen circuit was found to be the most efficient among the classification configurations tested in this work. A higher sharpness of separation value of 4.1 and a lower value of the water split to the oversize stream of 17% were achieved. This is evident that screen classifiers are better classifying units compared to cyclones whose highest sharpness of separation was found to be 2.0 in this work.

- The inclined cyclone circuit configuration showed a lower sharpness of separation of value of 0.54. This is indicative that the classification efficiency was poor. However, a relatively lower water split to the underflow stream of 30% was achieved.

- The fish-hook effect at particle sizes less than 38μm was observed for classification circuit configurations incorporating a fine screen and an inclined cyclone. The effect was more pronounced in classification configurations involving screens.

6.3 Conclusions

The following conclusions were made, based on the findings of the test work conducted in this study:

- The application of a hybrid configuration containing of cyclone(s) and a screen in closed-circuit grinding operations will improve the performance of classification circuits compared to configurations with cyclones only. However, the degree of improvement is dependent on the type of hybrid configuration. A hybrid circuit with cyclone underflow reclassification exhibited a higher sharpness of separation value compared to a circuit with cyclone overflow reclassification.

- Reclassification of the cyclone underflow in a separate classifier unit will result in reduced fines bypass irrespective of the type of configuration employed. However,

a hybrid cyclone-fine screen configuration will provide lower fines bypass than a two-stage cyclone configuration. The results showed that a hybrid configuration reduced fines bypass from 40% in the primary cyclone to 20% for the overall circuit. In the same duty, a two-stage cyclone configuration reduced fines bypass from 45% in the primary cyclone to 34% for the overall circuit. In the case of cyclone overflow reclassification on a screen, a finer corrected cut size will be realised, though this is likely to increase fines bypass for the overall circuit.

6.4 Recommendations

Based on the findings and conclusions made, the following recommendations are made for future work:

- Mineralogical analysis of the feed and product streams size fractions should be performed for the hybrid classification configurations to access the deportment of the mineral components during classification - particularly for multi-density ore bodies such as the Black Mountain Mine ore formation.

- Perform simulations using multi-component models of the cyclone and screen to predict the performance of a hybrid classification system. This could be done using the data generated in this study after the models are upgraded to consider multi-component data.

- Assess the influence of applying cyclone-fine screen hybrid systems in closed grinding circuits on the overall plant performance in terms of metal recovery.

- Conduct a study to assess the effects of varying cyclone apex and vortex finder diameters on the performance of hybrid classification system.

- Conduct an economic analysis to validate the benefits of applying cyclone-fine screen hybrid circuits in closed-circuit grinding operations.

7 REFERENCES

Albert, E. 1945. Characteristics of screen circuit products. *Min.Tech*. T.P.1820(May).

Albuquerque, L.G., Wheeler, J., Valine, S.B. & Ganahl, B. 2008. Application of high frequency screens in closing grinding circuits. *International Mineral Processing Seminar–Gecamin*. (1).

Arterburn, R.A. 1976. *The sizing and selection of hydrocyclones*.

Asomah, A.K. & Napier-Munn, T.J. 1997. An empirical model of hydrocyclones, incorporating angle of cyclone inclination. *Minerals Engineering*. 10(3):339–347. DOI: 10.1016/S0892-6875(97)00008-3.

Asomah, I.K. & Napier-Munn, T.J. 1996. The performance of inclined hydrocyclones in mineral processing. In *Proceedings Hydrocyclones '96*. D. Caxton, L. Svarovsky, & M. Thew, Eds. 273–288.

Barkhuysen, N.J. 2009. Implementing strategies to improve mill capacity and efficiency through classification by particle size only, with case studies. In *Base Metal Conference SAIMM*. 101–114.

Barrios, G.F. 2006. Increasing the Capacity of the Grinding Circuits without Installing More Mills. *The Fourth Southern African Conference on Base Metals SAIMM*. 433–444.

Becker, M., Mainza, A.N., Powell, M.S., Bradshaw, D.J. & Knopjes, B. 2008. Quantifying the influence of classification with the 3 product cyclone on liberation and recovery of PGMs in UG2 ore. *Minerals Engineering*. 21(7):549–558. DOI: 10.1016/j.mineng.2007.11.001.

Bhaskar, K.U., Govindarajan, B., Barnwal, J.P., Rao, K.K. & Rao, T.C. 2004. Modelling studies on a 100mm water-injected cyclone. *Physical Separation in Science and Engineering*. 13(3):89–99. DOI: 10.1080/14786470412331286580.

Bourgeois, F. & Majumder, A.K. 2013. Is the fish-hook effect in hydrocyclones a real phenomenon ? *Powder Technology*. 237:367–375. DOI: 10.1016/j.powtec.2012.12.017.

Bradley, D. 1965. *The hydrocyclone*. Oxford, UK: Pergamon Press.

Brodzik, P. 2009. Application of Derrick Corporation stack sizer technology for slimes reduction in 6Inch clean coal hydrocyclone circuit.

Chu, L. & Luo, Q. 1994. Hydrocyclone with high sharpness of separation. *Filtration & Separation*. (November):733–736.

Concha, F., Barrientos, A., Montero, J. & Sampaio, R. 1996. Air core and roping in hydrocyclones. *International Journal of Mineral Processing*. 44–45:743–749. DOI: 10.1016/0301-7516(95)00080-1.

Dahlstrom, D.A. & Kam, W. 1988. Potential energy savings in comminution by two stage classification. *International Journal of Mineral Processing*. 22:239–250.

Davies, E.W. 1925. Ball mill crushed in closed circuits with screens. *Bulletin University of Minnesota*. 10.

Drzymala, J. 2007. *Mineral processing, foundations of theory and practice of minerallurgy*. Wroclaw, Poland.

Dündar, H., Kalugin, A., Delgado, M., Palomino, A., Turkistanli, A., Aquino, B. & Lynch, A. 2014. Screens and cyclones in closed grinding circuits. *XXVII International Mineral Processing Congress*. 1–11.

Farghaly, M.G., Golyk, V., Ibrahim, G.A., Ahmed, M.M. & Neesse, T. 2010. Controlled wash water injection to the hydrocyclone underflow. *Minerals Engineering*. 23(4):321–325. DOI: 10.1016/j.mineng.2009.09.021.

Ferrara, G., Preti, U. & Schena, G.D. 1987. Computer-aided use of a screening process model. In *Proceeding of the 20th International Symposium on the Application of Computers and Mathematics in the Mineral Industries*. Johannesbery: SAIMM. 153–166.

Finch, J.A. 1983. Modelling a fish-hook in hydrocyclone selectivity curves. *Powder Technology*. 36:127–129.

Firth, B. & O'Brien, M. 2003. Hydrocyclone Circuits. *Coal Preparation*. 23:167–183. DOI: 10.1080/07349340390210997.

Firth, B., O'Brien, M., Edward, D. & Clarkson, C. 1999. Fine coal classification. *Final report Acarp Project*. C3084.

Flintoff, B.C., Plitt, L.R. & Turak, A.A. 1987. Cyclone modelling: A review of present technology. *CIM Bulletin*. 80:39–50.

Fowler, R.T. & Lim, S.C. 1959. The influence of various factors upon the effectiveness of separation finely divided solid by a vibrating screen. *Chemical Engineering Science*. 10:163–170.

Frachon, M. & Cilliers, J.J. 1999. A general model for hydrocyclone partition curves. *Chemical Engineering Journal*. 73(1):53–59. DOI: 10.1016/S1385-8947(99)00040-6.

Fuerstenau, M.C. & Han, K.N. 2003. *Principles of Mineral Processing*. Littleton: SME.

Gaudin, A.M. 1937. *Principles of Mineral dressing*. First ed. New York & London: McGraw-Hill Book Company Inc.

Gupta, A. & Yan, D.S. 2006. *Mineral processing, design and operation*. Perth, Australia.: Elsevier Science.

Heiskanen, K. 1993. *Particle Classification*. United Kingdom: Chapman and Hall.

Heiskanen, K., Vesanto, A. & Eronen, H. 1987. A high performance hydrocyclone design - The Twin Vortex cyclone. In *The 3rd International Conference on Hydrocyclones*. Oxford, England. 263–268.

Honaker, R.Q., Ozsever, A. V, Singh, N. & Parekh, B.K. 2001. Apex water injection for improved hydrocyclone classification efficiency. *Minerals Engineering*. 14(11):1445–1457.

Honaker, R.Q., Boaten, F. & Luttrell, G.H. 2007. Ultrafine coal classification using 150 mm gMax cyclone circuits. *Minerals Engineering*. 20:1218–1226. DOI: 10.1016/j.mineng.2007.06.004.

Hukki, R.T. 1975. About the ways and means to improve the performance of closed grinding circuits. *Fourth European Symposium on Comminution*. Preprints:319–330.

Hukki, R.T. & Heiskanen, K. 1981. Two stage hydraulic classification - A report on industrial application.

Ibrahim, G.A. & Ahmed, M.M. 2007. The performance of three-product hydrocyclone: distribution of the feed solids content in the product streams. *Journal of Engineering Sciences*. 35(2):527–544.

Jankovic, A. & Valery, W. 2012. The impact of classification on energy efficiency of grinding circuits - The hidden opportunity. In *11th Mill Operator's Conference*. 65–69.

Jankovic, A. & Valery, W. 2013. Closed circuit ball mill – Basics revisited. *Minerals Engineering*. 43–44:148–153. DOI: 10.1016/j.mineng.2012.11.006.

Kawatra, S.K., Bakshi, A.K. & Rusesky, M.T. 1996. The effect of slurry viscosity on hydrocyclone classification. *International Journal of Mineral Processing*. 48:39–50.

Kelly, E.G. & Spottiswood, D.J. 1982. *Introduction to mineral processing*. First ed. New York: Wiley.

Kelsall, D.F. 1953. A further study of the hydraulic cyclone. *Chem. Eng. Sci.* 2(6):254–272.

Kelsall, D.F. & Holmes, J.A. 1960. Improvements in classification efficiency in hydraulic cyclones by water injection. *Proceedings of the 5th Mineral Processing Congress*. 9.

Kelsall, D.F., Stewart, P.S.B. & Restarick, C.J. 1974. A practical multiple cyclone arrangement for improved classification. *European Conference on Mixing and Centrifugal Separation*. E5-83-E5-93.

Kılavuz, F.Ş. & Gülsoy, Ö.Y. 2011. The effect of cone ratio on the separation efficiency of small diameter hydrocyclones. *International Journal of Mineral Processing*. 98(3–4):163–167. DOI: 10.1016/j.minpro.2010.11.006.

Laplante, A.R. & Finch, J.A. 1984. The origin of unusual cyclone performance curves. *International Journal of Mineral Processing*. 13(1):1–11.

Lawrence, L.R. & Beddow, J.K. 1968. Powder segregation during die filling. *Powder Technology*. 2:253–259.

Luckie, P. & Hogg, R. 1980. A review of two fine particle processing units operations - Classification and mixing. In *Proceedings of the International Symposium on Fine Particles Processing*. V. 1. P. Somasundaran, Ed. Las Vegas: American Institute of Mining, Metallurgical, and Petroleum Engineers, Inc. 167–180.

Luckie, P.T. & Austin, L.G. 1973. Technique for the derivation of selectivity functions from experimental data. In *Proceedings of 10th IMPC IMM*.

Luckie, P., Hogg, R. & Schaller, R. 1980. A review of two fine particle processing unit operations - Calssification and Mixing. In *Fine Particle Processing AIME*. V. 1. Somasundaran, Ed.

Lusinga, D., Angombe, J. & Mainza, A.N. 2009. Assessing the effects of the cone force ratio on the performance of hydrocyclones. *Journal of the Southern African Institute of Mining and Metallurgy*. 109(4):239–243.

Lynch, A.J. 1977. *Mineral crushing and grinding circuits: Their simulation, optimisation, design and control*. V. 1. Elsevier.

Lynch, A.J. & Rao, T.C. 1975a. Modelling and scale-up of hydrocyclone classifiers. In *Proceedings of the 11th International Mineral Processing Congress*. Ca-gliari.

Lynch, A.J. & Rao, T.C. 1975b. Modelling and scale-up of hydrocyclone classifiers. *Indian Journal of Technology*. 4(6):106–114.

Lynch, A.J., Rao, T.C. & Prisbrey, K.A. 1974. The influence of hydrocyclone diameter on reduced-efficiency curves. *International Journal of Mineral Processing*. 1(2):173–181.

Lynch, A.J., Rao, T.C. & Bailey, C.W. 1975. The influence of design and operating variables on the capacities of hydrocyclone classifiers. *International Journal of Mineral Processing*. 2(1):29–37.

Mabote, S. 2016. Development of a wet fine screen model integrating the effect of operating and design variables on screen performance. University of Cape Town.

Mainza, A.N. 2006. Contribution to the understanding of the three-product cyclone on classification of a dual density platinum ore. University of Cape Town.

Mainza, A.N. 2016. Contribution of the classifers to comminution and separation processes in mineral processing. In *IMPC 2016 : XXVIII International Mineral Processing Congress Proceedings*. Canadian Institute of Mining , Metallurgy and Petroleum IMPC 2016. 1–11.

Mainza, A., Powell, M.S. & Knopjes, B. 2004a. Differential classification of dense material in a three-product cyclone. *Minerals Engineering*. 17(5):573–579. DOI: 10.1016/j.mineng.2004.01.023.

Mainza, A., Powell, M.S. & Knopjes, B. 2004b. A comparison of different cyclones in addressing challenges in the classification of the dual density UG2 platinum ore. In *International Platinum Conference" Platinum Adding Value". The Southern African Institute of Mining and Metallurgy*. 95–102.

Matthew, C.W. 1985. General classes of screens. In *Mineral Processing Handbook*. N.L. Weiss, Ed. SME. 3E–1–3E41.

Metso. 2015. *Basics in minerals processing*.

Mohanty, M.K., Palit, A. & Dube, B. 2002. A comparative evaluation of new fine particle size separation technologies. *Minerals Engineering*. 15:727–736.

Muzanenhamo, P. 2014. Assessing the effect of cone ratio , feed solids concentration and viscosity on hydrocyclone performance. Univerisity of Cape Town.

Mwale, A.N. 2015. Model for fine wet screening. University of Cape Town.

Nageswararao, K. 1978. Further developments in the modelling and scale-up of industrial hydrocyclones. University of Queensland.

Nageswararao, K. 1995. A generalised model for hydrocyclone classifiers. *AusIMM Proceedings*. 2(21).

Nageswararao, K. 2000. A critical analysis of the fish hook effect in hydrocyclone classifiers. *Chemical engineering journal*. 80(1–3):251–256. DOI: 10.1016/S1383-5866(00)00098-8.

Nageswararao, K. 2014. Comment on : "Is the fish-hook effect in hydrocyclones a real phenomenon?" by F . Bourgeois and A . K . Majumder [Powder Technology 237 (2013) 367 – 375]. *Powder Technology*. 262:194–197. DOI: 10.1016/j.powtec.2014.04.068.

Napier-Munn, T.J., Morrell, S., Morrison, R.D. & Kojovic, T. 2005. *7. Napier-Munn, T. J., Morrell, S., Morrison, R. D. & Kojovic, T.* University of Queensland, Australia: JKMRC Monograph Series, Julius Kruttschnitt Mineral Research Centre.

Narasimha, M., Mainza, A.N., Holtham, P.N., Powell, M.S. & Brennan, M.S. 2014. A semi-mechanistic model of hydrocyclones - Developed from industrial data and inputs from CFD. *International Journal of Mineral Processing*. 133:1–12. DOI: 10.1016/j.minpro.2014.08.006.

Obeng, D.P. & Morrell, S. 2003. The JK three-product cyclone — performance and potential applications. *International Journal of Mineral Processing*. 69:129–142.

Olson, T.J. & Turner, P.A. 2002. Hydrocyclone selection for plant design. In *Mineral Processing Plant Design, Practice and Control Proceedings*. V. 1. A.L. Mular, D.N. Halbe, & D.J. Barratt,

Eds. Colorado: SME. 880–893.

Peterson, R.D. & Herbst, J.A. 1984. The effects of two-stage hydrocyclone classification on mineral processing plant performance. *Canadian Metallurgical Quarterly*. 23(4):383–391.

Plitt, L.R. 1976. A mathematical model of the hydrocyclone classifier. *CIM Bulletin*. 69(776):114–123.

Pryor, E.J. 1965. *Mineral Processing*. London: Applied Science Publishers.

Rao, T.C., Nageswararao, K. & Lynch, A.J. 1976. Influence of feed inlet diameter on the hydrocyclone behaviour. *International Journal of Mineral Processing*. 3(4):357–363.

Rogers, R.S.C. 1982. A classification function for vibrating screens. *Powder Technology*. 31(1):135–137. DOI: 10.1016/0032-5910(82)80015-6.

Rogers, R.S.C. & Brame, K.A. 1985. An analysis of the high-frequency screening of fine slurries. *Powder Technology*. 42(3):297–304. DOI: 10.1016/0032-5910(85)80069-3.

Rogers, R.S.C., Hukki, A.M., Steiner, G.J. & Arterburn, R.A. 1981. An evaluation of the use of two vs one stage of hydrocyclones in a pilot scale ball mill. *AIME Annual Meeting*. 81–125.

Rong, R. & Napier-Munn, T.J. 2003. Development of a more efficient classifying cyclone. *Coal Preparation*. 23:149–165. DOI: 10.1080/07349340390211004.

Soldinger, M. 1999. Interrelation of stratification and passage in the screening process. *Minerals Engineering*. 12(5):497–516. DOI: 10.1016/S0892-6875(99)00033-3.

Soldinger, M. 2000. Influence of particle size and bed thickness on the screening process. *Minerals Engineering*. 13(3):297–312. DOI: 10.1016/S0892-6875(00)00009-1.

Standish, N., Bharadwaj, A.K. & Hariri-Akbari, G. 1986. A study of the effect of operating variables on the efficiency of a vibrating screen. *Powder Technology*. 48(2):161–172. DOI: 10.1016/0032-5910(86)80075-4.

Subasinghe, G.K.N.S., Schaap, W. & Kelly, E.G. 1989. Modelling the screening process - A probabilistic approach. *Minerals Engineering*. 59:37–44. DOI: 10.1016/0892-6875(89)90044-7.

Svarovsky, L. 1984. *Hydrocyclones*. Eastbourne, London, UK: Holt, Rinehart & Winston Ltd.

Svarovsky, L. & Thew, M.T. 1992. *Hydrocyclones: Analysis and Applications*. Letchworth, England: Springer Science + Bussiness Media LLC.

Tarr Jr., D.T. 1985. Hdrocyclones. In *Mineral Processing Handbook*. N.L. Weiss, Ed. New York & London: SME. 3D–10–3D–38.

Trawinski, H.F. 1980. Current liquid-solid separation technology. Paper presented at Second World Filtration Congress. *Filtration & Separation*. 17(4):326–335.

Tromp, K.F. 1937. “New methods of computing the washability of coals”. *Gluckauf*. 37:125–131.

Trumic, M. & Magdalinovic, N. 2011. New model of screening kinetics. *Minerals Engineering*. 24(1):42–49. DOI: 10.1016/j.mineng.2010.09.013.

Vakamalla, T.R., Kumbhar, K.S., Gujjula, R. & Mangadoddy, N. 2014. Computational and experimental study of the effect of inclination on hydrocyclone performance. *Separation and Purification Technology*. 138:104–117. DOI: 10.1016/j.seppur.2014.10.013.

Valine, S.B. & Wennen, J.E. 2002. Fine screening in mineral processing operations. In *Mineral Processing Plant Design, Practice and Control Proceedings*. V. 1. A.L. Mular, D.N. Halbe, & D.J. Barratt, Eds. Colorado: SME. 917–928.

Valine, S.B., Wheeler, J. & Albuquerque, L.G. 2009. Fine sizing with the Derrick Stack Sizer screen. In *Recent Advances in Mineral Processing Plant Design.* Society for Mining, Metallurgy and Exploration. 433–443.

Del villar, R. & Finch, J.A. 1992. Modelling the cyclone performance with a size dependent entrainment factor. *Minerals Engineering*. 5(6):661–669.

Waters, J.G. 2012. The influence of slurry viscosity on hydrocyclone performance. University of Cape Town.

Wills, B.A. & Napier-Munn, T.J. 2006. *Mineral processing technology: An introduction to the practical aspects of ore treatment and mineral recovery*. 7th Editio ed. Elsevier Science & Technology Books.

8 APPENDICES

8.1 Appendix A: Time graph series of the operational data during the survey campaigns.

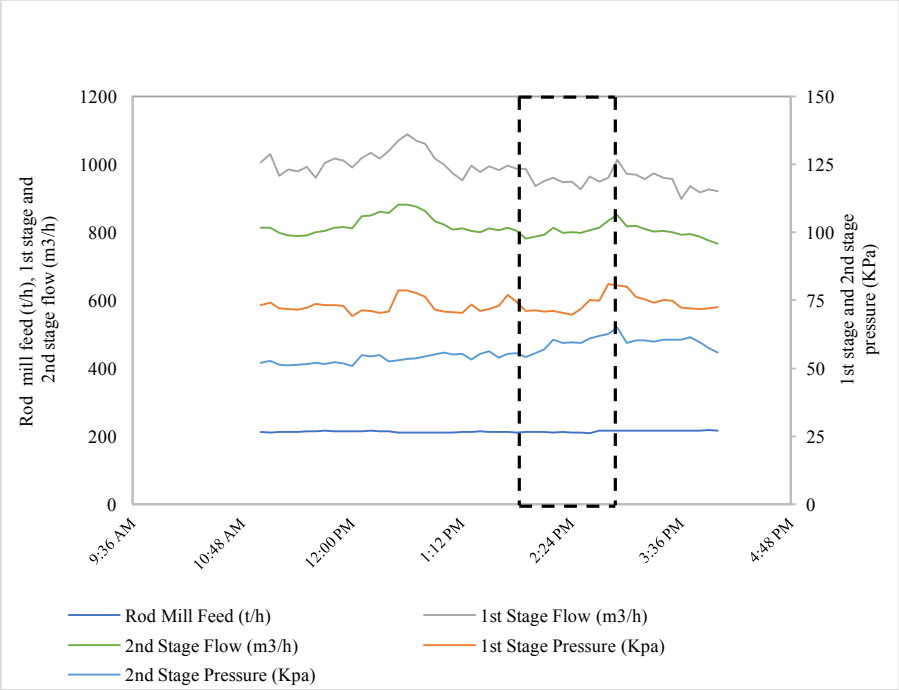

Figure 8-1: Operational data logged on the SCADA during survey 4 campaign

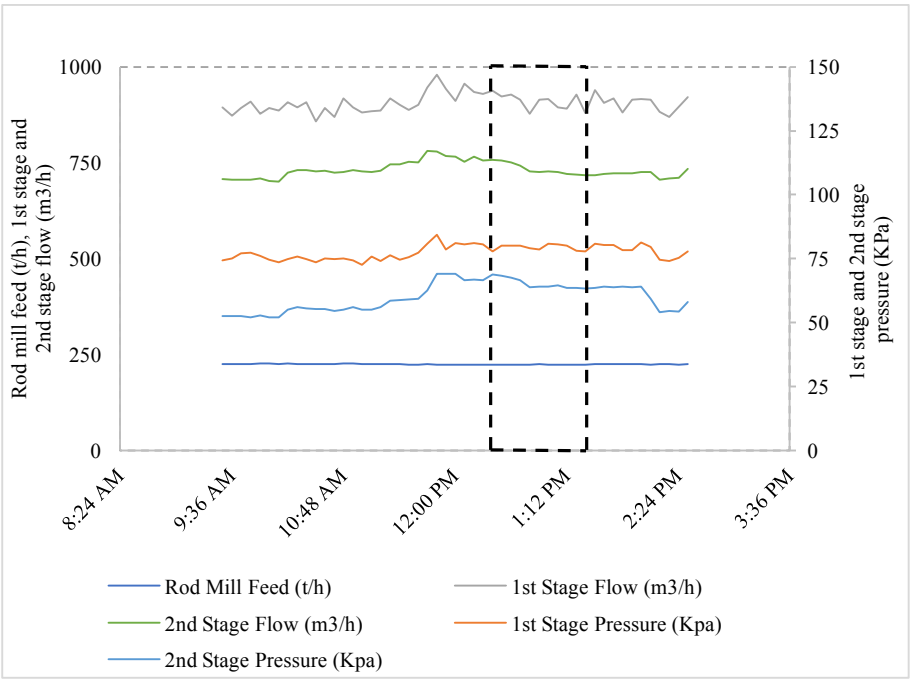

Figure 8-2: Operational data logged on the SCADA during survey 5 campaign

8.2 Appendix B: Experimental and mass balanced data

Table 8-1: Experimental and balanced data for the inclined cyclone circuit configuration

Operational parameters	**Feed**		**U/F**		**O/F**	
	Exp.	**Bal**	**Exp.**	**Bal**	**Exp.**	**Bal**
TPH Solids	1213.73	1213.74	771.98	777.01	441.76	436.73
Solids SG (t/m^3)	4.60	4.60	4.60	4.60	4.60	4.60
TPH Water	531.64	539.73	127.21	126.09	419.71	413.64
% Solids	69.54	69.22	85.85	86.04	51.28	51.36
Pulp SG (t/m^3)	2.19	2.18	3.05	3.06	1.67	1.67
Flowrate (m^3/h)	795.49	803.59	295.03	295.00	515.74	508.58
%-0.075 (mm)	24.15	23.63	13.05	13.27	41.84	42.05
80 % passes (mm)	0.335	0.345	0.441	0.426	0.198	0.197
Size (mm)	**% Retained**					
2.800	0.00	0.00	0.00	0.00	0.00	0.00
2.000	0.24	0.27	0.44	0.42	0.02	0.01
1.400	0.76	0.84	1.34	1.25	0.14	0.13
1.000	1.66	1.75	2.65	2.56	0.32	0.31
0.850	1.45	1.52	2.25	2.19	0.33	0.32
0.600	4.20	4.43	6.50	6.24	1.25	1.23
0.425	5.20	5.46	7.69	7.43	1.97	1.94
0.300	9.83	9.96	12.67	12.67	5.18	5.14
0.212	12.03	12.21	14.47	14.44	8.34	8.23
0.150	16.18	16.08	17.21	17.36	13.81	13.79
0.106	12.98	12.70	12.14	12.40	13.20	13.24
0.075	11.32	11.15	9.59	9.78	13.60	13.60
0.053	6.88	6.53	4.48	4.61	9.81	9.95
0.038	5.27	5.03	2.94	3.01	8.48	8.62
0.025	2.51	2.46	1.07	1.08	4.89	4.92
-0.025	9.49	9.60	4.56	4.56	18.66	18.56

Table 8-2:Experimental and balanced data for the fine screen circuit configuration

Operational parameters	Feed		O/S		U/S	
	Exp.	**Bal**	**Exp.**	**Bal**	**Exp.**	**Bal**
TPH Solids	797.66	797.67	630.78	630.86	166.88	166.81
Solids SG (t/m^3)	5.10	5.10	5.10	5.10	5.10	5.10
TPH Water	5263.32	5309.50	2119.36	2105.80	3211.26	3203.69
% Solids	13.16	13.06	22.94	23.05	4.94	4.95
Pulp SG (t/m^3)	1.12	1.12	1.23	1.23	1.04	1.04
Flowrate (m^3/h)	5419.73	5465.90	2243.04	2229.50	3243.98	3236.40
%-0.075 (mm)	18.93	18.98	4.25	4.24	74.80	74.72
80 % passes (mm)	0.386	0.392	0.47	0.46	0.08	0.08
Size (mm)	**% Retained**					
2.800	0.00	0.00	0.00	0.00	0.00	0.00
2.000	0.25	0.22	0.26	0.28	0.00	0.00
1.400	0.77	0.78	0.99	0.98	0.00	0.00
1.000	1.87	1.93	2.50	2.43	0.06	0.06
0.850	1.82	1.87	2.40	2.34	0.09	0.09
0.600	5.68	5.84	7.50	7.31	0.28	0.28
0.425	6.73	6.93	8.88	8.65	0.44	0.44
0.300	11.10	11.27	14.07	13.97	1.08	1.08
0.212	12.99	13.16	16.35	16.24	1.53	1.53
0.150	16.98	16.73	20.32	20.55	2.31	2.32
0.106	12.76	12.35	14.05	14.40	4.57	4.60
0.075	10.12	9.92	8.43	8.60	14.84	14.89
0.053	5.71	5.76	2.14	2.13	19.51	19.49
0.038	4.05	3.95	0.75	0.76	15.90	15.99
0.025	1.98	2.05	0.25	0.24	9.05	8.89
-0.025	7.19	7.22	1.11	1.11	30.34	30.34

Table 8-3 Experimental and balanced data for the hybrid cyclone-fine screen circuit configuration

Operational parameters	Cyclone feed		U/F		O/F		Screen feed		O/S		U/S		O/F + U/S	
	Exp.	**Bal**	**Exp.**	**Bal**	**Exp.**	**Bal**	**Exp.**	**Bal**	**Exp.**	**Bal**	**Exp.**	**Bal**	**Exp.**	**Bal**
TPH Solids	1498.10	1498.10	1271.50	1271.50	226.59	226.59	1271.50	1271.50	1153.41	1152.32	118.10	119.18	344.69	345.78
Solids SG (t/m^3)	6.09	6.09	6.09	6.09	6.09	6.09	6.09	6.09	6.09	6.09	6.09	6.09	6.09	6.09
TPH Water	711.27	711.16	291.23	295.41	420.04	420.07	2655.70	2680.75	1723.34	1703.49	932.36	940.20	1352.40	1347.33
% Solids	67.81	67.81	81.36	81.15	35.04	35.04	32.38	32.17	40.09	40.35	11.24	11.25	20.31	20.42
Pulp SG (t/m^3)	2.31	2.31	3.13	3.11	1.41	1.41	1.37	1.37	1.50	1.51	1.10	1.10	1.20	1.21
Flowrate (m^3/h)	957.26	957.15	500.02	504.20	457.24	457.28	2864.49	2889.54	1912.73	1892.71	951.75	959.77	1409.00	1404.11
%-0.075 (mm)	23.75	23.65	15.25	15.25	71.45	71.45	15.25	14.89	8.91	9.08	77.24	77.37	73.43	73.49
P80 (mm)	0.322	0.316	0.357	0.352	0.096	0.096	0.357	0.361	0.378	0.386	0.079	0.079	0.088	0.088
Size (mm)	**% Retained**													
2.800	0.00	0.00	0.00	0.00	0.00	0.00	0.00	0.00	0.00	0.00	0.00	0.00	0.00	0.00
2.000	0.24	0.26	0.28	0.28	0.00	0.00	0.28	0.35	0.31	0.25	0.00	0.00	0.00	0.00
1.400	0.62	0.55	0.73	0.74	0.00	0.00	0.73	0.82	0.80	0.78	0.00	0.00	0.00	0.00
1.000	1.40	1.29	1.65	1.64	0.00	0.00	1.65	1.89	1.82	1.76	0.03	0.03	0.01	0.01
0.850	1.25	1.18	1.48	1.47	0.01	0.01	1.48	1.48	1.62	1.71	0.04	0.04	0.02	0.02
0.600	4.01	3.91	4.71	4.55	0.07	0.07	4.71	4.79	5.18	5.42	0.15	0.15	0.09	0.09
0.425	5.04	4.89	5.89	5.66	0.24	0.24	5.89	5.96	6.47	6.89	0.24	0.24	0.24	0.25
0.300	9.58	9.53	11.05	11.04	1.31	1.31	11.05	10.69	12.13	12.49	0.54	0.54	1.05	1.05
0.212	12.35	12.32	14.06	14.11	2.73	2.74	14.06	13.81	15.41	15.59	0.82	0.82	2.08	2.07
0.150	17.09	17.18	19.17	19.43	5.40	5.40	19.17	19.09	21.00	20.75	1.30	1.30	3.99	3.99
0.106	13.21	13.63	14.28	14.42	7.16	7.15	14.28	14.46	15.39	14.76	3.49	3.47	5.91	5.88
0.075	11.46	11.61	11.43	11.41	11.63	11.63	11.43	11.77	10.95	10.52	16.14	16.04	13.17	13.15
0.053	6.65	6.61	5.78	6.02	11.50	11.52	5.78	5.70	4.05	3.99	22.65	22.56	15.32	15.32
0.038	4.99	5.00	3.46	3.31	13.56	13.54	3.46	3.20	1.77	1.94	20.00	20.13	15.77	15.81
0.025	2.56	2.57	1.43	1.42	8.89	8.86	1.43	1.31	0.60	0.66	9.58	9.73	9.12	9.16
-0.025	9.56	9.47	4.58	4.50	37.50	37.53	4.58	4.68	2.49	2.49	25.01	24.95	33.22	33.20

Table 8-4: Experimental and balanced data for the hybrid two cyclones-fine screen circuit configuration

Operational parameters	Cyclone feed 1		Cyclone U/F 1		Cyclone O/F 1		Cyclone feed 2		Cyclone U/F 2		Cyclone O/F 2		Screen feed		Screen O/S		Screen U/S		O/F 1 + U/S		U/F 2 + O/S	
	Exp.	Bal	Exp.	Bal	Exp.	Bal	Exp.	Bal	Exp.	Bal	Exp.	Bal	Exp.	Bal	Exp.	Bal	Exp.	Bal	Exp.	Bal	Exp.	Bal
TPH Solids	1424.07	1423.93	1209.15	1209.14	214.92	214.79	1209.15	1209.14	1026.67	1026.67	182.49	182.47	182.49	182.47	157.02	157.05	25.47	25.42	240.39	240.21	1183.68	1183.72
Solids SG	5.10	5.10	5.10	5.10	5.10	5.10	5.10	5.10	5.10	5.10	5.10	5.10	5.10	5.10	5.10	5.10	5.10	5.10	5.10	5.10	5.10	5.10
TPH Water	659.85	668.08	263.27	261.51	408.82	406.57	555.26	547.53	295.70	302.28	242.10	245.25	400.37	408.68	309.59	303.46	105.76	105.23	499.73	511.79	598.90	605.74
% Solids	68.34	68.07	82.12	82.22	34.46	34.57	68.53	68.83	77.64	77.25	42.98	42.66	31.31	30.87	33.65	34.10	19.41	19.46	32.48	31.94	66.40	66.15
Pulp SG	2.22	2.21	2.94	2.95	1.38	1.38	2.23	2.24	2.66	2.64	1.53	1.52	1.34	1.33	1.37	1.38	1.18	1.19	1.35	1.35	2.15	2.14
Flowrate (m^3/h)	939.08	947.28	500.36	498.60	450.96	448.68	792.35	784.62	497.01	503.59	277.89	281.03	436.15	444.46	340.38	334.25	110.75	110.21	546.86	558.89	830.99	837.84
%-0.075 (mm)	23.81	24.76	15.10	16.48	71.51	71.37	15.10	16.48	12.13	11.03	45.11	47.14	45.11	47.14	43.99	39.95	91.76	91.55	73.65	73.51	16.35	14.86
P80 (mm)	0.301	0.302	0.344	0.333	0.095	0.096	0.344	0.333	0.354	0.361	0.164	0.160	0.164	0.160	0.166	0.173	0.054	0.055	0.090	0.091	0.330	0.338
Size (mm)	**% Retained**																					
2.800	0.00	0.00	0.00	0.00	0.00	0.00	0.00	0.00	0.00	0.00	0.00	0.00	0.00	0.00	0.00	0.00	0.00	0.00	0.00	0.00	0.00	0.00
2.000	0.10	0.13	0.19	0.15	0.00	0.00	0.19	0.15	0.16	0.18	0.00	0.00	0.00	0.00	0.00	0.00	0.00	0.00	0.00	0.00	0.13	0.15
1.400	0.34	0.40	0.49	0.47	0.00	0.00	0.49	0.47	0.57	0.56	0.00	0.00	0.00	0.00	0.00	0.00	0.00	0.00	0.00	0.00	0.51	0.48
1.000	0.91	1.02	1.27	1.20	0.00	0.00	1.27	1.20	1.40	1.40	0.06	0.05	0.06	0.05	0.05	0.06	0.00	0.00	0.00	0.00	1.22	1.22
0.850	0.98	1.03	1.27	1.22	0.00	0.00	1.27	1.22	1.40	1.42	0.08	0.08	0.08	0.08	0.08	0.09	0.00	0.00	0.00	0.00	1.22	1.24
0.600	3.46	3.50	4.38	4.12	0.04	0.04	4.38	4.12	4.55	4.76	0.51	0.48	0.51	0.48	0.51	0.56	0.00	0.01	0.04	0.04	4.02	4.20
0.425	4.78	4.78	5.90	5.59	0.22	0.22	5.90	5.59	6.10	6.37	1.20	1.17	1.20	1.17	1.29	1.35	0.05	0.05	0.20	0.20	5.46	5.70
0.300	9.52	9.32	11.19	10.79	1.06	1.06	11.19	10.79	11.68	12.08	3.60	3.50	3.60	3.50	3.82	4.05	0.15	0.15	0.96	0.96	10.63	11.02
0.212	12.69	12.29	14.23	14.03	2.45	2.46	14.23	14.03	15.23	15.50	6.02	5.77	6.02	5.77	6.13	6.66	0.26	0.27	2.21	2.22	14.02	14.33
0.150	17.74	17.28	19.62	19.40	5.33	5.37	19.62	19.40	20.56	20.84	11.84	11.26	11.84	11.26	11.85	13.01	0.48	0.49	4.82	4.85	19.41	19.80
0.106	14.07	13.67	14.62	14.74	7.56	7.62	14.62	14.74	15.01	14.91	14.55	13.79	14.55	13.79	14.41	15.82	1.22	1.24	6.89	6.95	14.93	15.03
0.075	11.60	11.83	11.74	11.82	11.83	11.86	11.74	11.82	11.21	10.95	17.03	16.74	17.03	16.74	17.87	18.45	6.08	6.23	11.23	11.27	12.10	11.94
0.053	6.96	6.99	5.81	6.00	12.50	12.54	5.81	6.00	4.99	4.82	12.45	12.67	12.45	12.67	12.94	12.61	12.87	13.02	12.53	12.59	6.04	5.85
0.038	5.33	5.49	3.67	4.06	13.48	13.50	3.67	4.06	3.15	2.80	10.78	11.17	10.78	11.17	10.33	9.47	21.66	21.70	14.35	14.37	4.10	3.68
0.025	2.24	2.62	1.40	1.55	8.87	8.64	1.40	1.55	1.03	0.87	5.00	5.40	5.00	5.40	4.81	4.00	14.25	14.02	9.44	9.21	1.53	1.29